DYNAMIC HYDROLOGIC ECONOMIC MODELING OF TRADEOFFS
IN HYDROELECTRIC SYSTEMS

Jordan D. Kern

A dissertation submitted to the faculty at the University of North Carolina at Chapel Hill in partial fulfillment of the requirements for the degree of Doctor of Philosophy in the Department of Environmental Sciences and Engineering in the Gillings School of Global Public Health.

Chapel Hill
2014

Approved by:

Gregory Characklis

Martin Doyle

Jackie MacDonald

Dalia Patino-Echeverri

Marc Serre

ABSTRACT

Jordan D. Kern: Dynamic Hydrologic Economic Modeling of Tradeoffs in Hydroelectric Systems
(Under the direction of Gregory Characklis)

Hydropower producers face a future beset by unprecedented changes in the electric power industry, including the rapid growth of installed wind power capacity and a vastly increased supply of natural gas due to horizontal hydraulic fracturing (or "fracking"). There is also increased concern surrounding the potential for climate change to impact the magnitude and frequency of droughts. These developments may significantly alter the financial landscape for hydropower producers and have important ramifications for the environmental impacts of dams.

Incorporating wind energy into electric power systems has the potential to affect price dynamics in electricity markets and, in so doing, alter the short-term financial signals on which dam operators rely to schedule reservoir releases. Chapter 1 of this doctoral dissertation develops an integrated reservoir-power system model for assessing the impact of large scale wind power integration of hydropower resources. Chapter 2 explores how efforts to reduce the carbon footprint of electric power systems by using wind energy to displace fossil fuel-based generation may inadvertently yield further impacts to river ecosystems by disrupting downstream flow patterns.

Increased concern about the potential for climate change to alter the frequency and magnitude of droughts has led to growing interest in "index insurance" that compensates hydropower producers when values of an environmental variable (or index), such as reservoir inflows, crosses an agreed upon threshold (e.g., low flow conditions). Chapter 3 demonstrates the need for such index insurance contracts to also account for changes in natural gas prices in order to be cost-effective.

Chapter 4 of this dissertation analyzes how recent low natural gas prices (partly attributable to fracking) have reduced the cost of implementing ramp rate restrictions at dams, which help restore sub-daily variability in river flows by limiting the flexibility of dam operators in scheduling reservoir releases concurrent with peak electricity demand.

To Greg, my adviser... thanks for everything.

ACKNOWLEDGEMENTS

TABLE OF CONTENTS

LIST OF TABLES

LIST OF FIGURES

xiv

LIST OF ABBREVIATIONS

CF – capacity factor

d_WMP – daily average wind market penetration

DA – day-ahead

DROM – daily reservoir operations model

ED – economic dispatch

EM – electricity market

EPA – US Environmental Protection Agency

EWITS – Eastern Wind Integration and Transmission Study

f_WE – forecast wind energy

FERC – Federal Energy Regulatory Commission

GW – gigawatt

GWh – gigawatt-hour

IPP – independent power producer

LSE – load serving entity

MMBtu –million British thermal units

MW – megawatt

MWh – megawatt-hour

NGCC – natural gas combined cycle

NGCT – natural gas combustion turbine

RBF – Richards-Baker flashiness index

RMF – risk mitigation factor

ROR – run of river

RT – real-time

UC – unit commitment

INTRODUCTION

On an annual basis hydroelectric dams account for a significant fraction (about 7%) of total U.S. electricity generation and roughly two-thirds of the nation's renewable electricity generation. Although these are important contributions, it is the unmatched operational flexibility and extremely low variable costs of hydroelectric dams that distinguish them as prized assets in electric power systems. Dams can increase electricity output from zero to maximum plant capacity—or decrease it by the same amount—in a matter of minutes. They are also highly efficient ($> 90\%$) at converting potential energy (hydraulic head) to electrical energy, and they entail no fuel costs.

These operating characteristics give hydroelectric dams a tremendous competitive advantage over thermal generation sources (i.e., coal, nuclear, natural gas and oil)—simply put, dams are a cleaner, cheaper and faster way to produce electricity. For more than 75 years, hydroelectric dams have been used by utilities as giant batteries: to store potential energy (reservoir inflows) when electricity demand is low, and produce electricity at maximum rates during high demand periods. This practice decreases system-wide reliance on fossil fuel-based power plants (thereby reducing emissions of CO_2 and other pollutants into the atmosphere) and lowers electricity prices. Hydroelectric dams are also used to provide emergency back-up power during unexpected de-ratings and shut downs at thermal power plants. Thus, they also play a critical role in maintaining system reliability.

Despite the critical role that hydroelectric dams play in electric power systems, they are known to have an array of negative environmental consequences for riparian ecosystems. In particular, dams block the transport of sediment and nutrients downstream, degrade downstream water quality, and radically alter natural river flow patterns downstream. Hydroelectric dams are also highly susceptible to sustained periods of low reservoir inflows, i.e., droughts. Reduced water availability limits the ability of

hydroelectric dams to help meet peak electricity demand in power systems and can cause harmful financial consequences for hydropower producers.

Over the last several decades, research in engineering, hydrology, ecology and economics has contributed to an improved understanding of the tradeoffs that exist between the benefits of hydroelectric dams and their environmental impacts, and has begun to explore the vulnerability of dams (and larger electric power systems) to drought. Through the Federal dam relicensing process—and on occasion, the court system—this research has made headway in establishing management practices at dams that integrate consideration of financial goals, water availability and the protection of river ecosystems.

Nonetheless, hydropower producers face a future beset by unprecedented changes in the electric power industry, including the rapid growth of installed wind power capacity and a vastly increased supply of natural gas due to horizontal hydraulic fracturing (or "fracking"). There is also increased concern surrounding the potential for climate change to impact the magnitude and frequency of droughts. These developments may significantly alter the financial landscape for hydropower producers and have important ramifications for the environmental impacts of dams.

Hydropower is also linked to other forms of renewable energy (e.g., solar, wind), largely by virtue of its ability to complement these highly variable sources. Although the U.S. currently derives only 4% of its total electricity needs from wind power, annual wind energy production has increased 2200% since the year 2000, and in 2012 construction of wind turbines made up 43% of all new generating capacity. Incorporating wind energy into electric power systems reduces the amount of electricity needed from other generation resources, but it also requires other power plants to more frequently change power output to compensate for wind's intermittency. As such, wind power development has the potential to affect price dynamics in electricity markets and, in so doing, alter the short-term financial signals on which dam operators rely to schedule reservoir releases. Previous efforts to evaluate the potential for wind power development to impact decision making at hydroelectric dams have, however, relied mostly on pair-wise analysis of hypothetical wind-hydro projects. This approach omits consideration of the roles that both dams and wind energy play in the operation of larger electric power systems with diverse generation

2

portfolios. Chapter 1 of this doctoral dissertation presents a system-based approach for assessing the impact of large scale wind power integration of hydropower resources using an integrated reservoir-power system model. Chapter 2 explores how efforts to reduce the carbon footprint of electric power systems by using wind energy to displace fossil fuel-based generation may inadvertently yield further impacts to river ecosystems by disrupting downstream flow patterns. Due to the operational flexibility of hydropower, dams have been suggested as an ideal resource for compensating for both the variability and unpredictability of wind energy. However, coordinated use of wind and hydropower may exacerbate dams' current impacts on downstream environmental flows, i.e., the magnitude and timing of water flows needed to sustain river ecosystems.

Increased awareness of the vulnerability of hydroelectric dams to drought (along with concern about the potential for climate change to alter the frequency and magnitude of these events) has led to growing interest in risk management strategies that can reduce hydropower producers' exposure to periods of low reservoir inflows. In recent years, efforts have focused on a risk transfer tool known as "index insurance", a type of third party contract designed to compensate hydropower producers during droughts. Index insurance is designed to pay-out when values of an environmental variable (or index), such as reservoir inflows, crosses an agreed upon threshold (e.g., low flow conditions). These types of agreements have the potential to dramatically reduce the frequency of very low revenue years for hydropower producers. However, they may also be susceptible to fluctuations in peak electricity prices (i.e., changes in the value of hydropower)—in particular, those caused by price volatility in natural gas markets. Chapter 3 evaluates the need to account for changes in natural gas prices in the design of index-based financial hedging strategies that aim to protect hydropower producers against drought-related damages.

Previous efforts to reduce the impacts of hydroelectric dams on downstream river ecosystems have included the use of ramp rate restrictions, which help restore sub-daily variability in river flows by limiting the flexibility of dam operators in scheduling reservoir releases concurrent with peak electricity demand. These restrictions impose significant financial penalties on dam owners that are a function of: 1)

the "spread" (difference) between peak and off-peak electricity prices; and 2) total generation at dams (i.e., the availability of water for hydropower production). Variability in these two factors may cause significant seasonal and year-to-year fluctuations in the cost of ramp rate restrictions at dams. This variability may be particularly problematic for downstream stakeholders interested in "purchasing" environmental flow benefits (i.e., compensating a hydropower producer in exchange for the implementation of ramp rate restrictions). More recently, however, advances in gas extraction technology (i.e., horizontal hydraulic fracturing) have led to low natural gas prices. As a consequence, it may be less costly than in the past to implement ramp rate restrictions at dams. Chapter 4 of this dissertation analyzes the impact of recent low natural gas prices on the cost of implementing ramp rate restrictions at dams, and proposes a method for providing financial certainty to purchasers of environmental flow benefits by hedging against year-to-year changes in these costs.

CHAPTER 1: AN INTEGRATED RESERVOIR-POWER SYSTEM MODEL FOR EVALUATING THE IMPACTS OF WIND POWER INTEGRATION ON HYDROPOWER RESOURCES

1. INTRODUCTION

The extent to which large scale integration of wind energy in electric power systems will impact market prices, system costs and reliability may depend greatly on the availability of sources that can quickly change (or 'ramp') electricity output [1,2,3]. Due to their capacity for energy storage, low marginal costs, and fast ramp rates, hydroelectric dams are often regarded as an ideal resource for mitigating problematic issues related to wind's intermittency and unpredictability [4]. In recent years, researchers have investigated a wide range of topics concerning the coordinated use of wind and hydropower. However, few studies to date have made use of comprehensive reservoir and power system models in assessing the costs and benefits of wind-hydro projects, and the development of such models remains a limiting factor in addressing a number of unanswered questions in this area.

Previous studies of wind-hydro projects can be separated conceptually into two categories of analysis: 'pairwise' and 'system-based' [4]. Pairwise analyses evaluate the costs and benefits of wind-hydro projects operated in isolation (i.e., somewhat disconnected from other elements of a larger electric power system). Simpler examples include investigations of the capacity value [5] and firm energy costs [6,7] of wind-hydro projects. More sophisticated pairwise studies have used historical market prices to represent wind-hydro projects' connection to larger electric power systems. Examples include previous research on: the value of energy storage in wind-hydro systems [8,9]; the financial and environmental costs of dams' providing a 'wind firming' service [10]; project optimization [11]; the use of dams to

increase wind market penetration [12]; and the use of multipurpose dams to integrate wind energy [13]. Pairwise wind-hydro studies, particularly those that include some consideration of a project's system context, can offer valuable insights. However, they are generally less capable of capturing the more complex, endogenous economic and operational consequences of large scale wind integration for generators and consumers [4].

More comprehensive 'system-based' models simulate the effect of wind power integration on the workings of entire electric power systems made up of many different sizes and types of generators. As such, they offer the significant advantage of being able to simulate changes in market prices and system costs that may occur as a result of wind power integration, and then evaluate how these changes could impact the use of hydroelectric dams. However, most previous system-based wind-hydro studies have been conducted by electric power utilities, and detailed modeling information (and even results) from these studies is generally considered proprietary [4]. Examples of system-based studies from academic literature include investigations of the impacts of wind-hydro projects on: the value of wind energy [14]; and the cost of reducing CO_2 emissions [15].

Few wind-hydro studies to date have taken a system-based approach. As a consequence, significant gaps in knowledge remain as to how wind power integration may impact hydropower resources. For example: in all but a few US states, hydropower meets less than 10% of total annual electricity demand; but most (if not all) system-based wind-hydro studies have focused on 'hydro dominant' systems, in which hydropower makes up a much larger percentage of total system generation. The effects of wind power integration on dam operations may be much different in a system with relatively little hydropower capacity. There has likewise been little consideration in previous studies given to the role of market type (i.e., regulated versus competitive) in framing the incentive structure for hydroelectric dams to help integrate intermittent wind energy. In addition, no system-based study has addressed the potential for wind energy to impact environmental flows downstream of hydroelectric dams. Investigation of these topics requires models that can simulate the effects of wind power integration on hydroelectric dams

6

under a variety of structural, economic, and hydrological conditions, while also maintaining the operational complexity of interconnected reservoir and electric power systems.

At present, there are few systems-based wind-hydro studies available in the scientific literature. This work represents an attempt to begin filling this gap through the development of a systems-based modeling framework for analysis of wind power integration and its impacts on hydropower resources. The model, which relies entirely on publically available information, was developed to assess the effects of wind energy on hydroelectric dams in a power system typical of the Southeastern US (i.e., one in which hydropower makes up < 10% of total system capacity). However, the model can easily reflect different power mixes; it can also be used to simulate reservoir releases at self-scheduled (profit maximizing) dams or ones operated in coordination with other generators to minimize total system costs. The modeling framework offers flexibility in setting: the level and geographical distribution of installed wind power capacity; reservoir management rules, and static or dynamic fuel prices for power plants. In addition, the model also includes an hourly 'natural' flow component designed expressly for the purpose of assessing changes in hourly flow patterns that may occur as a consequence of wind power integration.

2. METHODS

The reservoir-power system model consists of: 1) an electricity market (EM) model; and 2) a reservoir system model. The EM model iteratively solves two linked mixed integer optimization programs, a unit commitment and economic dispatch problem, to allow a power system operator to meet fluctuating hourly electricity demand. A single iteration of the EM model and its two sub problems yields hourly market prices for a single 24 hour period.

The reservoir system model consists of: 1) an hourly natural flow model that simulates 'natural' (pre-dam) flows at dam sites; 2) a daily reservoir operations model that determines available reservoir storage for hydropower production; and 3) a hydropower dispatch model that schedules hourly reservoir

7

releases in order to maximize dam profits. Figure 1 shows a schematic of the integrated reservoir

(components shown in dark grey) and EM (components shown in light grey) model.
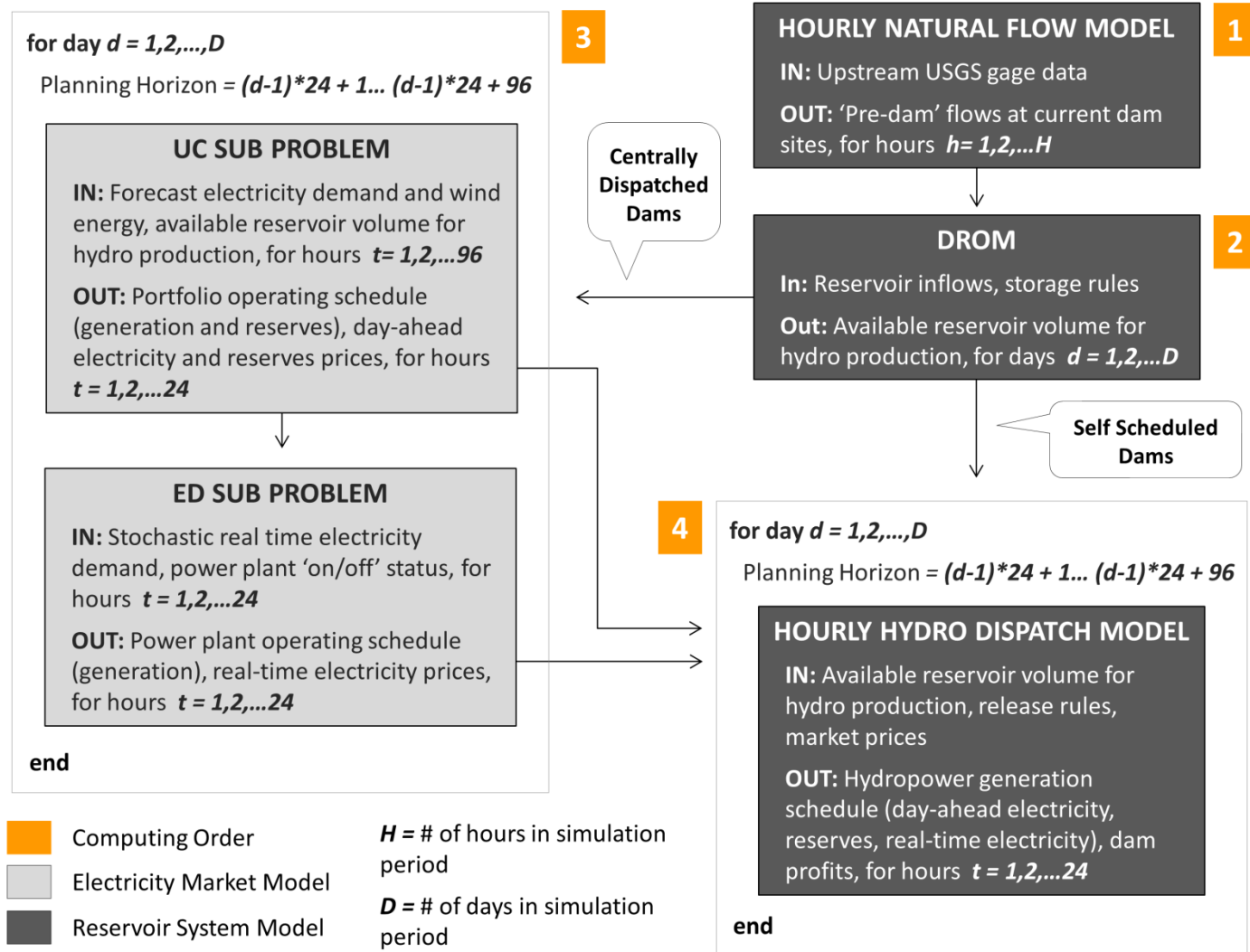
Figure 1. Conceptual framework of integrated reservoir-power system model. Orange boxes denote computing order; light grey boxes denote components of the electricity market (EM) model; and dark grey boxes denote components of the reservoir system model.

2.1 Electricity Market Model

The EM model was developed in order to simulate the operation of a large power system based on the Dominion Zone of PJM Interconnection (a wholesale electricity market located in the Mid-Atlantic region of the U.S). Dominion's total generation capacity is approximately 23 gigawatts (GW), with a peak annual electricity demand of roughly 19 GWh. Using the Environmental Protection Agency's (EPA) 2010 eGrid database, each generator in the utility's footprint was catalogued by generating capacity (MW), age, fuel type, prime mover and average heat rate (MMBtu/MWh). Specific operating constraints parameters were estimated for each size and type of plant using industry, governmental and academic sources. To reduce the computational complexity of the EM model (i.e., maintain reasonable solution times) units from each plant type were clustered by fixed and variable costs of electricity and reserves, with each cluster of similar generators forming a 'composite' plant. The total number of power plants represented in the model was reduced from 68 to a more manageable, yet representative, quantity (24)—with total system wide capacity remaining the same. Each generator in the modeled system belongs to one of eight different power plant types: conventional hydropower, pumped storage hydropower, coal, combined cycle natural gas (NGCC), combustion turbine natural gas (NGCT), oil, nuclear or biomass. Appendix 1 contains detailed operating characteristics of each plant in the modeled generation portfolio.

The EM model has two main components: 1) a unit commitment (UC) problem that represents both 'day ahead' electricity and 'reserves' markets; and 2) an economic dispatch (ED) problem that represents a 'real time' electricity market [16].

2.1.1   Unit Commitment Problem

The UC problem uses information regarding the costs (variable, fixed, and start) of participating power plants to schedule the status (on/off) and generation (MWh) at each plant in the system 24 hours in advance. The UC problem is responsible for meeting forecast 'day ahead' (DA) electricity demand and

satisfying system wide requirements for the provision of spinning and non-spinning 'reserves' (unscheduled generating capacity that is set aside for the next day as 'back up'). The objective function of the UC problem is to minimize the cost of meeting forecast electricity demand and reserve requirements over a 96 hour planning horizon, given a diverse generation portfolio:

$$\text{Minimize } Z_{UC} \ \sum_{t=1}^{96} \sum_{j}^{J} [(DA\_MWh_{t,j} * VC_j) + (ON_{t,j} * FC_j) \qquad (1)$$

$$+ \ (SRV\_MW_{t,j} * VC\_SR_j) + \ (SRV\_ON_{t,j} * FC\_SR_j) + (NRV\_MW_{t,j} * VC\_NR_j)$$

$$+ (START_{t,j} * SC_j)]$$

where, $t =$ hour in planning horizon $\in \{1,2, \dots 96\}$

$j =$ generator in system portfolio

Decision Variables:

$DA\_MWh_{t,j} =$ DA electricity scheduled in hour t at generator j (MWh)

$ON_{t,j} =$ Binary 'on/off' variable indicating DA electricity production

$SRV\_MW_{t,j} =$ Spinning reserve capacity scheduled in hour t at generator j (MW)

$SRV\_ON_{t,j} =$ Binary 'on/off' variable indicating spinning reserve provision

$NRV\_MW_{t,j} =$ Non spinning reserve capacity scheduled in hour t at generator j (MW)

$START_{t,j} =$ Binary 'on/off' variable indicating plant start

Parameters

$VC_j =$ Variable cost of DA electricity production at generator j ($/MWh)

$FC_j =$ Fixed cost of DA electricity production at generator j ($)

$VC\_SR_j =$ Variable cost of spinning reserve at generator j ($/MWh)

FC_SR_j = Fixed cost of spinning reserve provision at generator j ($)

VC_NR_j = Variable cost of non spinning reserve at generator j ($/MW)

SC_j = Start cost of generator j

Solution of the UC problem yields a preliminary hourly schedule of DA electricity generation and provision of reserves for each plant in the system over the entire planning horizon ($t = 1,2,...96$). However, only the first 24 hours of the calculated operating schedule is considered 'locked in'—scheduled generation and reserves for later hours, i.e., $t = 25, 26,... 96$, are immediately discarded. This strategy ensures that plant operating schedules are conditioned on multi-day forecast information for electricity demand, wind availability, and hydropower capacity, but it also makes sure plant operations are formally scheduled no more than 24 hours in advance. Market prices for both DA electricity and reserves for hours $t = 1,2,...24$ are then determined by the variable cost of the most expensive plant used to meet demand in each market, respectively.

2.1.2 Economic Dispatch Problem

After the UC problem is solved, the model adjusts in real time via the economic dispatch (ED) problem. The ED problem represents the operation of a 'real time' (RT) electricity market that compensates for demand forecast error, forced reductions in power plant output, and/or wind forecast errors by scheduling generation from system reserves. The objective function for the ED problem is to minimize the cost of meeting RT electricity demand over a 24 hour planning horizon ($t = 1,2,...24$) using generation capacity that was designated one day prior as reserves by the UC problem:

$$\text{Minimize } Z_{ED} : \sum_{t=1}^{24} \sum_{p}^{P} (RT\_MWh_{t,p} * VC_p) \tag{2}$$

$$+ \sum_{t=1}^{24} \sum_{n}^{N} [(RT\_MWh_{t,n} * VC_n) + (RT\_ON_{t,n} * FC_n) + (START_{t,n} * SC_n)]$$

where, t = hour in planning horizon $\in \{1, 2, \dots 24\}$

p = generator in spinning reserves portfolio

n = generator in non-spinning reserves portfolio

Decision Variables:

$RT\_MWh_{t,p}$ = RT electricity produced in hour t using spinning reserves from

generator s (MWh)

$RT\_MWh_{t,n}$ = RT electricity produced in hour t using non spinning reserves from

generator n (MWh)

$RT\_ON_{t,n}$ = Binary on/off variable indicating real time electricity production

from non spinning reserves at generator n

$START_{t,n}$ = Binary 'on/off' variable indicating plant start (non-spinning generator)

Parameters:

VC_p = Variable cost of RT electricity production at generator p ($/MWh)

VC_n = Variable cost of RT electricity production at generator n ($/MWh)

FC_n = Fixed cost of electricity production at generator n ($)

SC_n = Start cost of generator n

Solution of the ED problem yields an hourly schedule of RT electricity generation from each plant in the system's combined spinning and non-spinning reserves portfolio over the planning horizon (t = 1,2,...24). RT electricity prices are then set by the variable cost of the most expensive generator used to meet demand in each hour. After the ED problem is solved, the larger electricity market (EM) model shifts 24 hours into the future and begins its two stage process again.

13

Both the UC and ED problems are subject to a number of constraints, which can be separated conceptually into two classes: 1) constraints that enforce adherence to plant specific operating characteristics (e.g., minimum/maximum generating capacities, maximum ramp rates, minimum up/down times, etc.); and 2) constraints that apply to overall system operation (e.g., the system must always meet hourly demand for electricity and reserves). It is important to note that the EM model does not include consideration of transmission constraints and therefore assumes infinite transmission capacity on all lines. Further details regarding the EM model, including plant specific operating parameters for the modeled generation portfolio, problem constraints, and modeling assumptions, and full mathematical formulations can be found in Appendix 1 section 1.

2.1.3 Wind Development Scenarios

The EM model can represent a wide array of potential wind development pathways using hourly wind data from the Eastern Wind Integration and Transmission Study (EWITS) dataset [17]. Wind development scenarios are developed for testing by specifying a desired: 1) geographical source region(s) (e.g., Mid West, Offshore Atlantic coast, etc.); 2) wind site distribution (i.e., single or multi region); and 3) average annual wind penetration (wind energy as a fraction of total electricity demand— e.g., 5%, 15%, or 25%). After these three parameters have been specified, the EWITS database is filtered to remove wind sites outside the desired geographical region(s); then the remaining wind sites are sorted by capacity factor (CF) and selected one at a time (highest CF value first) until the product of cumulative installed wind capacity (MW) and average wind site CF (%) is equivalent to the product of target wind market penetration (%) and average annual DA electricity demand (MWh). This wind site selection algorithm inherently assumes that in order to maximize return on investment, wind power developers will first exhaust sites with higher capacity factors before installing wind turbines in areas where wind is less active. This assumption does not, however, account for the cost of transmission infrastructure, which may

make the distance between wind sites and demand centers a more important concern than capacity factor

[18].

The wind site selection algorithm yields an assembly of individually modeled wind sites, each of which is associated with two unique time series: 1) a vector of hourly DA wind energy forecasts (MWh); and 2) a vector of hourly wind forecast errors, i.e., actual minus forecast wind energy output (MWh). For a given wind development scenario, time series data are summed across all individually selected sites, yielding a pair of composite wind data vectors—the first describing total DA forecast wind energy across all selected wind sites, and the second describing total wind energy forecast error across the same collection of wind sites.

2.1.4 Day Ahead and Real Time Electricity Demand

Forecast wind energy is incorporated into the DA electricity market as 'demand reduction' by estimating hourly net demand as equal to forecast DA electricity demand (taken from historical databases maintained by PJM Interconnection) [19] minus forecast wind energy (taken from the EWITS database) (Equation 3). RT electricity demand in each hour is simulated stochastically as the sum of three different factors: 1) forced reductions in plant output; 2) demand forecast errors in the DA electricity market; and 3) wind forecast errors:

$$Net\_DA\_Demand_{s,t} = DA\_Demand_t - Wind\_For_{s,t} \tag{3}$$

$$RT\_Demand_{s,t} = \max(Dem\_Err_t + \sum_j^J Out\_Gen_{t,j} - Wind\_Err_{s,t}, 0) \tag{4}$$

where, $DA\_Demand_{s,t}$ = forecast DA electricity demand in hour t (MWh)

$Wind\_For_{s,t}$ = forecast wind energy supply for scenario s in hour t (MWh)

Dem_Err_t = DA electricity demand forecast error (actual minus forecast) in

hour t (MWh)

$Out\_Gen_{t,j}$ = Forced reduction in electricity output at generator j in hour t (MW)

$Wind\_Err_{s,t}$ = DA wind error (actual minus forecast)in hour t in scenario s (MWh)

s = wind scenario

t = hour in simulation period

j = generator in system portfolio

The ***max*** operator in Equation 4 ensures that RT electricity demand is always greater than or equal to zero, thereby disregarding cases when forecast errors can lead to negative demand. Details regarding the stochastic model used to simulate RT electricity demand are described in section 1.3 of Appendix 1.

2.1.5 Reserve Requirements

Each wind scenario tested assumes a static, baseline reserve requirement consistent with an N minus 1 criterion (i.e., the system operator must always have enough reserves to be able to compensate for the loss of its single largest generator). In addition, each scenario includes an additional dynamic reserve component set as a fixed percentage of forecast wind energy in each hour. The total hourly system reserve requirement for each scenario is then calculated as:

$$Reserve_{s,t} = NM1 + \alpha_s * WindFor_{s,t} \tag{5}$$

where, s = a given wind scenario

t = hour in simulation run

$NM1$ =static N minus 1 reserve requirement (MWh)

α_s = fixed percentage specified for wind scenario s

An approach similar to those described in [20, 21] is used to determine values of α_s. Values of α_s are selected for each scenario such that loss of load probability is equivalent to baseline conditions (i.e., system reliability is equivalent to that of a system with 0% wind market penetration). Detailed discussion of the reserve requirement calculation process, along with typical values of α_s found for different wind levels, can be found in section 1.4 of Appendix 1.

2.2 Reservoir System Model

The reservoir system model is based on a three dam cascade in the Roanoke River basin, which spans both North Carolina and Virginia (Figure 2). The reservoir system model comprises: 1) an hourly natural flow model that simulates reservoir inflows into the furthest upstream reservoir (John H. Kerr Dam), as well as natural flows at the present day site of the furthest downstream dam in the basin (Roanoke Rapids Dam); 2) a daily reservoir operations model that outputs daily volumes of reservoir storage available for hydropower production at each dam; and 3) a hydropower dispatch model that optimizes hourly reservoir releases. The hydropower dispatch model is only used to schedule releases (maximize hydropower profits) at dams that are assumed to be self-scheduled. If dams are assumed to be controlled by a central operator, they are included as generators in the EM model and scheduled in a manner consistent with the system's minimum cost objectives.
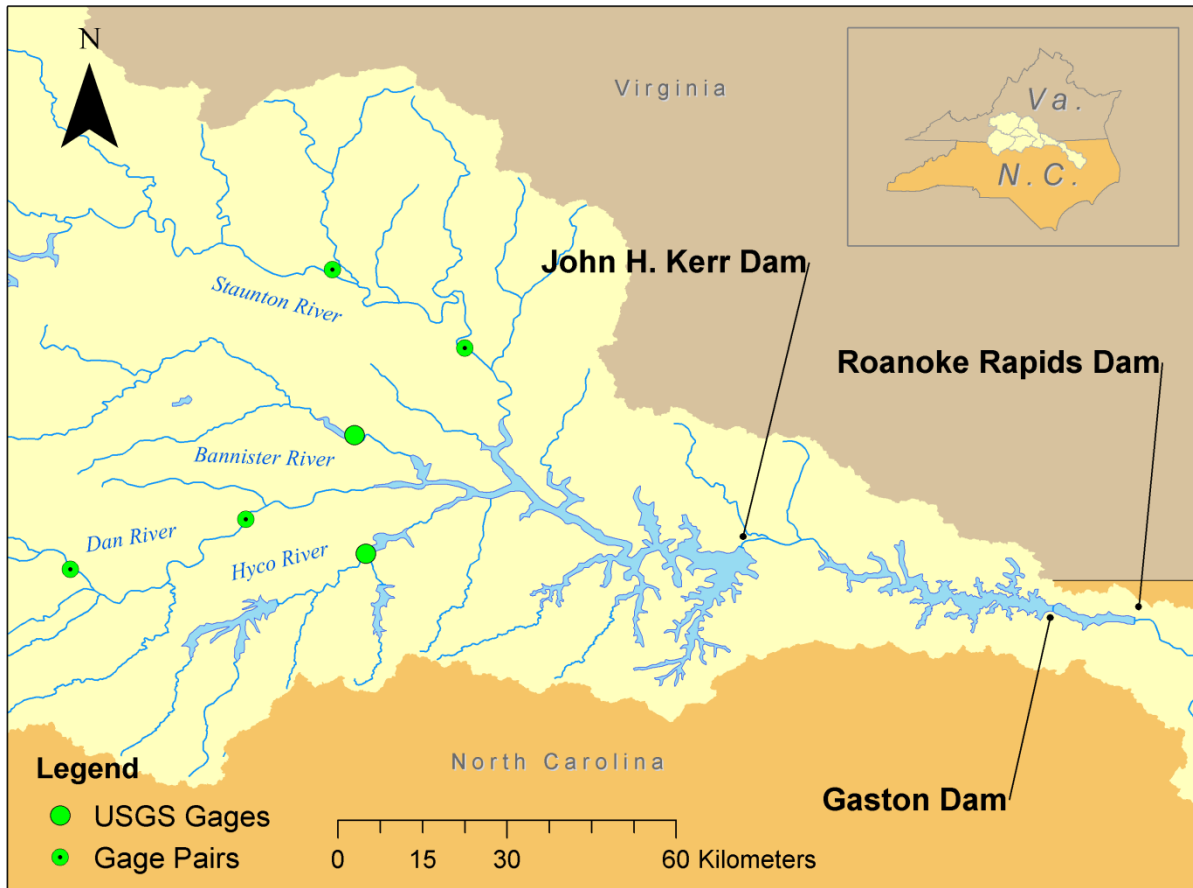
Figure 2. Three dam cascade in Roanoke River basin. USGS gages used to calculate hourly inflows at John H. Kerr reservoir and at the present day site of Roanoke Rapids Dam are shown in green.

2.2.1 Hourly Natural Flow Model

In many regions, there is considerable interest in how flow patterns below hydroelectric dams influenced by wind development would compare to flows under both baseline (0% wind) and 'natural' (pre-dam) conditions. However, despite widespread availability of historical daily flow data, no records of hourly, pre-dam flows exist for many present day dam sites. In order to simulate natural hourly flow dynamics at the sites of present day hydroelectric dams, an hourly river flow model was developed using a signal processing technique similar to that used by Knapp [22]. Details on model construction and validation can be found in section 2.1 of Appendix 1.

18

2.2.2 Daily Reservoir Operations Model

Reservoir inflows to the furthest upstream dam in the system (John H. Kerr Dam) simulated by the hourly natural flow model are fed directly to a daily reservoir operations model (DROM), which uses time series inputs of inflows, precipitation, and evaporation to drive water balance equations at all three reservoirs. The DROM calculates available storage for hydropower generation at each dam on a daily basis as a function of: reservoir guide curves (schedules of target lake elevation for each day of the calendar year); beginning of period reservoir storage values; hydropower turbine capacities; minimum flow requirements, and water supply contracts. Output from the DROM (in the form of daily volumes of water for release) is then fed to the EM model (for centrally controlled dams) or the hourly hydropower dispatch model (for self-scheduled dams) for more detailed hourly scheduling. For more information on the daily reservoir operations model (data sources, reservoir operating parameters, and model validation), please refer to Kern et al. [23].

2.2.3 Hourly Hydropower Dispatch Model

Any dam assumed to be controlled by a central system operator is scheduled by the EM model, consistent with the objective of minimizing system cost. For self-scheduled dams, however, an hourly hydropower dispatch model is used to maximize profits from the sale of DA electricity, reserves and RT electricity. The hydropower dispatch model works by iteratively solving a deterministic optimization program with the following objective function:

$$\text{Maximize Profits: } \sum_{t=1}^{96}(DA\_MWh_t * DA\_P_t) + (RV\_MW_t * RV\_P_t) \tag{6}$$
$$+ (RT\_MWh_t * RT\_P_t) - (ON_t * \text{Fixed Cost}) - (START_t * \text{Start Cost})$$

where, t = hour of planning horizon, $\in \{1, 2, \ldots 96\}$

Decision Variables:

DA_MWh_t = Electricity (MWh) sold in DA market in hour t

RV_MW_t = Capacity (MW) sold in reserves market in hour t

RT_MWh_t = Electricity (MWh) sold in RT market in hour t

ON_t = Binary 'on/off' variable indicating electricity production

$START_t$ = Binary 'on/off' variable indicating plant start

Time Series Parameters:

DA_P_t = DA electricity price in hour t ($/MWh)

RV_P_t = Reserves price in hour t ($/MWh)

RT_P_t = RT electricity price in hour t ($/MWh)

A single iteration of the hydropower dispatch model's core optimization program yields an hourly schedule of hydropower production in each market (i.e., DA electricity, reserves, and RT electricity) for hours t = 1,2,...96. However, only the first 24 hours of the proposed hydropower schedule are considered 'locked in'. Sales of electricity and reserves in other hours (t = 25,26,...96) are discarded immediately, and water associated with these discarded sales are retained as available storage. This strategy ensures that reservoir releases are conditioned on expectations of future water availability and market prices, but also makes sure that releases are formally scheduled no more than 24 hours in advance. After the hydropower dispatch model schedules reservoir releases for a single 24 hour period, the planning horizon is shifted one day into the future. The model gives the dam operator some degree of perfect foresight for future day-ahead, reserves and real-time prices. Thus, the solutions obtained are considered an upper

bound to the profits a dam would make in reality by responding to market prices. Further discussion of the hydropower dispatch model for self-scheduled hydroelectric dams (including a complete mathematical formulation) is presented in section 2.2 of Appendix 1.

3. RESULTS

In the following section, we present results on computational performance and discuss model validation of the reservoir and EM models. In addition, results from three yearlong wind development scenarios are presented in order to demonstrate the capabilities of the integrated modeling framework in evaluating the impact of wind power integration on hydropower resources.

3.1 Computing Environment and Solver Algorithm Performance

The hourly natural flow model and daily reservoir operations model were implemented in Matlab. All optimization problems (the EM and hydropower dispatch models) were formulated using the AMPL language and solved using CPLEX.

By far, the most computationally intensive component of the integrated model is the UC problem of the EM model, due to the large number of binary variables involved in its mathematical structure (three binary variables per generation unit (24), per hour (96), for a total of 6912). As such, efforts to shorten the average simulation time of the larger integrated model focused on limiting the UC model's role as a performance bottleneck. Solution times for a single iteration of the UC problem—a single iteration simulates hourly prices in the DA electricity and reserves markets for one day—were restricted to four minutes. This time restriction, which ensures that a yearlong modeling run requires roughly 24 hours of computing time (or less), was selected heuristically based on tradeoffs between model detail and solution optimality.

The solver CPLEX works by first identifying the non integer based solution of a linear program; then it employs branch and bound and simplex algorithms to identify integer based solutions whose

21

objective function values approximate that of the non integer solution. The relative degree of separation between the objective functions of integer and non integer solutions (Equation 7) can be viewed as a measure of solution optimality, and is calculated as:

$$Relative\ MIP\ Gap = \frac{OBJ_n - OBJ_i}{OBJ_n} \qquad (7)$$

where, OBJ_n = objective function value for non integer solution

OBJ_i = objective function value for integer solution

The effect of a four minute time restriction on the solver's ability to achieve optimal solutions is explored in Figure 3. A cumulative probability distribution function (CDF) was derived from relative MIP gap values observed in 19 separate yearlong simulation runs of the UC problem (each representing a different wind development scenario). Figure 3 shows that roughly 83% of all UC problem iterations were within 1% of the non integer objective function value (i.e., total system costs in $US), and 99.4% of all solutions were within 10% of the non integer objective function value. Thus, even with a time restriction of four minutes, the solver is able to closely approximate the optimal non integer solutions to the UC problem over a range of wind development scenarios.
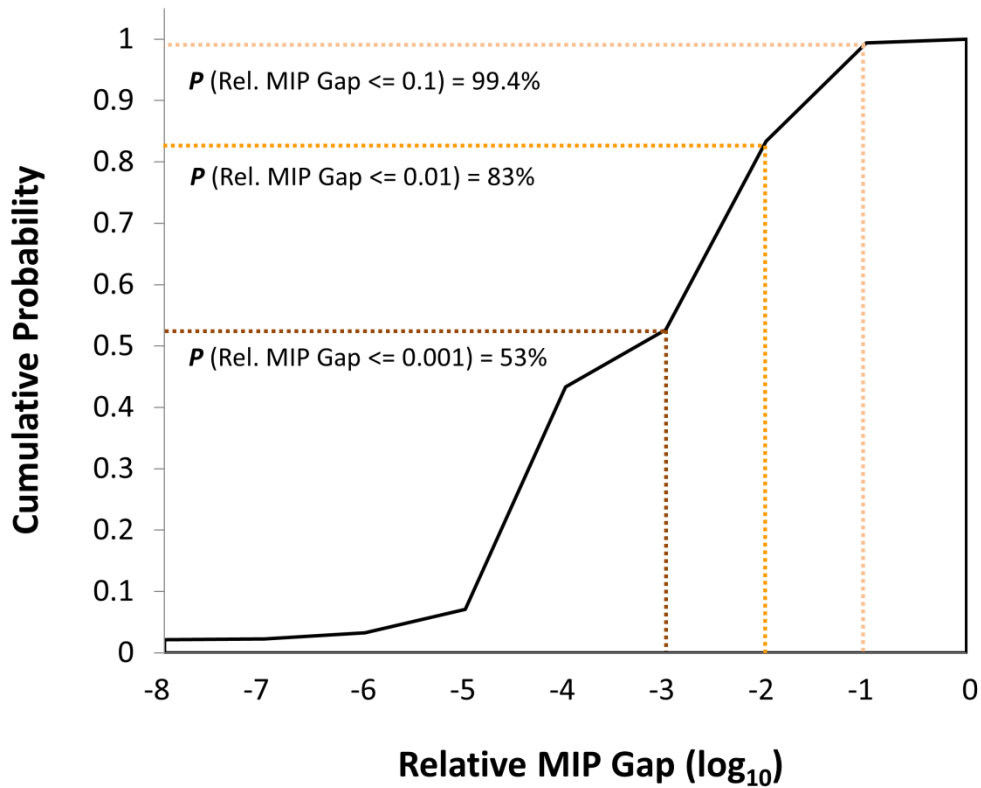
Figure 3. Cumulative probability distribution function of relative MIP gap values for the UC problem from 19 yearlong simulation runs (6935 model solutions), using a four-minute restriction on solution time by CPLEX. 83% of all individual solutions are within 1% of the optimal non-integer objective function value.

3.2 Model Validation

3.2.1 Electricity Market Model

Figure 4 compares historical mean daily prices for DA electricity in the Dominion Zone of PJM alongside prices simulated by the UC problem of the EM model for the year 2006. Panel A, which shows CDFs for both historical and simulated DA prices, suggests that the simulation underestimates most prices by between $15 and $25/MWh. This error may be due to underestimated fuel prices and plant heat rates; is also likely due to generators in Dominion's actual portfolio submitting bids to provide electricity at rates higher than their marginal costs to recoup fixed operational and start costs (or, possibly, take

advantage of market power). In panel B of Figure 4, frequency histograms are shown for historical DA electricity prices and 'corrected' prices simulated by the UC problem (i.e., simulated prices + $19/MWh). Histograms for both historical and corrected prices are mean centered on $55/MWh, but the distribution of corrected prices shows significantly more kurtosis, due to the smaller number of generating units and corresponding unique prices possible in the EM model. Nonetheless, panels B and C of Figure 4 demonstrate that the UC problem is able to accurately reproduce historical dynamics in DA electricity prices over different timescales.

The UC model also demonstrates a high degree of success in replicating the time series characteristics and statistical moments of historical reserves prices, which, compared to electricity prices, tend to be significantly much lower and less volatile (typically fluctuating between $5 and $15/MW).

RT electricity demand in the ED component of the EM model is driven by stochastic models for demand forecast error and forced unit outages; as such, no effort was made to reproduce the exact historical sequence of RT electricity prices in the Dominion Zone of PJM. However, it is worth nothing that, like historical RT electricity prices, those simulated by the ED problem tend to be lower on average (but more volatile) than DA prices. The main discrepancy between historical and simulated RT electricity prices is a higher frequency of simulated prices with a value of $0/MWh; this is due to the EM model's hourly temporal resolution, which precludes it from considering minute to minute markets for load following electricity or frequency regulation.
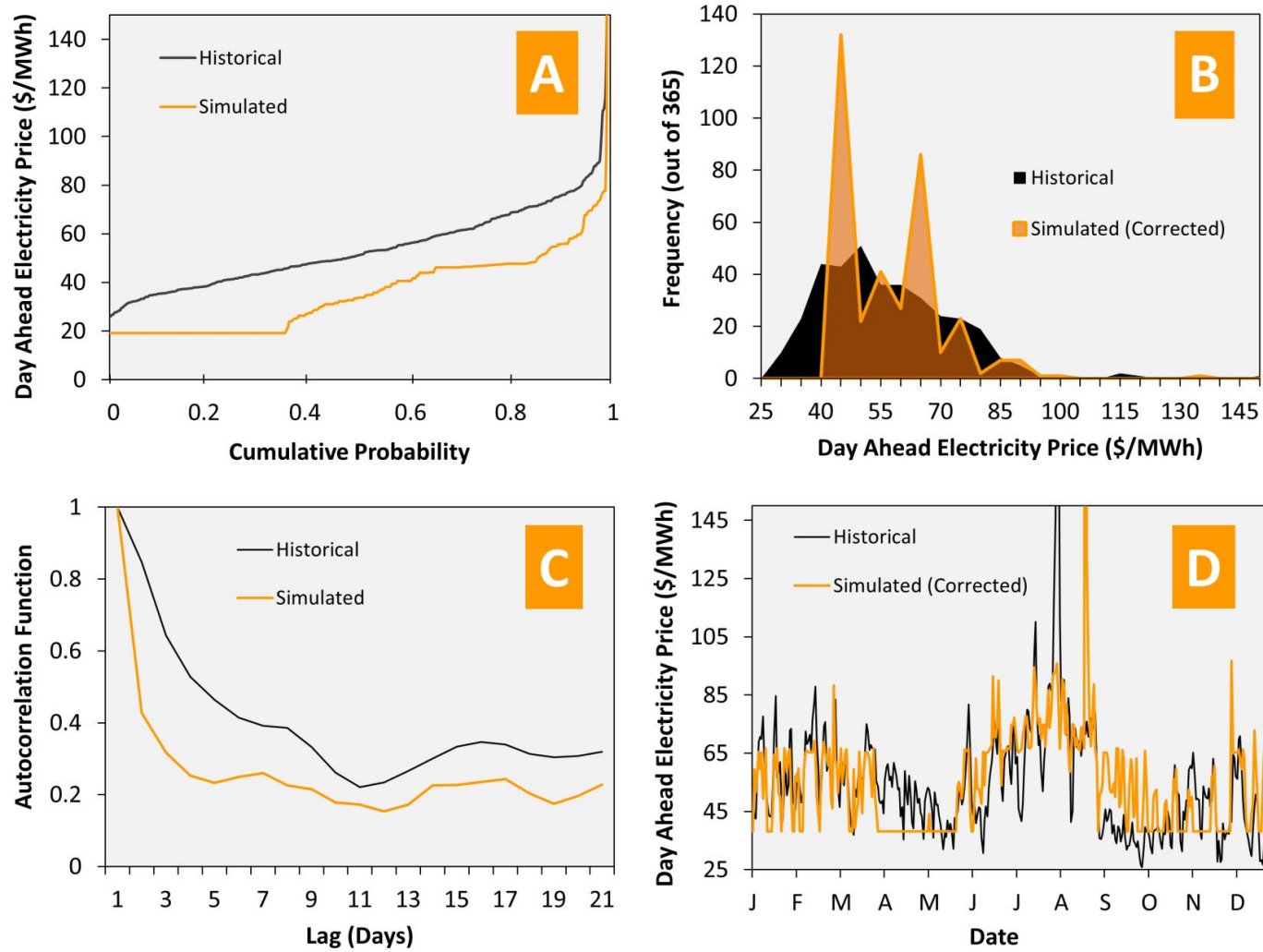
Figure 4. Validation of unit commitment problem of electricity market model. A) cumulative probability distribution functions for simulated and historical mean daily day-ahead electricity prices; B) histogram of corrected (simulated + $19/MWh) and historical mean daily day-ahead electricity prices; C) daily autocorrelation functions for simulated and historical electricity prices; D) time series of corrected and historical mean day-ahead electricity prices.

3.2.2 Reservoir System Model

The hourly natural flow model developed in order to simulate 'pre-dam' river flows and current dam sites was able to closely reproduce hourly time series characteristics of natural river flows; however, the model does underestimate total annual inflows to the three dam system by roughly 11%, because it does not account for runoff from floodplains adjacent to the river. A detailed validation of the hourly natural flow model can be found in section 2.1 of Appendix 1. The DROM, which calculates available storage for hydropower generation at each dam on a daily basis, was fully developed as part of a previous study. For details on the DROM (including data sources, reservoir operating parameters, and model validation), please refer to Kern et al. [26].

Output from the DROM (daily volumes of reservoir storage available for hydropower production) is fed to the EM model (for centrally controlled dams) or the hourly hydropower dispatch model (for self-scheduled dams) for hourly scheduling. Figure 5 compares historical hourly reservoir releases at Roanoke Rapids Dam for the year 2006 alongside releases simulated by the EM model (i.e., Roanoke Rapids Dam is assumed to be controlled by the centralized system operator). Panel A of Figure 5 shows a count of simulated and historical hourly flows compartmentalized into four quadrants: i) hours of historical 'peak' releases (i.e., reservoir discharges >= 280kL/s) that were correctly simulated as such; ii) hours of historical minimum flow releases (i.e, flows < 280kL/s) that were simulated as peak releases; iii) hours of minimum flow releases that were correctly simulated as such; and iv) hours of historical peak releases that were simulated as minimum flow releases. Approximately 80% of all simulated flows are located in quadrant (i) or (iii), i.e., they are correctly matched to historical reservoir releases. The largest source of error (accounting for roughly 15% of simulated hourly flows) is the EM model scheduling minimum flows at Roanoke Rapids Dam during hours of historical peak flow. The primary source of this error is the hourly natural flow model, which underestimates inflows to the reservoir system (and thereby reduces reservoir storage available for peak hydropower releases. Panel B of Figure 5 shows that overall, however, the reservoir system model does well at replicating typical reservoir release schedules.

26
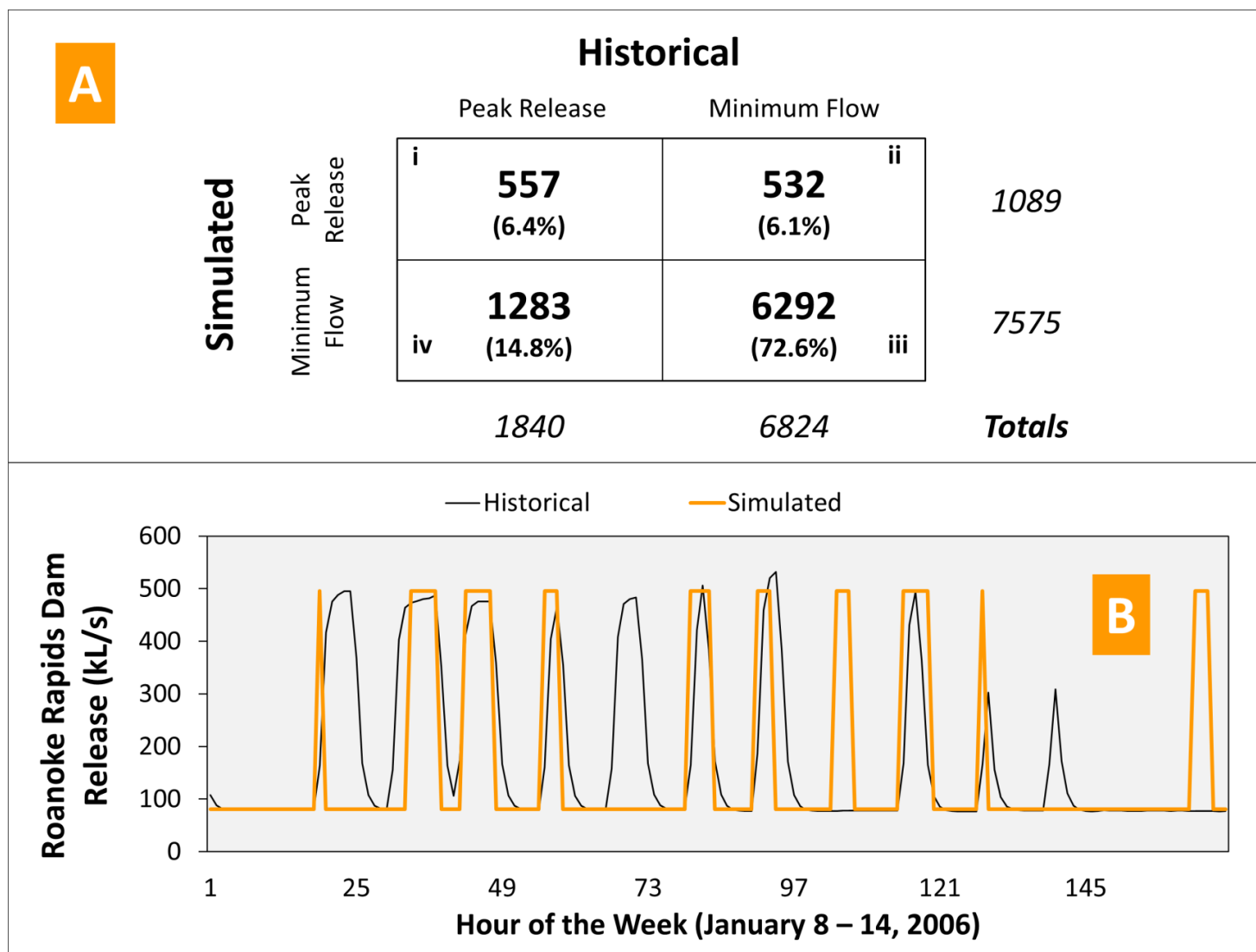
Figure 5. Comparison of historical and simulated hourly hydropower releases at Roanoke Rapids Dam. A) Historical and simulated flows presented in tabular form show the model correctly predicts hourly flows 80% of the time; B) Time-series of historical and simulated reservoir releases.

3.3 Wind Integration Case Study

The EM model was used to simulate market prices for DA and RT electricity and reserves under three different levels (0%, 5% and 25%) of average daily wind market penetration (i.e., wind energy consumed as a fraction of total electricity demand) using land based wind sites located in the Mid-Atlantic region of the US.

Figure 6 shows CDFs of mean daily prices for DA (panel A) and RT electricity (panel B), estimated from the results of a yearlong simulation that assumed average 2010 fuel prices for coal and natural gas power plants (of about $1.62/MMBtu, and $4.86/MMBtu respectively) [24]. Each panel also indicates the plant type that is dominant in setting the hourly market clearing price for each section of the CDF. Panel A shows that a modest amount (i.e., 5% market penetration) of low cost wind energy reduces the market share of combined cycle natural gas (NGCC) generators in the DA electricity market, which results in less expensive coal generators setting the market clearing price more often. At 25% wind penetration, however, the system relies much more on NGCC generators in order to accommodate lower, more volatile net electricity demand patterns and increased demand for spinning reserves; as a result, NGCC units more frequently set the market clearing price and the bottom 2/3 of the cumulative probability distribution increases in value. At the same time, 25% wind market penetration reduces the frequency of DA price spikes (e.g., especially those caused by periods of peak summer demand) associated with the use of more expensive oil and combustion turbine natural gas generators. Thus, panel A shows that the upper quartile of the DA price distribution is reduced at 25% wind penetration.

In the RT electricity market (Figure 6, panel B) wind energy has two main effects on prices: 1) positive wind forecast errors offset other sources of RT electricity demand and result in more frequent hours with a RT price of $0/MWh; and 2) negative wind forecast errors increase RT electricity demand and cause more frequent occurrences of high RT prices. Particularly at 25% market penetration, wind energy causes the bottom portion of the cumulative probability distribution function for RT prices to decrease, while the top half increases.
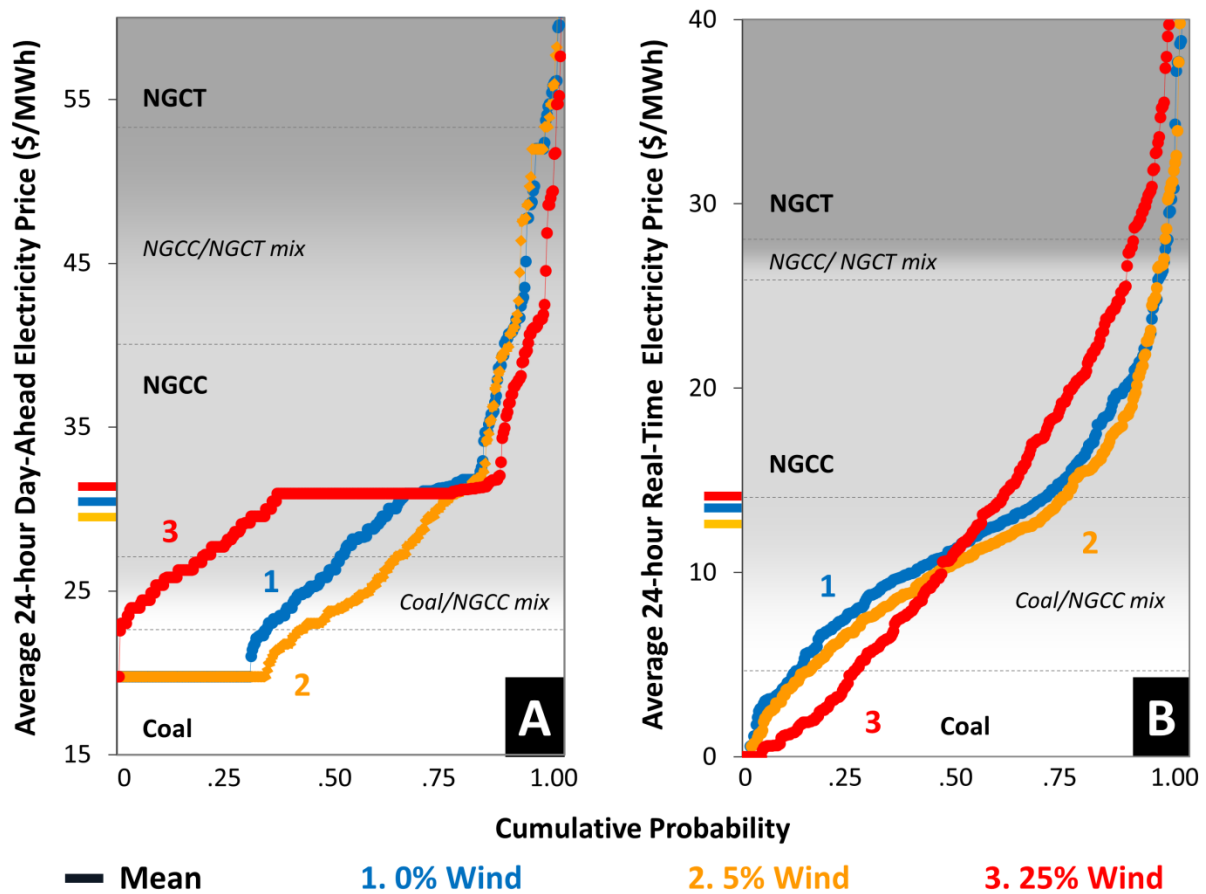
Figure 6. Cumulative probability distribution functions of DA (panel A) and real time (panel B) electricity prices at baseline (0%), 5% and 25% average daily wind market penetration. Market clearing plant types are noted at each price level.

In order to illustrate the ability of the integrated model to capture changes in dam operations and revenues as a consequence of wind power integration, results are also presented from the hydropower dispatch model under 0%, 5%, and 25% average daily wind market penetration (i.e., here Roanoke Rapids Dam is assumed to be a self-scheduled, profit maximizing entity). Figure 7 shows that at 0% wind market penetration, the ratio of total annual DA electricity to reserves sold is roughly 8:5 in favor of the DA market. At 5% wind market penetration, Roanoke Rapids Dam sells slightly more reserves and RT electricity and less DA electricity. Average prices in each market decrease due to wind energy's effect on

the market share of NGCC plants, and annual profits at the dam decrease from $US 8.13 million at baseline to $US 7.81 million at 5% wind penetration.

At 25% wind market penetration, average prices in each market increase due to increased market share of NGCC plants—and profits at the dam increase to $US 9.44 million. More severe negative wind forecast errors entice the dam to significantly increase its sale of reserves and RT electricity on an annual basis, resulting in a sales volume ratio of roughly 1:1 (DA electricity to reserves). This considerable increase in the Dam's sale of reserves may entail more 'stop/start' reservoir releases, which could negatively impact the operational efficiency and longevity of power equipment, and river flows downstream. However, further investigation is needed to develop a robust understanding of these effects on the dam from wind energy.
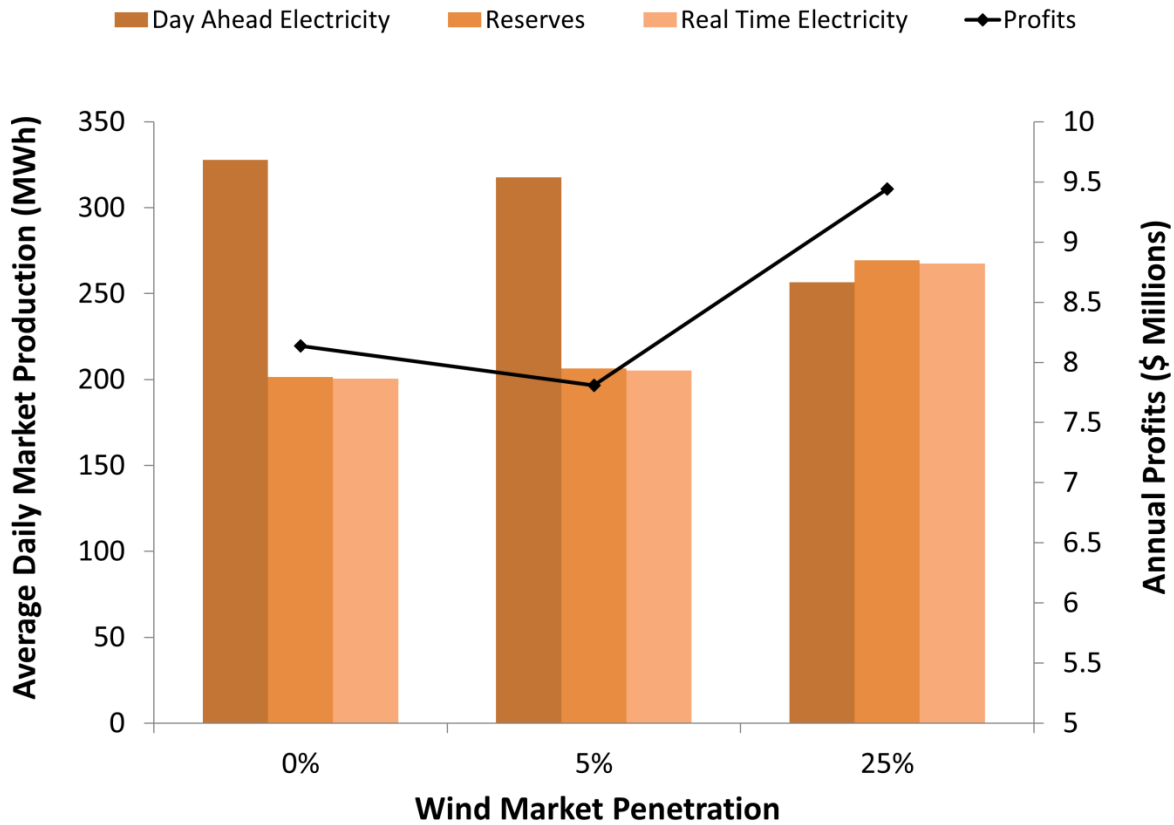
Figure 7. Impact of wind market penetration on market production (primary y-axis) and annual profits (secondary y-axis) at Roanoke Rapids Dam. Results show the dam selling significantly more reserves (and less DA electricity) at 25% wind market penetration.

4. CONCLUSIONS

Building a more complete understanding of the costs and benefits of incorporating intermittent energy resources will require comprehensive, yet transferable, modeling approaches that can be adapted to different circumstances. This paper presents an integrated reservoir-power system model specifically designed for system-based analysis of the effects of wind power integration on hydropower resources. The model relies only on publically available information from government, industry and academic sources, and model detail can be tailored to a desired solution time to accommodate available computing resources. It can incorporate a large number of assumptions regarding power system makeup and fuel

prices, wind development pathways, and reservoir management strategies. As such, it is capable of addressing many unanswered questions concerning the use of hydroelectric dams as a complement to wind energy.

REFERENCES

[1] Lund, H. 2005. Large scale integration of wind power into different energy systems. Energy 30 (13), p. 2402 2412.

[2] U.S. DOE Office of Energy Efficiency and Renewable Energy (EERE). July 2008. 20% *Wind Energy by 2030: Increasing Wind Energy's Contribution to U.S. Electric Supply*. DOE/GO 102008 2567. Washington: EERE. http://www1.eere.energy. gov/windandhydro/pdfs/41869.pdf.

[3] van Kooten, G.C. 2009. Wind power: the economic impact of intermittency. Lett. Spat. Resour. Sci. 3, 1 17.

[4] International Energy Agency. 2011. "Integration of Wind and Hydropower Systems. Volume 1: Issues, Impacts, and Economics of Wind and Hydropower Integration."

[5] Belanger, C. and Gagnon, L. "Adding wind energy to hydropower." Energy Policy 30 (2002) 1279 1284.

[6] Bakos, George. 2002. "Feasibility study of a hybrid wind/hydro power system for low cost electricity production." Applied Energy. 72, pp. 599 608.

[7] Jaramillo, O. et al. 'Using hydropower to compliment wind energy: a hybrid system to provide firm power.' Renewable Energy. 29 (2004) 1887 – 1909.

[8] Bathurst, G.N. and Strbac, G. 2003. "Value of Combining Energy Storage and Wind in Short Term Energy and Balancing Markets. Electric Power Systems Research. Vol. 67, pp. 1 8.

[9] Angarita, J.M. and Usaola, J.G. 2007. "Combining hydro generation and wind energy. Bidding and operation on electricity spot markets." Electric Power Systems Research. Vol. 77, Issues 5 6, pp. 393 400.

[10] Fernandez, Alisha, Seth Blumsack and Patrick Reed, 2012. "Evaluating Wind Following and Ecosystem Services for Hydroelectric Dams," *Journal of Regulatory Economics* 41:1, pp. 139 154. DOI: 10.1007/s11149 011 9177 9.

[11] Castronuovo, E. and Lopes, J.A. 'On the optimization of the daily operation of a wind-hydro power plant.' IEEE Transactions on Power Systems, Vol. 19, No. 3, August 2004.

[12] Matevosyan, J. et al. 'Hydropower planning coordinated with wind power in areas with congestion problems for trading on the spot and the regulating market.' Electrical Power Systems Research. 79 (2009) 39 48.

[13] Fernandez, Alisha, Blumsack, Seth, and Reed, Patrick. 2013. "Operating constraints and hydrologic variability limit hydropower in supporting wind integration." Environmental Research Letters. Vol. 8, No. 2.

[14] Vogstad, K. 2003. 'Utilising the complementary characteristics of wind power and hydropower through coordinated hydro production scheduling using the EMPS model.' Dep. Of Electrical Engineering, NTNU.

[15] Scorah, H. et al. "The economics of storage, transmission and drought: integrating variable wind power into spatially separated electricity grids." Energy Economics. 2012. Vol. 34, No. 2. pp. 536-541.

[16] Kirschen, Daniel and Strbac, Goran. Fundamentals of Power System Economics. 2004. Wiley Publishing.

[17] National Renewable Energy Laboratory. "Eastern Wind Integration and Transmission Study." 2011.

[18] Hoppock, D., and Echeverri, D. 2010. "Cost of Wind Energy: Comparing Distant Wind Resources to Local Resources in the Midwestern United States." Environmental Science and Technology. Vol. 44(22), pp. 8758 8765.

[19] PJM Interconnection. " DA Energy Market." Website. http://www.pjm.com/markets and operations/energy/ DA.aspx. Accessed October 10, 2012.

[20] EnerNex Corporation. "Final Report – 2006 Minnesota Wind Integration Study." 2006.

[21] Gooi, H.B. et al., "Optimal scheduling of spinning reserve," *IEEE Transactions on Power Systems,* vol. 14, no. 4, pp. 1485 1492, November 1999.

[22] Knapp, C. 1976. "The generalized correlation method for estimation of time delay." IEEE Transactions on Acoustics, Speech and Signal Processing. Volume 24, Issue 4. p. 320 327.

[23] Kern, J. et al. 2011. "Influence of Deregulated Markets on Hydropower Generation and Downstream Flow Regime." Journal of Water Resources Planning and Management.

[24] Energy Information Administration. Website. http://www.eia.gov. September 2012.

[25] Johnson, R., Oren, S., Svoboda, A. 1997. "Equity and Efficiency of Unit Commitment in Competitive Electricity Markets." Utilities Policy. Vol. 6, No. 1, p. 9 19.

[26] Lu, B., and Shahidehpour, M. 2005. "Unit Commitment with Flexible Generating units." IEEE Transactions on Power Systems. Vol. 20, No. 2.

[27] Institute of Electrical and Electronics Engineers (IEEE). "IEEE Reliability Test System." 1979. IEEE Transactions on Power Apparatus and Systems. Vol. PAS 98, No. 6.

[28] Energy Information Administration. "Updated Capital Cost Estimates for Electricity Generation Plants." Independent Statistics and Analysis. November 2010.

[29] Peterson, W. L., and Brammer, S. R. 1995. "A Capacity Based Lagrangian Relaxation Unit Commitment with Ramp Rate Constraints." *IEEE Transactions on Power Systems,* Vol. 10, No. 2.

[30] Kumar, N., Besuner, P., Lefton, S., Agan, D., and Hilleman, D. 2012. "Power Plant Cycling Costs." Report prepared for National Renewable Energy Laboratory and Electricity Coordinating Council by Intertek APTECH.

[31] Papavasiliou, Anthony, Shmuel S. Oren, Richard P. O'Neill. 2011. "Reserve requirements for wind power integration: A scenario based stochastic programming framework." IEEE Transactions on Power Systems, Vol. 26, No. 4, p. 2197 2206

[32] North American Electric Reliability Corporation (NERC). "2006 to 2010 Generating Unit Statistical Brochure." Website. http://www.gadsopensource.com/NERCBroc.aspx. Accessed Oct. 2012

[33] Ortega Vasquez, M., and Kirschen, D. "Optimizing the Spinning Reserve Requirements Using a Cost/Benefit Analysis." 2007. IEEE Transactions on Power Systems, Vol. 22, No. 1.

[34] North American Electric Reliability Corporation (NERC). "Reliability Concepts." Website. http://www.nerc.com/files/concepts_v1.0.2.pdf. Accessed Oct. 2012

[35] National Renewable Energy Laboratory. "Operating Reserves and Wind Power Integration: An International Comparison." 2010.

[36] California Independent System Operator (CAISO). "Spinning Reserve and Non-spinning Reserve." Website. http://www.caiso.com/docs/2003/09/08/2003090815135425649.pdf

[37] Andracsek, R. "Protecting Your Plant's Zero to 60". 2013. Power Engineering Magazine. 117(3).

[38] Aggarwal, S., Saini, L., and Kumar, A. "Electricity price forecasting in deregulated markets: A review and evaluation." 2009. Electrical Power and Energy Systems. Vol. 31, 13 22.

[39] Bruynooghe, C., Eriksson, A., and Fulli, G. 2010. "Load following operating mode at Nuclear Power Plants (NPPs) and incidence on Operation and Maintenance Costs: Compatibility with Wind Power Variability." European Commission Joint Research Centre Scientific and Technical Papers. SPNR/POS/10 03 004 Rev. 05

[40] Deane, J.P., Chiodi, A., Gargiulo, M., and O'Gallachoir, B. "Soft linking of a power systems model to an energy systems model." 2012. Energy. Vol. 42, Issue 1, p. 303 312.

[41] Fenton Jr., F. "Survey of Cyclic Load Capabilities of Fossil Steam Generating Units." 1982. IEEE Transactions on Power Apparatus and Systems. Vol. PAS 101, No. 6.

[42] Gray, D. 2001. "Correlating Cycle Duty with Cost at Fossil Fuel Power Plants." Electric Power Research Institute (EPRI) Technical Papers. 1004010.

[43] Lindsay, J., and Dragoon, K. 2010. "Summary Report on Coal Plant Dynamic Performance Capability." Prepared as part of Renewable Northwest Project.

[44] MIT Energy Initiative. 2010. "Symposium on Managing Large Scale Penetration of Intermittent Renewables." Website. http://web.mit.edu/mitei/research/reports/intermittent renewables findings.pdf

[45] Puga, J.N. 2010. "The Importance of Combined Cycle Generating Plants in Integrating Large Levels of Wind Power Generation." *The Electricity Journal*. Vol. 23, Issue 7.

[46] PR&C Renewable Power Service. "Coal Wind Integration: Strange Bedfellows May Provide a New Supply Option." December 2003. RPS – 3.

[47] PJM Interconnection. "Operating Reserves Rules Real-time Update." Market Monitoring Unit. February, 2006. Website. http://www.monitoringanalytics.com/reports/Presentations/2006/20060222-real-time-update.pdf

CHAPTER 2: THE IMPACTS OF WIND POWER INTEGRATION ON SUB-DAILY VARIATION IN RIVER FLOWS DOWNSTREAM OF HYDROELECTRIC DAMS

1. INTRODUCTION

An increased reliance on intermittent wind energy by the electric power industry has augmented the need for sources of generation that can rapidly change power output [1]. Hydroelectric dams can do this more quickly and less expensively than thermal power plants (i.e., coal, natural gas, nuclear, or oil)—as such, they are ideally suited to compensate for the variability and unpredictability of wind energy production. The operational flexibility of dams allows them to start and rapidly increase electricity production when wind is unavailable, and/or curb output when wind is plentiful [2]; and unlike thermal power plants, operating hydroelectric dams in this manner does not entail significant sacrifices in plant efficiency or additional contributions to CO_2 emissions [3]. Nonetheless, the coordinated use of wind and hydropower may exacerbate dams' current impacts on downstream environmental flows, i.e., the magnitude and timing of water flows needed to sustain river ecosystems.

Due to their operational flexibility and low variable costs, hydroelectric dams are often used as "peaking" resources; i.e., they generate electricity at maximum turbine capacity during a few high demand periods per day and release much less water during other, less valuable hours. This practice triggers large, abrupt changes in flows that have been linked to numerous negative consequences for river ecosystems, including habitat loss, altered temperature and sediment dynamics, stranding of fish and other organisms, and/or the disruption of life cycle processes [4,5,6,7,8]. However, results from previous studies on the ecosystem impacts of hydropower peaking are predicated on traditional market dynamics, i.e., predictable fluctuations in electricity demand and prices that yield 1-2 peak periods (sustained reservoir releases) per day. Very little consideration has been given to the potential impacts of

hydroelectric dams on environmental flows in systems with higher levels of intermittent wind power penetrating the market.

Two previous studies have suggested that providing an exclusive "back-up" service to wind farms could compromise a hydroelectric dam's ability to meet instantaneous minimum flow targets [9,10]; as well as increase the intensity of short-term flow fluctuations [9]. But, these studies give little attention to the larger system context in which wind and hydropower resources operate. As a result, they do not capture the effect wind power integration could have on market prices for electricity and reserves. Market prices, along with reservoir inflows, are often the primary drivers of short-term reservoir release scheduling. These previous studies also omit consideration of coal and natural gas-fired power plants, which will help bear the brunt of wind power integration in regions with limited hydropower capacity [3]; as well as the level and geographical location of wind energy production, two factors that may be critical in determining how power systems accommodate a significant influx of new wind energy [11].

This study represents an effort to more fully understand the implications of wind power integration for river ecosystems using a system-based approach. An integrated reservoir-power system modeling framework is used to: 1) explore the effects of wind energy on market prices for electricity and reserves in a system with limited (<10%) hydropower capacity under different levels of wind market penetration; and 2) show how shifting financial incentives for hydropower producers could affect reservoir release schedules and impact sub-daily flow patterns below dams.

2. METHODS

2.1 Incorporating Wind Energy in Electric Power Systems

Wholesale electricity markets generally rely on three different mechanisms to meet demand on an hourly basis: 1) a "day-ahead" electricity market; 2) a "real-time" electricity market; and 3) a "reserves" market [12]. The vast majority of electricity produced and consumed in wholesale markets is bought and sold via day-ahead markets [13,14], in which participating power plants submit "bids" (an amount of

electricity in megawatt-hours (MWh) and an offer price in $/MWh) to provide electricity 24 hours in

advance. Bids are collected by a system operator, who uses them to meet forecast electricity demand

(schedule generation) for the next day at the lowest possible cost.

In real-time electricity markets, system operators schedule smaller amounts of generation in order

to compensate for real-time electricity demand (Equation 1), calculated as the sum of positive day-ahead

demand forecast errors (Equation 2), which typically range from 1-3% [15], and forced reductions in

power plant output.

$$Real\ Time\ Demand_t = (ED_t - f\_ED_t) + Outage_t \tag{1}$$

$$Demand\ Forecast\ Error_t = \frac{(ED_t - f\_ED_t)}{ED_t} * 100 \tag{2}$$

where, t = hour of the day

ED_t = actual electricity demand in hour t (MWh)

f_ED_t = day-ahead forecast electricity demand for hour t (MWh)

$Outage_t$ = forced reduction in output at power plants in hour t (MWh)

In order to ensure that adequate generation capacity is always available to meet potential real-time

electricity demand, system operators also manage markets for reserves, or unscheduled power capacity

(MW). In reserves markets, providers are paid for each unit of capacity they leave unscheduled (with the

understanding that, should the system have a need for real-time electricity, reserved capacity may be

called upon to provide it). Reserves can be provided by power plants that are already online (i.e.,

"spinning"), provided these plants are operating below their maximum generating capacity, or by units

that are offline (i.e., "non-spinning"), assuming these plants are able to start and increase production

quickly. Although rules vary by system, a commonly used requirement is that in any given hour 50% of a system's supply of reserves should be spinning [3].

Each type of market (i.e., day-ahead electricity, real-time electricity, and reserves) is associated with a separate hourly price generally set by the variable cost of the most expensive resource used to meet demand. Price dynamics in these three markets, which constitute a critical driver of hourly reservoir release schedules at hydroelectric dams, may be significantly affected by large-scale wind integration. Due to the extremely low variable costs of wind energy, forecast wind energy is generally incorporated into day-ahead electricity markets as "demand reduction"; that is, each unit (MWh) of forecast wind energy results in a commensurate reduction in "net" day-ahead electricity demand (Equation 3). Wind energy thus yields lower (but sometimes more volatile) demand patterns for day-ahead electricity.

$$Net\ Day\ Ahead\ Demand_t = f\_ED_t - f\_WE_t \tag{3}$$

where, f_WE_t = day-ahead forecast wind energy in hour t (MWh)

The effect of wind energy on demand for real-time electricity depends largely on wind forecasting skill (i.e., the magnitude and sign of wind forecast errors in each hour (Equation 4)), with positive errors serving to reduce real-time electricity demand, and negative errors increasing it (Equation 5).

$$WindErr_t = WE_t - f\_WE_t \tag{4}$$

$$Real\ Time\ Demand_t = (ED_t - f\_ED_t) + Outage_t - WindErr_t \tag{5}$$

where, WE_t = actual wind energy in hour t (MWh)

Wind power integration also increases demand in reserves markets, with the extent of this increase dependent on the amount of installed wind capacity and the accuracy of wind energy forecasting [16,17]. In this study we employ methods similar to those used in previous studies [3,18,19] to model hourly demand for reserves dynamically as a function of forecast wind energy (Equation 6) using proportionality constants (α) calculated based on the level of installed wind power capacity (MW) in the system, as well as the accuracy of wind forecasting at modeled wind sites. For the system presented in this paper, values of α range from 4.5% at lower levels of wind capacity up to 29% at higher levels of wind capacity (see Appendix 2 for α-values used in this study).

$$Reserve\ Requirement_t = NM1 + \alpha * f\_WE_t \qquad (6)$$

where, $t =$ hour in simulation run

$NM1 =$ fixed 'N minus 1' reserve requirement (i.e., contingency against loss of largest   power plant in the system

$\alpha =$ value between 0 and 1

2.2 Implications for Hydroelectric Dams

In its simplest form, the problem of maximizing profits at a hydroelectric dam can be viewed as a choice (made in each hour) between: 1) producing day-ahead electricity; and 2) offering reserves and selling real-time electricity. Alternatively, dam operators can choose to do neither and instead retain reservoir storage until a later, more valuable time, since the operational flexibility of dams allow operators to only sell electricity and reserves in hours when they anticipate high prices.

Based on the effects of wind power integration outlined above, we hypothesize that wind energy will decrease prices for day-ahead electricity and increase prices for reserves, and that a profit maximizing dam will respond by selling less day-ahead electricity and selling more reserves and real-time

electricity. In line with this shift in strategy, we also posit that the dam will make more frequent and shorter duration reservoir releases as power production at the dam is increasingly used to compensate for negative wind forecast errors, and that this change in behavior will drive "flashier" river flows downstream.

2.3 Modeling Framework

An electricity market (EM) model is used to represent the operation of the Dominion Zone of PJM Interconnection, a 23 gigawatt (GW) electric power system in the Mid-Atlantic region of the U.S. The EM model has two main components: a unit commitment problem, which is used to conduct separate hourly markets for day-ahead electricity and reserves, and an economic dispatch problem, which is used to conduct an hourly market for real-time electricity. Each generator in the system belongs to one of eight different power plant types. Listed by fraction of total system capacity, they are: coal (34.4%), natural gas combustion turbine (NGCT) (24.3%), nuclear (15.5%), natural gas combined cycle (NGCC) (13.4%), pumped storage hydropower (6.9%), biomass (1.9%), conventional hydropower (2.1%), and oil (1.5%). The EM model was used to simulate hourly market prices for day-ahead electricity, reserves, and real-time electricity over a 1-year period (2006), under baseline conditions (0MW wind power capacity) and under 15 different wind scenarios (varying the amount and geographical source of installed wind power capacity in the system).

Simulated market prices for each scenario were then sent to a reservoir system model representing the Lower Roanoke River basin (Virginia and North Carolina, U.S.). The reservoir system model uses a deterministic optimization framework along with inputs of market prices to schedule profit-maximizing, hourly reservoir releases at Roanoke Rapids Dam (100MW), subject to operational constraints and water availability. The resultant river flows simulated under baseline conditions and under the 15 wind scenarios were then compared alongside simulated "natural" (pre-dam) flows in terms of an ecologically

relevant flow metric, the Richards-Baker Flashiness index [20], to estimate the impacts of wind energy on sub-daily flow patterns.

A complete description of the integrated reservoir-power system model used in this study can be found in [21], which details validation, data sources and full mathematical formulations of the models, as well as plant-specific operating parameters for the modeled generation portfolio, and descriptions of methodologies used to simulate hourly real-time electricity demand and dynamic reserve requirements.

2.4 Wind Scenarios

The 15 wind scenarios explored in this study represent a range of potential development pathways by varying the geographical location and level of installed wind power capacity—two key factors that could determine the impacts of wind energy on market prices [11]. Five different regions in the U.S. are considered: 1) the Southern Plains; 2) the Northern Plains; 3) the Midwest; 4) the Mid-Atlantic; and 5) offshore Atlantic Coast. For each of the five geographical regions, three levels of installed wind power capacity are considered: LOW, MED, and HIGH. These capacity levels correspond to *average annual* wind market penetrations (a_WMP) (Equation 8) of 5%, 15%, and 25%, respectively. It is important to note the difference between a_WMP and *daily* wind market penetration (d_WMP) (Equation 9), which is a dynamic value that fluctuates depending on wind availability and electricity demand.

$$a\_WMP = \frac{1}{365} \sum_1^{365} d\_WMP_d \tag{8}$$

$$d\_WMP_d = \frac{1}{24} * \sum_1^{24} \frac{FWE_t}{FED_t} \tag{9}$$

where d = day of simulation year

t = hour of day d

Hourly wind data (day-ahead wind energy forecasts and forecast errors) were taken from the updated Eastern Wind Integration and Transmission Study (EWITS) dataset made publicly available by the National Renewable Energy Laboratory [22]. Details regarding contributing U.S. states, total installed wind capacity (GW), and average capacity factors for the 15 wind scenarios can be found in Appendix 2. The algorithm used to select individual wind sites for each scenario is explored in detail in [21].

2.5 River Flow Analysis

The use of flow metrics that describe one or more general characteristics of river flows (i.e., magnitude, duration, frequency, rate-of-change, and timing) is common in efforts to quantify the impact of hydroelectric dams on the downstream environment [23,24,25,26]. In this study, the Richards-Baker flashiness (RBF) index (Equation 10), which has been used in previous efforts to characterize changes in sub-daily flows due to human influences like dams [20,27], is employed to quantify the impacts of wind power integration on downstream flows.

$$RBF_d = \frac{\sum_{i=2}^{24} 0.5(|q_{i+1} - q_i| + |q_i - q_{i-1}|)}{\sum_{i=1}^{24} q_i} \tag{10}$$

where, q_i = average river flow in hour i (kilo liters per second)

The RBF index is a value assigned to each calendar day that approximates the length of a river's hydrograph within a 24-hour period, weighted inversely by total daily discharge. As such, the RBF index is a visually intuitive measure of the frequency and magnitude of fluctuations in hourly flows, with high RBF values indicating frequent, large flow fluctuations, and low RBF values denoting relatively static flows. The RBF index is also (in hydropower systems) highly correlated with metrics used in previous studies to address the response of fish populations to changes in hourly flows, such as coefficient of variation [28] and percentage of total flow [6]; it is also moderately correlated with the number of "flow

reversals," or successive periods of increasing and decreasing flow often produced from dams' practice of hydropower peaking [29]. It is important to note, however, that while the RBF index is useful for describing changes in hourly flow patterns (some of which may be associated with direct or indirect impacts to riparian ecosystems), results presented in terms of this flow metric cannot be viewed explicitly as measures of ecological damage—only the potential for it to occur. We expect the effects of wind power integration on market prices to incentivize a hydroelectric dam to make more frequent, shorter duration reservoir releases, and anticipate that this change in behavior will lead to higher values of the RBF index.

3. RESULTS

3.1 Impacts of Wind Energy on Market Prices

Figure 8 shows expected changes in mean daily prices, relative to baseline conditions, as a function of daily wind market penetration (d_WMP), using results from all 15 wind scenarios. In general, we find that prices in all three markets move in the same direction in response to increased wind market penetration, with prices decreasing at d_WMP less than 20% and increasing at d_WMP greater than 20%. This finding does not support the hypothesis that increased wind market penetration will have opposite effects on prices for day-ahead electricity and reserves. Nonetheless, increases in real-time electricity prices at d_WMP greater than 25% are found to be considerably larger than corresponding increases in day-ahead electricity prices or reserves (see Figure 8). These large increases in real-time electricity prices are caused by more severe negative wind forecast errors, and they represent the strongest potential for wind energy to financially incentivize a change in behavior at Roanoke Rapids Dam. The following two sections give more details about how wind energy causes price changes in each market.

45
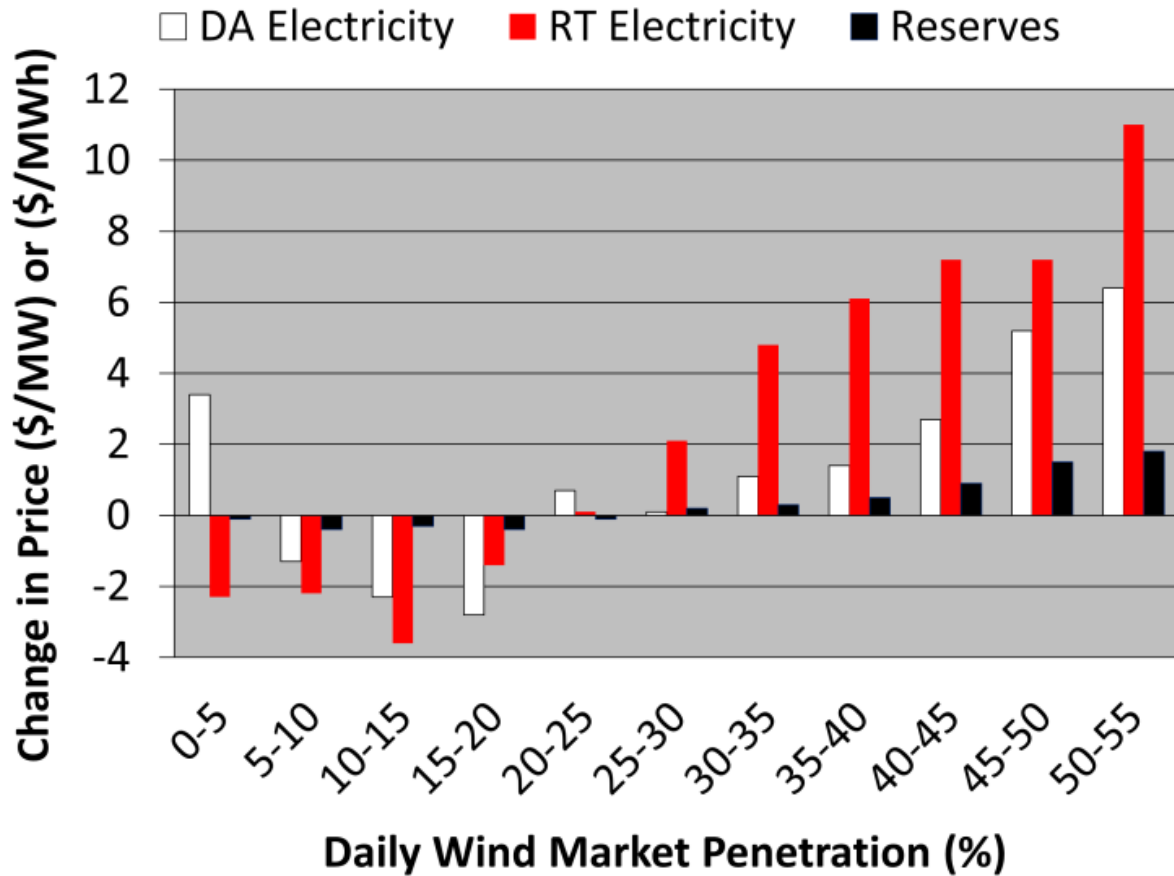
Figure 8. Expected changes in mean daily price at different levels of daily wind market penetration. Wind energy generally causes prices in all three markets to decrease at daily wind market penetration < 20%. Above this level, wind energy causes increases in prices.

3.1.1 Day-Ahead Electricity and Reserves

Figure 9 shows the modeled system's marginal cost curve for production of electricity. Under baseline conditions, market prices for both day-ahead electricity and reserves are set by either coal or natural gas combined cycle (NGCC) plants for a combined 90% of the simulation year (prices in the remaining 10% of the year set by more expensive natural gas combustion turbines or oil generators). The model assumes 2010 fuel prices for coal ($1.62/MMBtu) and natural gas ($4.86/MMBtu) [30]. With these fuel prices, NGCC plants have higher variable costs of electricity generation ($29-35/MWh) than coal plants ($14-20/MWh) (see Figure 9). NGCC plants also have more convex heat rate curves than coal

plants, which cause them to experience larger losses in efficiency when providing spinning reserves. As a result, the variable cost of spinning reserves from modeled NGCC plants ($7-9/MW) is also higher than that of coal plants ($4-6/MW).

At levels of d_WMP *below* 20%, forecast wind energy incorporated as "demand reduction" often displaces NGCC plants completely from the day-ahead electricity market (these NGCC plants would otherwise be turned on under baseline conditions). When this happens, the most common result is that less expensive coal plants become the marginal system generator and day-ahead prices decrease. Figure 9 shows a hypothetical example of how forecast wind energy can decrease day-ahead electricity prices by reducing net demand and allowing coal plants to set the market price. In the example shown, 1.5GWh of forecast wind energy reduces net demand by 10%, and the price of day-ahead electricity decreases from $26/MWh (the marginal cost of electricity from a NGCC plant) to $17/MWh (the marginal cost of electricity from a coal plant). Since demand for reserves increases as a function of forecast wind energy (see Equation 6) lower levels of d_WMP result in only modest increases in demand for reserves. If NGCC plants have been displaced from the day-ahead electricity market by wind energy (as shown in Figure 9), the system operator may also have to compensate for the loss of spinning reserves from NGCC plants, because NGCC plants cannot provide spinning reserves if they are offline. But, at lower wind market penetration the system is generally able to meet increased demand for reserves and absorb the loss of NGCC plants using less expensive coal plants and pumped storage. As a result, prices for reserves typically decrease alongside prices for day-ahead electricity.

At levels of d_WMP *above* 20%, prices for reserves and day-ahead electricity typically increase, relative to baseline conditions. High levels of d_WMP cause the system to experience very low net demand for day-ahead electricity and, simultaneously, high demand for spinning reserves. Under these circumstances, the system operator is forced to rely much more on NGCC plants. Compared to coal plants, NGCC plants have higher maximum "ramp rates", lower minimum output requirements, and lower start costs. As such, they can physically provide more reserves and are better suited to be turned on and off in response to changes in forecast wind energy under low net demand conditions. But, because

47

NGCC plants also have higher variable costs than coal plants, increased usage of NGCC plants at high

levels of d_WMP often leads to higher prices for reserves and day-ahead electricity.
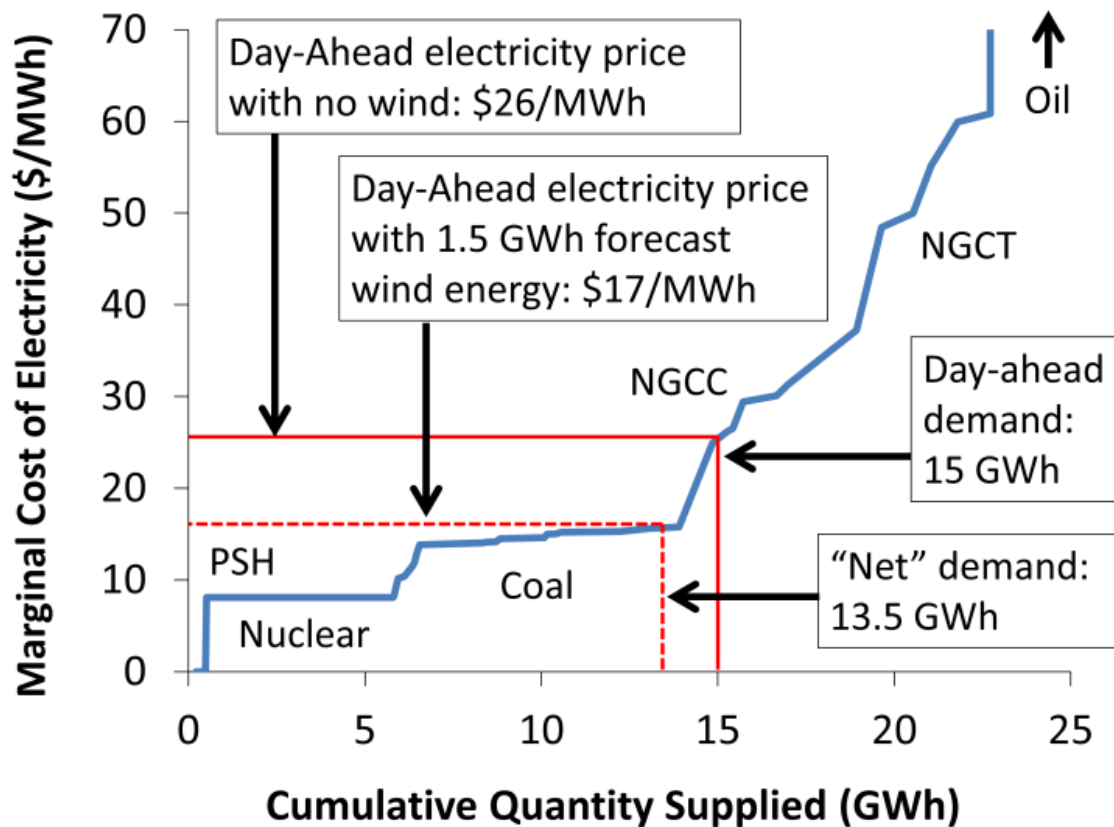
Figure 9. Effect of low-to-moderate forecast wind energy on the day-ahead electricity price. Figure shows 1.5GWh of forecast wind energy reducing "net" day-ahead electricity demand from 15GWh to 13.5GWh (10%) and the price decreasing from $26/MWh (marginal cost of electricity from a NGCC unit) to $17/MWh (marginal cost of electricity from a coal plant).

3.1.2 Real-Time Electricity

Real-time electricity prices are similarly affected by increases and decreases in the system's usage of NGCC plants. But the effect of wind energy on real-time electricity prices also depends strongly on the magnitude and sign of wind forecast errors. Panel A of Figure 10 shows the median and interquartile range (IQR) of wind forecast errors as a function of forecast wind energy (f_WE) for all 15 wind scenarios tested. This graph shows that at high levels of f_WE negative wind forecast errors (increases in real-time electricity demand) are much more likely to occur than positive wind forecast errors (reductions in real-time demand). Figure 10 also shows that the magnitude (absolute value) of negative wind forecast errors generally increases as a function of f_WE.

These two trends are due in part to the logical upper and lower bounds on the value of wind forecast errors. Panel A of Figure 10 may also reflect systematic errors in the forecasting technique used in the EWITS. Regardless, the positive relationship observed between f_WE and the frequency and severity of negative wind forecast errors has important implications for the effects of wind energy on the real-time electricity market. Panel B of Figure 10 shows probability distributions of hourly f_WE at LOW, MED and HIGH installed wind power capacity. Clearly, HIGH wind capacity is more likely to experience very large negative wind forecast errors (spikes in real-time electricity demand) than LOW and MED wind capacity. This trend explains the significant increases in real-time electricity prices observed at high levels of dWMP (see Figure 8) and likewise plays an important role in incentivizing changes in hydropower operations.
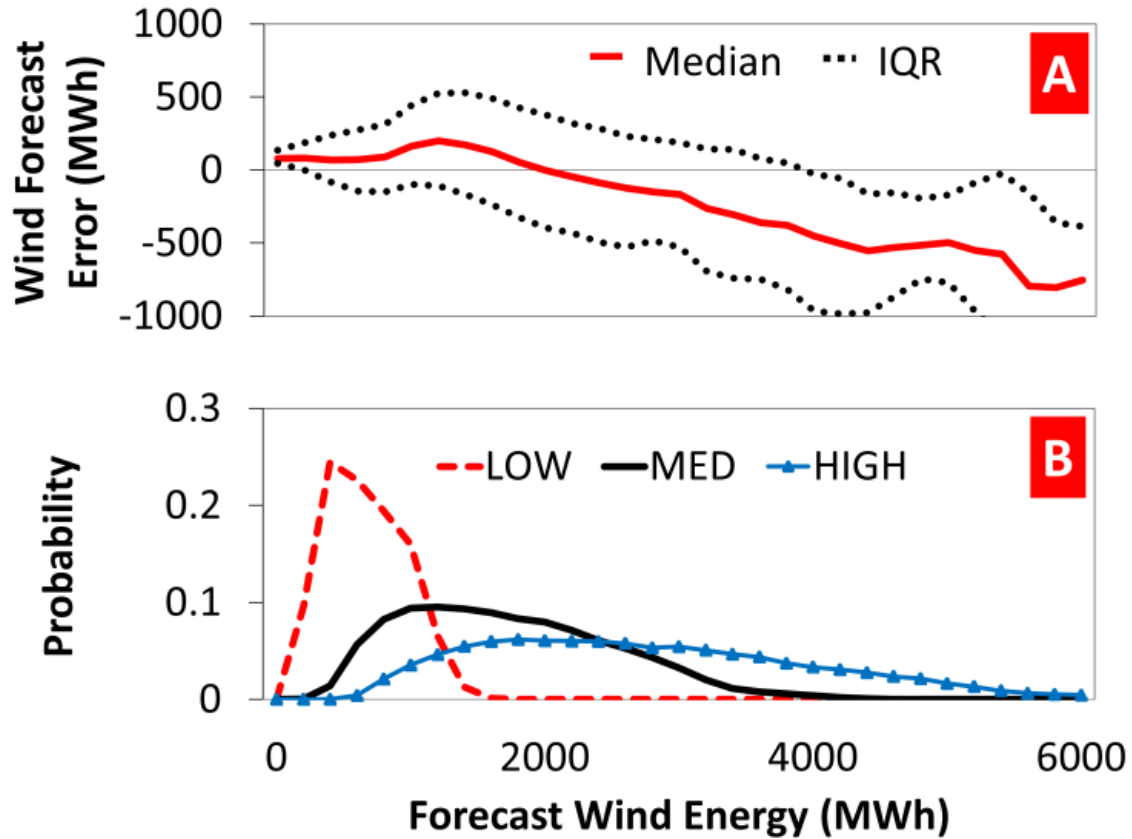
Figure 10. Wind forecast errors as a function of forecast wind energy (panel A) and probability distribution functions of forecast wind energy for each level of installed wind power capacity (panel B). Panel A shows median and IQR wind forecast errors for the 15 wind scenarios considered. Negative wind forecast errors (increases in real-time electricity demand) are much more likely to occur at HIGH wind capacity.

3.2 Impact of Market Price Changes on Dam Operations

Table 1 shows annual volumes of day-ahead electricity, reserves, and real-time electricity sold by Roanoke Rapids Dam (hereafter 'the Dam') at different levels of installed wind power capacity. Data for the wind scenarios (i.e., LOW, MED and HIGH wind capacity) are shown in terms of the average values and standard errors (in italics) for the five geographical regions tested.

We find little potential for wind power to impact the volumes of electricity and reserves sold at LOW and MED installed power capacity, due in large part to the similar manner in which prices in each market respond to increased wind market penetration. Table 1 shows that the Dam sells equivalent

amounts of day-ahead electricity and reserves at baseline conditions and LOW installed wind capacity, and only slightly less day-ahead electricity (more reserves) at MED wind capacity.

The strongest potential for wind energy to cause changes in hydropower operations occurs at HIGH wind capacity. At HIGH wind capacity the Dam sells significantly more reserves and less day-ahead electricity, relative to baseline conditions. This shift in strategy is not, however, due to any observed effects of wind energy on prices for day-ahead electricity and reserves. Rather, it reflects the increased likelihood of large negative wind forecast errors at higher levels of daily wind market penetration (see Figure 10). We find that real-time electricity price spikes caused by large negative wind forecast errors are the critical factor in incentivizing the Dam to shift capacity away from the day-ahead electricity market to reserves at HIGH wind capacity.

The Dam's decision to sell more reserves at HIGH capacity also has implications for reservoir release schedules. Table 1 shows that the expected duration of reservoir releases made at maximum turbine capacity decreases by 1.3 hours, relative to baseline conditions. Since the total volume of water passing through the dam on an annual basis is equal for each scenario, this likewise translates to more frequent reservoir releases made at turbine capacity. We also find that at HIGH wind capacity the frequency of days in which the Dam releases only static minimum flows decreases by 19, relative to baseline conditions. Collectively, these changes indicate that dam operators are scheduling hydropower production in smaller discretized amounts and spreading this production more evenly throughout the day and week, as opposed to simply concentrating production around traditional peak demand periods. This result is consistent with the Dam being used more frequently to compensate for brief periods of negative wind forecast errors, which occur somewhat randomly and are not tied to regular changes in electricity demand.

Table 1. Impacts of wind energy on dam operations and downstream flows. For the wind scenarios (i.e., LOW, MED and HIGH installed wind capacity) data are presented in terms of the means and standard errors (italics) across each of the 5 geographical regions considered.

	Installed Wind Capacity [average wind market penetration %]			
	Baseline [0%]	**LOW** [5%]	**MED** [15%]	**HIGH** [25%]
Day Ahead Electricity (GWh)	118.64	118.38 *(1.41)*	111.83 *(1.65)*	93.55 *(3.75)*
Reserves (GW)	72.90	71.50 *(1.53)*	78.72 *(1.59)*	96.94 *(3.83)*
Real Time Electricity (GWh)	72.57	71.00 *(1.53)*	78.11 *(1.63)*	96.39 *(3.88)*
Mean Reservoir Release Duration (hrs)	7.08	6.82 *(0.1)*	6.46 *(0.19)*	5.81 *(0.2)*
Static Minimum Flow Days (out of 365)	148	149.6 *(3.17)*	142.4 *(5.03)*	129 *(9.84)*
Richards Baker Flashiness (RBF) Index	0.339	0.354 *(.006)*	0.359 *(.018)*	0.404 *(.015)*

3.3 Impacts of Wind Energy on Richards-Baker Flashiness (RBF) Index

Table 1 shows that statistically significant increases (relative to baseline conditions) in the expected value of the Richards-Baker Flashiness (RBF) index occur at LOW and HIGH installed wind power capacity. The increase in the RBF index at LOW capacity occurs despite no significant difference in the volume of reserves sold by the Dam, indicating that other consequences of wind power integration (in particular, increased volatility of day-ahead electricity prices) are capable of exerting modest impacts on downstream flows, even if the Dam's annual production of day-ahead electricity and reserves remains the same. Nonetheless, the largest change in the RBF index occurs at HIGH wind capacity and is directly attributable to the Dam selling more reserves.

Figure 11 explores the link (at HIGH wind capacity) between wind market penetration, changes in the amount of reserves sold by the Dam, and changes in the RBF index. Daily RBF index values simulated under baseline conditions were subtracted from those simulated at HIGH wind capacity (Equation 11) for each of the five geographical regions considered, yielding a total of 1790 time-series data points (5 simulation runs x 358 days). These RBF index differentials ($\Delta_{RBF,d}$) were then sorted into bivariate bins according to daily wind market penetration (d_WMP) and reserve differentials (Equation 12).

$$\Delta_{RBF,d} = RBF_{HIGH,d} - RBF_{Baseline,d} \tag{11}$$

$$\Delta_{Reserves,d} = Reserves_{HIGH,d} - Reserves_{Baseline,d} \tag{12}$$

where, d = day of simulation year

$RBF_{HIGH,d}$ = RBF index value at HIGH wind capacity in day d

$RBF_{Baseline,d}$ = RBF index value under baseline conditions in day d

$Reserves_{HIGH,d}$ = reserves sold by dam under HIGH wind capacity in day d (MW)

$$Reserves_{Baseline,d} = \text{reserves sold by dam under baseline conditions in day } d \ (MW)$$

Figure 11 shows a histogram of $\Delta_{RBF.d}$ values sorted by d_WMP and reserve differentials ($\Delta_{Reserves,d}$). Cell numbers denote the frequency of simulated days (out of 1790) contained in each bivariate bin (empty cells have a frequency of zero), and cell coloration indicates the expected value of $\Delta_{RBF,d}$ for each bin. Red cells, which indicate an expected increase in the RBF index ($E[\Delta_{RBF,d}] > 0$), account for 89% of the days in which the Dam sells more reserves ($\Delta_{Reserves,d} > 0$); conversely, blue cells, which indicate an expected decrease in the RBF index ($E[\Delta_{RBF,d}] < 0$), account for 78% of the days in which the Dam sells less reserves ($\Delta_{Reserves,d} < 0$). We thus fund that, on average, increases in the Dam's daily provision of reserves *exacerbate* sub-daily variation in river flows, while decreases in reserves sold *reduce* said variation.
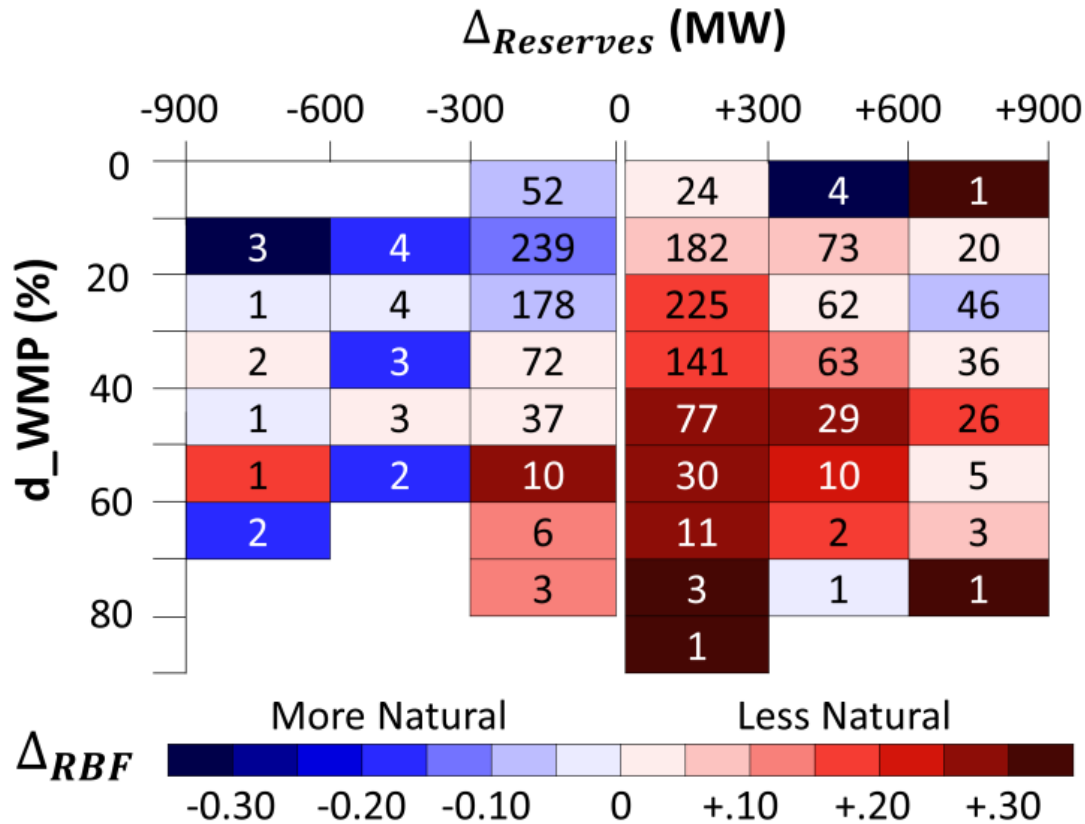
Figure 11. Relationship at HIGH installed wind capacity between wind market penetration (d_WMP), changes in the amount of reserves sold by the Dam ($\Delta_{Reserves}$), and changes in the Richards-Baker Flashiness (Δ_{RBF}) index. Cell numbers denote the frequency of simulated days contained in each bivariate bin. Those days in which the dam sells more reserves ($\Delta_{Reserves} > 0$) are strongly associated with an expected increase in the RBF index (red cells, less natural flows).

Another important question is how changes in wind market penetration impact flow patterns relative to the current impacts of the dam. Figure 12 shows a bar graph of annual expected values of the RBF index for "natural" (pre-dam) flows, baseline conditions, and the three levels of installed wind capacity tested. Figure 12 also shows the marginal impact of each scenario on the expected value of the RBF index, calculated as the difference between a given scenario and its neighbor to the left (e.g., baseline conditions minus natural flows, LOW wind capacity minus baseline conditions, etc.). Despite the potential for wind power integration (in particular, HIGH wind power capacity) to increase values of the RBF index, Figure 12 nonetheless shows that the marginal impacts of the wind scenarios are considerably

smaller than the initial change exerted on natural flows by dam construction (and the Dam's subsequent use as a peaking resource under baseline conditions). The largest impact from wind energy occurs at HIGH wind capacity, when the expected value of the RBF index increases by +0.065, relative to baseline conditions. But, this change is equivalent to a relatively small fraction of the increase in the RBF index that occurs moving from natural flows to baseline conditions (+0.328).
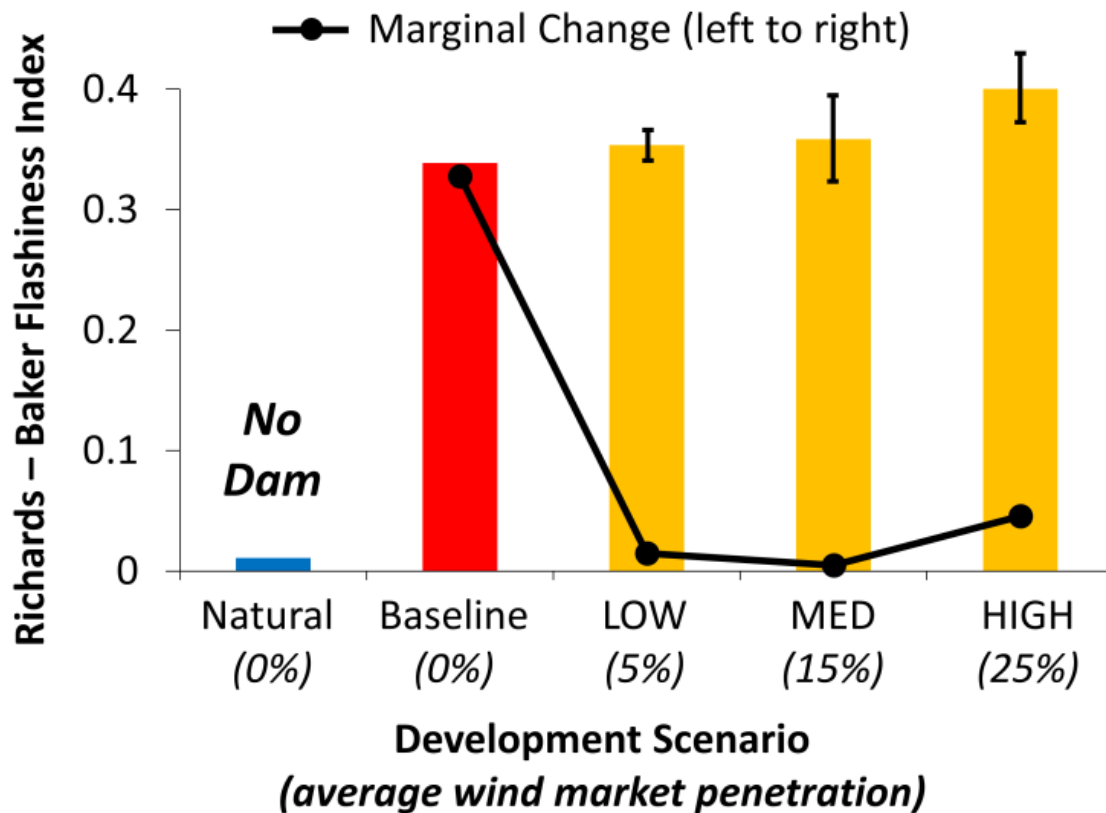
Figure 12. Impacts of wind power integration on values of the Richards-Baker Flashiness (RBF) index. Marginal changes (dotted line) are calculated as the difference between a given scenario and its neighbor to the left. Statistically significant increases in RBF index values occur at LOW and HIGH installed wind capacity, but the marginal impacts of wind energy on downstream flows are considerably lower than the impact of initial dam construction (baseline conditions).

4. CONCLUSIONS

Increased wind market penetration was expected to decrease prices for day-ahead electricity and increase prices for reserves, and incentivize a profit-maximizing hydroelectric dam to sell more reserves and less day-ahead electricity on an annual basis. We hypothesized that greater participation by dam operators in the reserves market would more directly link reservoir releases to spikes in real-time electricity prices caused by negative wind forecast errors, and that this would exacerbate existing levels of sub-daily variation in downstream flows (increase RBF index values).

Our results, however, indicate that in a power system dominated by coal and natural gas plants (assuming 2010 fuel costs), prices for day-ahead electricity and reserves decrease and increase together as a function of daily wind market penetration. Accordingly, we find limited potential for wind power integration to financially incentivize dams to sell more reserves except at HIGH wind capacity (an average annual market penetration of 25%), when large negative wind forecast errors (i.e., spikes in real-time electricity demand) are more prevalent. At HIGH wind capacity the Dam is found to sell significantly more reserves in order to exploit substantial increases in real-time electricity prices, and reservoir releases made at turbine capacity become shorter and more frequent. This, in turn, yields increased sub-daily variation in downstream flows.

It is important to note that the deterministic optimization framework used to schedule hydropower releases at the Dam gives operators perfect foresight regarding market prices, including increases in real-time prices caused by negative wind forecast errors. Although wind data used in this study (taken from the EWITS) indicate that large negative wind forecast errors are much more likely to occur at higher forecast wind energy levels, results presented in this paper should be viewed as an upper bound on the Dam's ability to take advantage of changes in market prices. Even with a heightened ability to predict real-time prices, however, we do not find that the Dam uses its capacity exclusively to provide reserves under any wind scenario (even at HIGH wind capacity, roughly half of the Dam's capacity remains in the day-ahead electricity market).

Thus, although our results confirm some potential for wind power integration to increase RBF index values (in particular, at HIGH wind capacity), the greatest marginal impacts to hourly flow patterns are shown to occur as a result of initial dam construction (and the Dam's subsequent use as a peaking resource under baseline conditions). The additional effects of wind energy on downstream flows are relatively minor, due in part to the significant degree of flow impairment that exists below the Dam under baseline conditions. Moreover, the critical role of wind forecast errors in pushing the dam to sell more reserves suggests that improvements in forecasting methods would eliminate most of the potential that does exist for wind energy to exacerbate sub-daily variation in river flows below the Dam.

A number of results from this study may be transferrable to other systems—in particular, the impacts of wind energy on market prices in fossil-fuel based systems, and the limited ability of wind energy to exacerbate dams' current impacts on hourly flows. It is likely, however, that the findings of this paper are most applicable in systems similar to the one presented in this paper. The effects of increased wind market penetration on dams in different systems, e.g., ones with significantly different generation mixes or systems in which dams are centrally controlled (scheduled to help minimize total system costs, rather than maximize hydropower revenues), could vary from the results presented in this paper. For example, in power systems that derive larger fractions of total electricity generation from hydropower (e.g., the Pacific Northwest region of the U.S.) there may be considerably less potential for wind integration to alter market prices and financially incentivize a change in operations at any one project. Alternatively, systems of dams structured as cascades (with little free flowing river between impoundments) may facilitate the designation of upstream dams as "wind-following" while allowing for better protections at downstream projects whose operations impact sensitive river ecosystems.

Another important factor that could influence the effects of wind power development on dam operations and downstream flows (albeit on larger temporal scales) is seasonal wind availability. If strong seasonal patterns in wind availability exist, then it may be beneficial to both dam owners and power system operators to alter seasonal reservoir storage strategies to reflect when hydropower is needed most (is most valuable) in accommodating the availability of wind.

REFERENCES

[1] U.S. DOE Office of Energy Efficiency and Renewable Energy (EERE). July 2008. 20% *Wind Energy by 2030: Increasing Wind Energy's Contribution to U.S. Electric Supply*. DOE/GO-102008-2567. Washington: EERE.

[2] International Energy Agency. 2011. "Integration of Wind and Hydropower Systems. Volume 1: Issues, Impacts, and Economics of Wind and Hydropower Integration."

[3] Valentino, L., Valenzuela, V., Botterud, A., Zhou, Z., and Conzelmann, G. "System-wide Implications of Increased Wind Power Penetration." 2012. Environmental Science and Technology. Vol. 46, 4200-4206.

[4] Cushman, R.M. 1985. Review of ecological effects of rapidly varying flows downstream from hydroelectric facilities. North American Journal of Fisheries Management 5: 330–339.

[5] Blinn, W., Shannon, JP., Stevens, LE., Carder, JP. 1995. Consequences of fluctuating discharge for lotic communities. Journal of the North American Benthological Society 14: 233–248.

[6] Freeman MC, Bowen ZH, Bovee KD, Irwin ER. 2001. Flow and habitat effects on juvenile fish abundance in natural and altered flow regimes. Ecological Applications 11: 179–190.

[7] Grand TC, Railsback SF, Hayse JW, Lagory KE. 2006. A physical habitat model for predicting the effects of flow fluctuations in nursery habitats of the endangered Colorado pikeminnow (Ptychocheilus lucius). River Research and Applications 22: 1125–1142.

[8] van Looy K, Jochems H, Vanacker S, Lommelen E. 2007. Hydropeaking impact on a riparian ground beetle community. River Research and Applications 23: 223–233.

[9] Belanger, C. and Gagnon, L. "Adding wind energy to hydropower." Energy Policy 30 (2002) 1279-1284.

[10] Fernandez, A., Blumsack, S. and Reed, P. 2012. "Evaluating Wind-Following and Ecosystem Services for Hydroelectric Dams," *Journal of Regulatory Economics* 41:1, pp.139-154. DOI: 10.1007/s11149-011-9177-9.

[11] Holtinnen, H., et al. 2007. "Design and operation of power systems with large amounts of wind power: State of the art report." International Energy Agency. VTT Publishing.

[12] Kirschen, Daniel and Strbac, Goran. <u>Fundamentals of Power System Economics</u>. 2004. Wiley Publishing.

[13] Monitoring Analytics, LLC. "State of the Market Report for PJM." 2011.

[14] Potomac Economics, Ltd. "2011 State of the Market Report for the ERCOT Wholesale Electricity Markets." July, 2012.

[15] GE Energy, Enernex, AWS Truewind, 2009: Technical Requirements for Wind Generation Interconnection and Integration. For ISO-New England, 118 pp.

[16] Brown, Phillip. 2012. "U.S. Renewable Electricity: How Does Wind Generation Impact Competitive Power Markets?" US Congressional Research Service.

[17] National Renewable Energy Laboratory. "Operating Reserves and Wind Power Integration: An International Comparison." 2010.

[18] EnerNex Corporation. "Final Report – 2006 Minnesota Wind Integration Study." 2006.

[19] Gooi, H.B. et al., "Optimal scheduling of spinning reserve," *IEEE Transactions on Power Systems,* vol. 14, no. 4, pp. 1485 1492, November 1999.

[20] Baker, D.B., Richards, R.P., Loftus, T.T., Kramer, J.W. 2004. "A new flashiness index: characteristics and applications to Midwestern rivers and streams." Journal of the American Water Resources Association 40: 503–522.

[21] Kern, J., et al., 2013. "An Integrated Reservoir – Power System Model for Evaluating the Impact of Wind Power Integration on Hydropower Resources." Renewable Energy. Submitted.

[22] National Renewable Energy Laboratory. "Eastern Wind Integration and Transmission Study." 2011. Website. http://www.nrel.gov/electricity/transmission/eastern_wind_dataset.html. Accessed on October 12, 2012.

[23] Richter, B. et al. 1996. "A Method for Assessing Hydrologic Alteration within Ecosystems." *Conservation Biology*. Vol. 10, No. 4. pp. 1163-1174.

[24] Pearsall, S. et al. 2005. "Adaptive Management of Flows in the Lower Roanoke River, North Carolina, USA." *Environmental Management*. Vol. 35, No.4. pp. 353-367.

[25] Matthews, R and Richter, B. 2007. "Application of the Indicators of Hydrologic Alteration Software in Environmental Flow Setting." Journal of the American Water Resources Association. Vol. 4, No. 6. pp. 1400-1413.

[26] Kern, J. et al. 2011. "Influence of Deregulated Markets on Hydropower Generation and Downstream Flow Regime." Journal of Water Resources Planning and Management.

[27] Zimmerman, J, Letcher, B, Nislow, K, Lutz, K, Magilligan, F. 2010. "Determining the Effects of Dams on Sub-Daily Variation in River Flows at a Whole-Basin Scale." River Research and Applications. 26: 124

[28] McKinney, T., Speas, D.W., Rogers, R.S., Persons, W. 2001. Rainbow trout in a regulated river below Glen Canyon Dam, Arizona, following increased minimum flows and reduced discharge variability. North American Journal of Fisheries Management 21: 216–222.

[29] The Nature Conservancy. 2007. "Indicators of Hydrologic Alteration Version 7 User's Manual. The Nature Conservancy: Arlington, VA.

[30] Energy Information Administration. Website. http://www.eia.gov. September 2012.

CHAPTER 3: NATURAL GAS PRICE UNCERTAINTY AND THE SUCCESS OF FINANCIAL HEDGING STRATEGIES FOR HYDROPOWER PRODUCERS

1. INTRODUCTION

Conventional hydroelectric dams are associated with extremely low variable costs of electricity production and an ability to increase power output to maximum plant capacity within minutes of starting [1]. As a result, hydroelectric dams are typically operated within electric power systems as highly valuable "peaking" plants—i.e., they are used to produce electricity at maximum rates during high demand hours and produce as little as possible in other, less valuable periods. Nonetheless, extended periods of low reservoir inflows (i.e., droughts) limit the ability of hydroelectric dams to provide peak power and can impact the balance sheets of dam owners in two different ways: 1) by decreasing total generation (revenues); and/or 2) by forcing a power producer to rely on more expensive sources of electricity to compensate for lower than expected hydropower generation (i.e., increasing total costs) [2,3]. In either case, drought contributes to increased volatility in the net income streams of power producers with significant hydropower capacity. This increased financial instability can in turn result in a higher cost of capital, reductions in shareholder value (for publically traded companies), difficulty paying off existing debt, and in extreme cases, even bankruptcy [4,5].

In recent years, "index insurance" has emerged as a potentially useful tool for mitigating the financial impacts of extreme hydrological conditions. Previous work has investigated the use of index insurance to indemnify agricultural producers [6,7,8,9,10] municipalities [11,12] and hydropower producers [13] against drought, as well as protect communities against losses associated with flooding [14]. Unlike conventional insurance, which guarantees a payout to policyholders in the event of a loss, index insurance makes payouts based on levels of an environmental variable or "index". The index itself

62

is typically based on some form of transparent, publically available data (e.g., precipitation or streamflows). Structuring insurance contracts to pay out based on such an index reduces transaction costs for insurers and policyholders, and it also limits concerns over moral hazard while reducing opportunities for outright fraud [8].

In general, reservoir inflows and hydropower generation are highly correlated on seasonal and annual time scales [13]. Therefore, it is logical that index insurance for hydropower producers be based either wholly or in part on reservoir inflows (or some reasonable proxy for inflows, such as localized stream flow or precipitation totals). Such contracts are designed so that whenever hydrological conditions (as measured by the index) fall below a predetermined threshold, payouts are made to the policyholder. In recent years, risk transfer products of this type have been implemented in a small handful of systems in the U.S. and abroad [15,16]. However, apart from recent work by Foster and Characklis [13], there is little evidence that strategies for hedging against hydrological risk in hydropower production have been considered in the scientific literature. As a result, a number of critical issues remain concerning the design and use of index insurance contracts for hydropower producers. One particularly important issue that has not been explored is how the "basis risk" of such contracts (i.e., the correlation between losses experienced by the policyholder and payouts triggered by the index) may be susceptible to volatility in natural gas markets. Since peak electricity prices are generally set by the marginal cost of electricity production at natural gas plants [17], the value of hydropower generation is closely tied to the price of natural gas (high gas prices make hydropower more valuable, and low gas prices make it less valuable).

During droughts, dam owners that are contractually obligated to meet their customers' electricity demand (known as "load serving entities" (LSEs)) must often compensate for reduced hydropower generation by purchasing electricity from another utility via the "spot" market (see Figure 13a). Since much of this generation is likely to come from natural gas plants, droughts cause LSEs with hydropower assets to experience unexpected higher costs, and this financial risk becomes much more acute *when dry periods overlap with high natural gas prices*. A well-known example of coincident drought and high gas prices causing financial hardship for LSEs is the California energy crisis of 2001, when wholesale

electricity costs soared as a result of both reduced hydropower production and high gas prices, even as revenues (retail electricity prices) remained relatively constant due to price caps [5].

On the other hand, for hydropower producers with little or no firm power commitments, i.e., independent "non-utility" power producers (IPPs), drought does not impact total costs—rather, it reduces total generation (decreases revenues). In terms of foregone hydropower revenues, droughts that coincide with higher natural gas prices (i.e., higher peak electricity prices) are likewise more costly for IPPs. High natural gas prices can, however also act as a stabilizing influence on an IPP's revenue stream in dry years (less hydropower is sold, but that generation earns a higher price). In fact, for an IPP primarily concerned about the incidence of years with extremely low revenues, *coincident drought and low natural gas prices—that is, reduced generation and low electricity prices—represent a worst case scenario* (see Figure 13b).

Failure to account for natural gas price volatility in the design of index insurance for hydropower producers (for either a LSE or an IPP) is likely to result in higher levels of basis risk (i.e., a lower correlation between losses experienced by the policyholder and contract payouts) and, accordingly, less effective mitigation of drought-related financial losses. In order to reduce basis risk, it may be desirable to explicitly tie insurance payouts to natural gas prices by employing a joint hydrologic-natural gas index. Another viable alternative (one that would also circumvent the need for a single counterparty to absorb all of a hydropower producer's financial risk) could be the use of exchange-based natural gas derivatives (i.e., put options) in conjunction with index insurance based on hydrological measures alone.

This study addresses an important gap in our knowledge of how natural gas prices affect the performance of index insurance designed to protect hydropower producers against the harmful financial impacts of drought. Using an integrated reservoir-power system model, we assess the cost-effectiveness of index insurance designed to reduce the financial exposure of a hydropower producer without firm power commitments (i.e., an IPP whose lowest annual revenues occur in dry years with low natural gas prices). Several different contract types (which vary primarily in their respective treatments of natural gas prices) are tested under three different levels of historical natural gas price volatility: low (2010-2012);

average (1997-2012); and high (2003-2005). In addition, we evaluate the potential for exchange based

natural gas derivatives (i.e., put options) to be used alongside index insurance contracts based on

hydrologic factors alone in order to reduce a hydropower producer's risk exposure. Results from this

study are meant to provide hydropower producers with a more comprehensive quantitative understanding

of how natural gas prices impact the financial risks posed by drought, along with a menu of options for

mitigating this type of exposure.
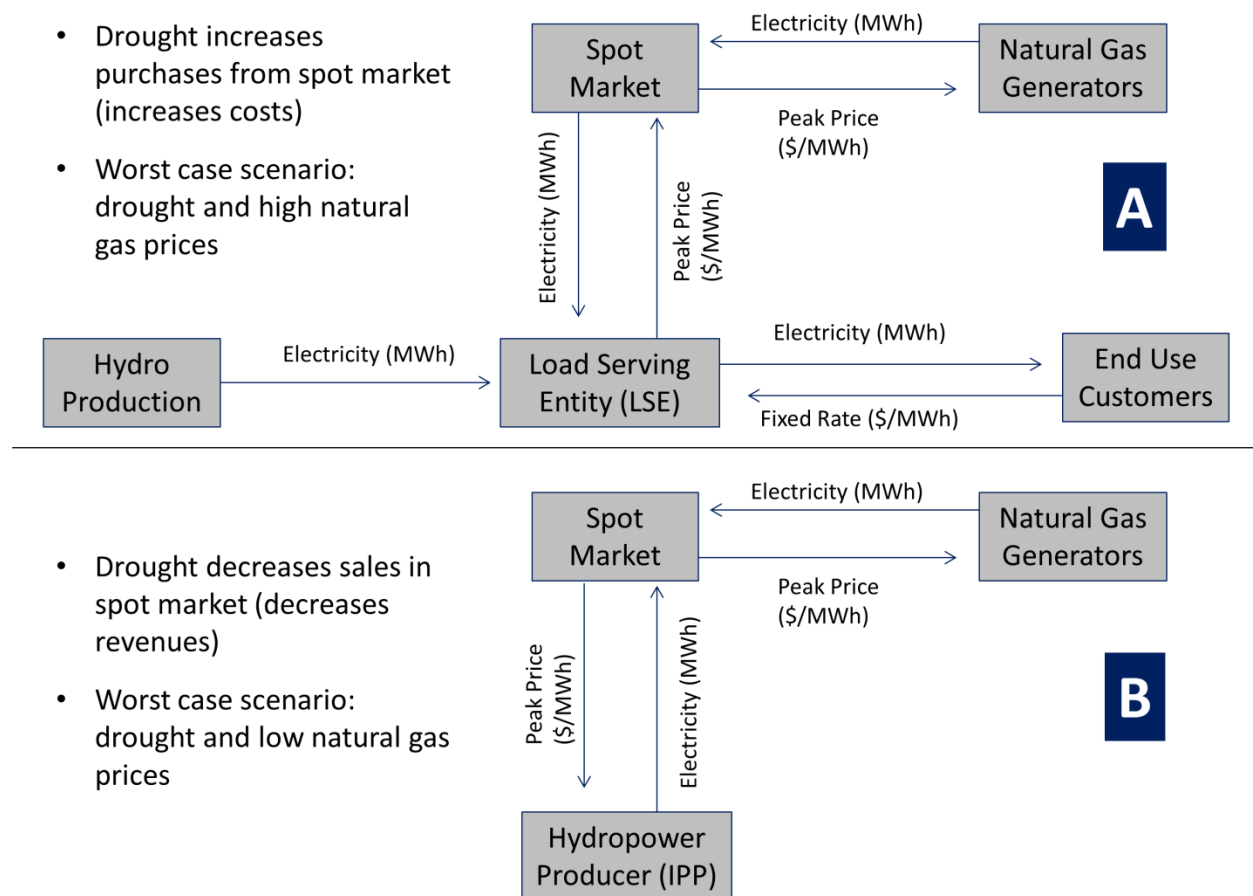
Figure 13. Power marketing setup for load serving entity (LSE) with end use customers (A) and independent power producers (IPPs) (B). For IPPs, the lowest revenues from hydropower production occur in dry years with low natural gas prices.

2. METHODS

2.1 Modeling Platform and Study Area

This study makes use of an integrated reservoir-power system modeling framework adapted from previous work by the authors [18] that simulates the simultaneous operation of a series of hydroelectric dams in the Roanoke River basin (Virginia and North Carolina, U.S.) and the Dominion Zone of PJM Interconnection, a large deregulated electricity market in the Mid-Atlantic region of the U.S. The power system model iteratively solves a mixed-integer optimization program whose objective function is to minimize the total cost of meeting peak electricity demand (MWh) using a diverse fleet of thermal generation (nuclear, coal, natural gas and oil) and hydropower (conventional and pumped storage). Power system model inputs include time-series of electricity demand, fuel prices and water availability for hydropower production, and outputs are peak electricity prices ($/MWh) for each day, determined by the marginal cost of the most expensive generator used to meet demand.

The reservoir system model uses hydrologic inputs of run-off, precipitation and evaporation, along with existing reservoir operating rules, to drive water balance equations and allocate daily volumes of water for release (hydropower production) at dams. Daily volumes of water available for hydropower production are then scheduled for release on an hourly basis using a mixed integer optimization program that maximizes revenues from the sale of electricity using market prices simulated by the power system model. A detailed description of the reservoir-power system modeling framework can be found in Kern et al. [18].

Index insurance contracts developed in this paper are designed specifically to reduce the risk exposure of John H. Kerr Dam, a project that is owned and operated by the U.S. Army Corps of Engineers. Although the operation of Kerr Dam is represented here as an IPP without firm power commitments, in reality electricity produced by Kerr Dam is marketed by the Southeastern Power Administration (SEPA), which does maintain firm power contracts with a group of Federal power

customers. However, SEPA is not required to compensate for reduced hydropower production (i.e., buy electricity from the spot market) during droughts, and their total annual costs are dominated by constant expenditures related to the amortization of debt. Thus, while Kerr Dam is not strictly speaking owned by an IPP, SEPA is, similar to an IPP, concerned about the potential for drought to diminish annual revenues (as opposed to increase its costs).

It is also important to note that although the specific hedging strategies developed in this paper are different than what would be used for LSEs, the hedging principles explored can be easily tailored to fit any power producer's unique circumstances.

2.2 Study Framework

Figure 14 shows a schematic of the study framework used in this paper. Employing synthetically generated inputs of reservoir inflows, temperature, and natural gas prices, the reservoir-power system model is used to simulate electricity prices and hydropower revenues, which are in turn used to calibrate and test four different index insurance contract types for use at Kerr Dam (contract types are described at length in section 2.3).

Pricing of index insurance contracts for hydropower producers necessitates having an accurate understanding of: 1) the probability of damaging events occurring (in this case, drought); and 2) the magnitude of losses (i.e., reductions in hydropower revenues) distributed across a range of drought conditions. Developing such an understanding requires sufficiently long records of hydrological inputs (reservoir inflows, precipitation, and evaporation), fuel prices, and temperature data (the primary driver of electricity demand). In the Roanoke River basin, however, robust statistical characterization of these three inputs is limited by a lack of historical data. Although 84 years (1929-2012) of daily reservoir inflow data exists, only 66 years (1947-2012) of daily temperature data exists, and only the most recent 20 years (1993-2012) of prices for natural gas have been recorded. Thus, at most 20 consecutive years of concurrent historical data can be used to characterize the risk exposure of hydropower producers (and

likewise, of potential insurers) in this system. Rather than rely on such a limited data set in developing hedging strategies, synthetic time-series for each input are generated.

Synthetic daily time-series data for hydrological inputs and temperature (peak electricity demand) were calculated for two 300-year periods—one 300-year period for calibrating index insurance contracts (assessing the magnitude and frequency of drought related losses) and a second for evaluating contract performance—using a method developed by Nowak et al. [19]. For each 300-year dataset of synthetic hydrological and temperature inputs, three separate 300-year time-series of weekly natural gas prices were simulated via an Ornstein-Uhlenbeck (OU) stochastic difference process (representative of low, average, and high price volatility levels). Natural gas prices have historically displayed different levels of volatility as a result of technological changes, changes in production/distribution infrastructure, more widespread demand, and unexpected disruptions in supply (see Figure 15). In this paper, low, average and high natural gas volatility levels used in the OU model are represented by the annualized standard deviations of daily log returns for the periods 2010-2012; 1997-2012; and 2003-2005, respectively. In order to isolate the impacts of natural gas price volatility on contract performance, index insurance contracts were tested at each volatility level using the same hydrological and temperature data. Details regarding the methods used to generate synthetic time-series inputs for temperature, electricity demand, hydrological inputs and natural gas prices can be found in Appendix 3.
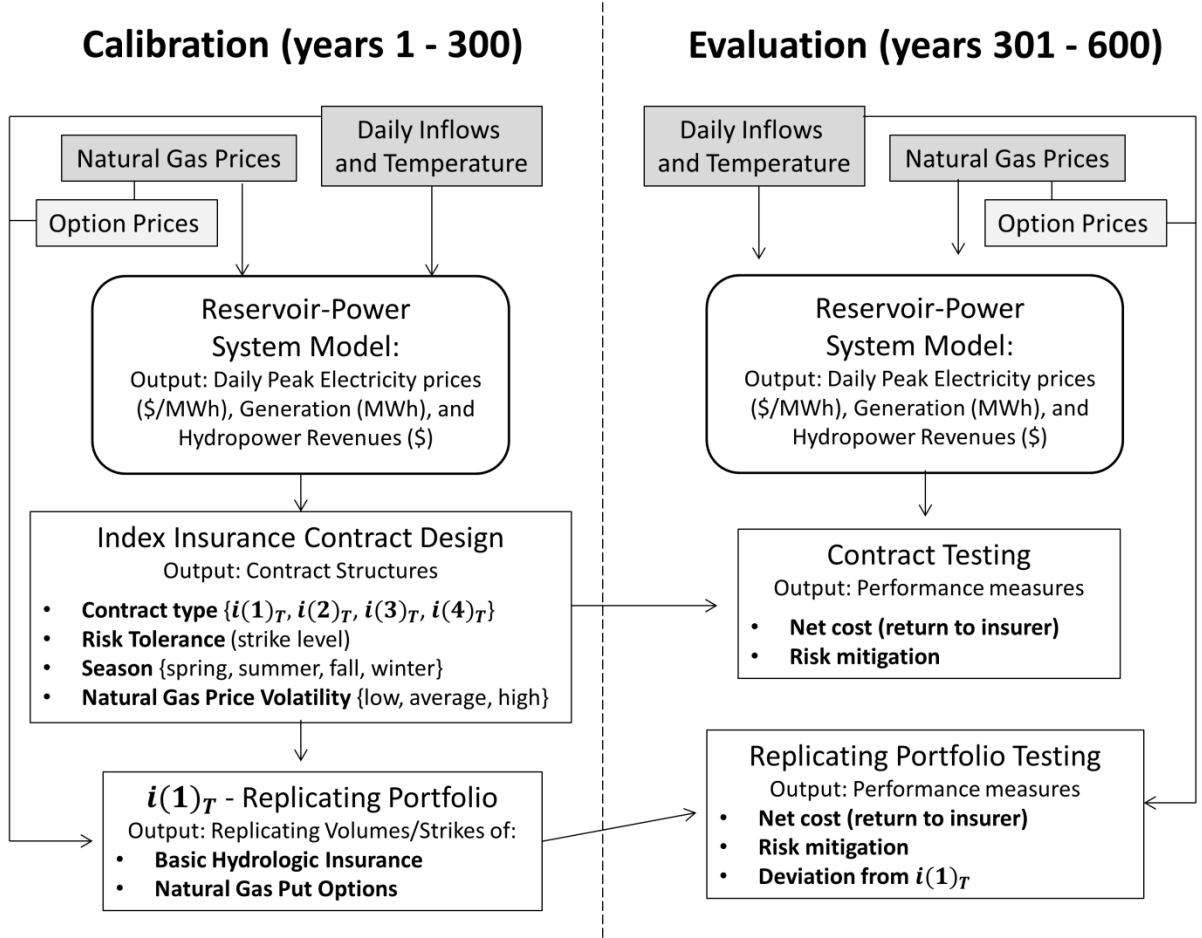
Figure 14. Schematic of study framework used in this paper. Grey boxes indicate synthetically generated system inputs.

2.3 Contract Design

All index insurance contracts considered in this paper are structured as contingent payoff functions $((H(i_T))$ that compensate a hydropower producer when the value of an agreed upon index falls below a predetermined threshold or "strike" level (Equation 1).

$$H(i_T) = \max(K - i_T, 0) \qquad (1)$$

where, K = predetermined index threshold (or "strike")

i_T = index value in coverage period T

Payoffs are not initiated until index values fall below the strike, and then compensation increases as a function of the difference $(K - i_T)$.

One of the primary challenges in establishing viable index insurance contracts is basis risk, i.e., disagreement between the underlying index and actual hydropower revenues that can lead to contract payouts occurring at the wrong time (and in the wrong quantities) and diminish the ability of insurance to mitigate a hydropower producer's risk. Ideally, the selected index (i_T) should correspond perfectly with hydropower revenues. If this is the case, then basis risk is said to minimized and the strike level (K) can be viewed as a revenue "floor", or minimum allowable revenue level; the dam owner's revenues will never be less than this floor (minus the purchase price of insurance), because if revenues drop below the strike level a commensurate insurance payment compensates for the loss.

The working assumption of this study is that the correlation between the index (i_T) and hydropower revenues (R_T) will improve if the index reflects both the amount of generation produced by a dam, as well as the value of that electricity (Equation 2).

$$R_T = \sum_{j=1}^{J} G_j * P_j \tag{2}$$

where, T = coverage period

j = hour in coverage period

G_j = hydropower generation in hour j (MWh)

P_j = peak electricity price in hour j $(\frac{\$}{\text{MWh}})$

Index insurance contracts are designed for seasonal coverage periods (T) (consecutive 3-month periods, i.e., Dec.-Feb., Mar.-May, June-Aug., and Sept.-Nov.). This is done for two reasons. First,

70

reservoir inflows at Kerr Dam are highly correlated ($R^2 = 0.94$) with total generation ($G_T = \sum_{j=1}^{J} G_j$) on a seasonal basis [13]. As such, seasonal inflows can be substituted as a good proxy for G_T in contract indices.

Besides ensuring a high correlation between reservoir inflows and generation, structuring contracts in this manner also allows for the control of seasonal changes in the peak price of electricity caused by fluctuations in electricity demand. Recent work by Foster and Characklis [13] showed that by designing index insurance contracts on a seasonal basis and assuming constant fuel prices, contracts written for any 3-month period (e.g., June-August) could reasonably assume an static seasonal peak price of electricity applicable in any year. This allowed the achievement of very high ($R^2 > 0.90$) correlations between seasonal inflows and hydropower revenues and the subsequent design index insurance contracts based solely on inflows.

However, accounting for changes in the seasonal peak price of electricity (($P_T = \frac{1}{J}\sum_{j=1}^{J} P_j$)) is in reality a more complex challenge than simply controlling for fluctuations in seasonal electricity demand. Since peak electricity prices typically correspond to the marginal cost of electricity production at natural gas power plants, fluctuations in natural gas prices have tremendous potential to cause year-to-year differences in P_T *for the same season*. Considering the degree of year-to-year variability present in historical natural gas prices over the last 20 years (see Figure 15), we hypothesize that explicitly accounting for fluctuations in gas prices may be vital in establishing an appropriate index (i_T) for use in insurance contracts. To test this hypothesis, we explore four different contracts that vary in their treatment of natural gas prices, specifically in how gas prices are incorporated in the insurance index.
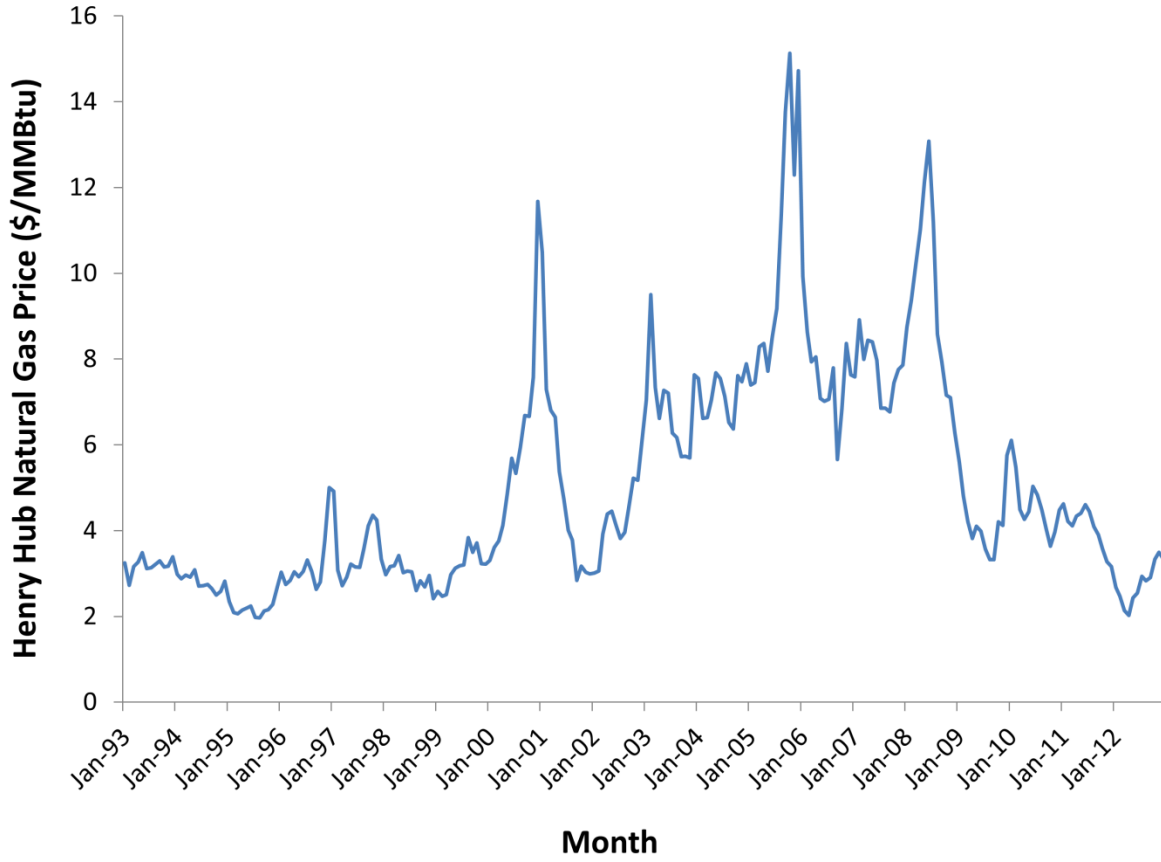
Figure 15. Monthly natural gas prices (1993-2012).

2.3.1 Explicit Consideration of Natural Gas Prices

The most comprehensive way to account for the effects of fluctuating natural gas prices on peak electricity prices is to explicitly include gas prices in the formulation of the index, such that index values (estimated hydropower revenues for a coverage period) are calculated as a linear combination of inflows and natural gas prices:

$$i(1)_T = \exp(a * \ln(F_T) + b * \ln(NGP_T) + \gamma) \tag{3}$$

where, $i(1)_T$ = index value for coverage period T

a = regression coefficient

F_T = cumulative 3 month reservoir inflows during coverage period (km^3)

b = regression coefficient

NGP_T = average 3 month price of natural gas during coverage period ($\frac{\$}{\text{MMBtu}}$)

γ = regression intercept

Multivariate regression of the index $i(1)_T$ on hydropower revenues (R_T) using ordinary least squares can then be used to identify the appropriate values of unknowns a, b, and γ. Ultimately, the degree to which the index $i(1)_T$ corresponds to seasonal hydropower revenues depends on the correlation between seasonal inflows (F_T) and generation (G_T) and the correlation between the seasonal peak electricity price (P_T) and natural gas price (NGP_T).

2.3.2 Historical Median Gas Price

The contract pricing methods used here (discussed in detail in section 2.4) assume that cumulative reservoir inflows for any given 3-month coverage period (F_T) can be considered an independent random variable. The validity of this assumption holds only if a long enough time lag is employed between contract inception and the coverage period in order to remove statistically significant levels of autocorrelation in streamflows (in the Roanoke River basin, the minimum required time lag is on the order of 4 months [13]). In this paper, we consider contracts that are initiated (signed) 1 year prior to the beginning of the coverage period, such that hydrologic conditions at the time the contract is signed are essentially independent of those experienced during the period covered by the contract.

If natural gas prices are not explicitly accounted for in the insurance index (as they are in $i(1)_T$), some prediction of future natural gas prices must then be made at the time of contract inception (i.e., contracts must assume some value of hydropower to use as a rate-of-compensation when making payouts during droughts). Three models of predicting future natural gas prices at contract inception are evaluated.

The most rudimentary of these models is an assumption that natural gas prices will not fluctuate and rather will remain fixed at the historical median level for the coverage period. Provided that natural gas prices are stationary (have a constant mean and volatility), in the long run such an assumption should overestimate seasonal peak electricity prices roughly half of the time, and underestimate prices the other half of the time. An insurance index comprising seasonal reservoir inflows and median historical natural gas prices (Equation 4) can be thus viewed as a baseline metric, one that implicitly assumes that changes in revenues are driven solely by variability in reservoir inflows.

$$i(2)_T = \exp(a * \ln(F_T) + b * \ln(NGP_{50}) + \gamma) \tag{4}$$

where, $NGP_{50} = $ historical median price of natural gas $(\frac{\$}{\text{MMBtu}})$

2.3.3 Price Parity at Contract Signing and during Coverage Period

A second, slightly more sophisticated option for predicting natural gas prices is to assume that prices in the coverage period (e.g., several months in the future) will equal prices at the time of contract signing. Although incorporating this assumption in an insurance index (as shown in Equation 5) conditions contract payouts on a lagging estimate of the price of gas, historical natural gas prices demonstrate significant levels of autocorrelation at a 12-month lag (R = .48). As a result, assuming parity between present and future gas prices should allow the index to reflect important, longer lasting changes in the value of hydropower.

$$i(3)_T = \exp(a * \ln(F_T) + b * \ln(NGP_0) + \gamma) \tag{5}$$

where, $NGP_0 = $ price of natural gas at contract signing $(\frac{\$}{\text{MMBtu}})$

2.3.4 Conditional expectation

In a third approach, conditional probabilities gathered from 2,500-year simulations of synthetic natural gas prices are used to forecast natural gas prices for the coverage period (NGP_T), given prices at contract inception (NGP_0). Because the Ornstein-Uhlenbeck (OU) model used to generate synthetic prices assumes stationarity (a constant mean and volatility), prices simulated by the model are mean-reverting. Accordingly, including the term $E[NGP_T|NGP_0]$ (i.e., the conditional expectation of gas prices in one year given the current price) in the insurance index (see Equation 6) ascribes a mean-reverting estimate of natural gas prices to the value of hydropower production. For example, if the mean natural gas price were \$5/MMBtu and the current price were \$3.50/MMBtu, then $E[NGP_T|NGP_0] > \$3.50$/MMBtu. Likewise, if the current price were \$6.50/MMBtu, then $E[NGP_T|NGP_0] < \$6.50$/MMBtu.

$$i(4)_T = \exp(a * \ln(F_T) + b * \ln(E[NGP_T|NGP_0]) + \gamma) \tag{6}$$

where, $E[NGP_T|NGP_0] = $ the expected price of natural gas in the coverage period T given the price at contract signing ($\frac{\$}{\text{MMBtu}}$)

2.4 Contract Premiums

The pricing of seasonal (3-month) contracts is performed using 300-year synthetic datasets of reservoir inflow data and natural gas prices in a manner similar to that presented in Foster and Characklis [13]. The following is a general step-by-step procedure of how contract premiums are determined.

- First, an index is selected along with a desired seasonal coverage period T (i.e, spring, summer, fall or winter).

- Premiums are calculated on an annual basis at contract signing (i.e., one year prior to the selected coverage period T).

- Each year, a distribution of possible index values (i_T) for the coverage period T is generated using a 300-year time-series of synthetic inflows from the calibration dataset, as well as some estimate of the future price of natural gas.

- Then, for a range of strike levels (percentiles of the distribution of (i_T)), a distribution of possible insurance payouts $H(i_T)$ is calculated from the distribution of (i_T) produced in the previous step.

- The empirical probability distribution of insurance payouts ($H(i_T)$) is then transformed (Equation 7) in order to account for the market price of risk [20]. This transform assigns more weight to the risk posed by large insurance payouts (rare instances when the index value is well below the predetermined strike level).

- Annual contract premiums (M_T) are then calculated as the annualized expected value of the payout function $H(i_T)$ after its density function has been altered by the Wang transform (Equation 8).

$$F^*(H(i_T)) = Q[\varphi^{-1}(F(H(i_T))) + \lambda] \tag{7}$$

where, $F^*(H(i_T))$ = risk adjusted probability density function (pdf)of payout function

Q = student T test with n degrees of freedom (n = sample size)

φ = standard normal cumulative distribution function

$F(H(i_T))$ = original pdf of payout function $H(i_T)$

λ = market price of risk

$$M_T = E[F^*(H(i_T)) *]*H(i_T) \tag{8}$$

Premiums calculated in this manner can then be said to equal an insurer's annualized expected cost of providing coverage for a hydropower producer plus an additional risk premium determined by the market price of risk (λ), which, like authors of previous studies on this subject, we assume to equal 0.25 [20,13].

Some important distinctions are made when calculating annual premiums for contracts with different indices (i.e., for contracts that make different assumptions about the price of natural gas). Premiums for contracts that use index $i(1)_T$ are based on the empirical distribution of $H(i(1)_T)$, which is made up of 90,000 values (each one representing a different combination of seasonal inflows (F_T) from the 300-year calibration dataset and 300-years of synthetic natural gas prices ($NGP_T|NGP_0$) generated via Monte Carlo simulation). In contrast, premiums for contracts based on the indices $i(2)_T$, $i(3)_T$ and $i(4)_T$) are based on empirical probability distributions of $H(i_T)$ made up of 300 possible values (one estimated future gas price and 300 seasonal inflow values).

Since contracts based on $i(2)_T$ assume a static price of natural gas (the historical median value), premiums (M_T) associated with this contract type do not change on a year-to-year basis. In contrast, contracts that include some dynamic consideration natural gas prices (i.e., ones that employ either $i(1)_T$, $i(3)_T$ or $i(4)_T$)) are associated with premiums that change each year depending on the current price of natural gas. For example, because insurance payouts are more likely to occur in drought years with low natural gas prices, premiums are higher if the price of natural gas is low at contract signing (and they are lower if the price of natural gas is high).

2.5 Contract Testing

The four contract types were then tested for a range of strike levels under low, average, and high natural gas price volatility using independently generated 300-year synthetic datasets.

Adjusted revenues accruing to the operators of Kerr Dam during each seasonal coverage period (a_R_T) were calculated as follows:

$$a\_R_T = R_T + \frac{H(i_T)}{(1+r)} - M_T \tag{9}$$

where, $r = $ risk free rate (e. g. , yield on 1 year US Treasury bond)

Note that seasonal values of hydropower revenues (R_T) and insurance premiums (M_T) are always greater than zero, whereas $H(i_T)$ is only greater than zero when payouts are triggered.

Using adjusted revenues calculated for the 300-year evaluation period, contracts were assessed in terms of their cost (reduction in mean revenues) and effectiveness (ability to reduce dam owners' exposure to incidences of very low seasonal revenues). It is important to note the distinction between the premiums associated with an insurance contract (i.e., the amount of money paid by a policyholder at regular intervals in order to receive insurance coverage) and the net cost of a contract. The net cost to the policyholder is the mean annual difference between revenues with insurance (a_R_T) and revenues without insurance (R_T). Net cost is also equivalent the total return for the insurer, i.e., the cumulative difference between insurance premiums and payouts.

$$Net\ Cost(\$) = \frac{1}{300}\sum_{T=1}^{300}(R_T - a\_R_T) = \frac{1}{300}\sum_{T=1}^{300}\left(M_T - \frac{H(i_T)}{(1+r)}\right) \tag{10}$$

This cost can also be standardized as a percentage decrease relative to (R_T).

$$Net\ Cost(\%) = \frac{\sum_{T=1}^{300}(R_T - a\_R_T)}{\sum_{T=1}^{300} R_T} \tag{11}$$

The effectiveness of index insurance contracts, in terms of their ability to mitigate financial risk, is measured as the difference between the single lowest value of R_T over the 300-year test period (i.e., the old revenue "floor" without insurance) and the single lowest value of a_R_T over the same period (i.e., the new revenue "floor" with insurance) (Equation 12). The degree of risk mitigation offered by an insurance contract can also be expressed as the ratio of the new floor divided by the old floor (Equation 13), which is henceforth referred to as the "risk mitigation factor" (RMF). An RMF value of 1 indicates no increase in the seasonal revenue floor; an RMF value of 2 indicates that the new floor is double the value of the floor without insurance; and a RMF value of 3 indicates that the new floor value is triple the value of the old floor.

$$Risk\ Mitigation\ (\$) = \min(a\_R_T) - \min(R_T), \quad T \in \{1 \dots 300\} \tag{12}$$

$$RMF = \min(a\_R_T) / \min(R_T), \quad T \in \{1 \dots 300\} \tag{13}$$

2.6 Replicating Portfolio

In addition to testing the four contract types described above, an alternative strategy that makes use of existing financial tools for mitigating risk in natural gas markets is explored. Here a hydropower producer's hydrological risk and natural gas price risk are managed separately via "replicating portfolios" made up of: 1) index insurance contracts based on reservoir inflows alone; and 2) natural gas derivatives (in particular, "put options"). In principle, this approach would circumvent the potential challenge of finding a single counterparty willing to absorb all of a hydropower producer's risk.

The hydrological index insurance contracts used in creating replicating portfolios are structured identically to Equation 1. In this case, however, the index i_T is set *equal* to seasonal reservoir inflows (F_T) and K is a seasonal inflow level against which a policyholder desires to be protected.

$$H(F_T) = \max(K - F_T, 0) \tag{14}$$

No consideration is given to the value of hydropower (i.e., the price of natural gas). Rather, an individual contract of this sort makes very small payouts equivalent to the term $(K - F_T)$ (the value of this term typically ranges from \$0 - \$3, if seasonal reservoir inflows are considered in units of cubic kilometers). In order to protect themselves fully against hydrological financial risk, a hydropower producer must therefore purchase a large number of these smaller hydrological insurance contracts. Premiums for these contracts are calculated at a range of strike levels in an identical manner as that described in section 2.4.

Index insurance based on inflows alone is paired with "European" style put options on natural gas, which also have payout structures identical to that of Equation 1, with the index i_T set equal to the price of natural gas in the coverage period, and K equaling the natural gas strike price.

$$H(NGP_T) = \max(K - NGP_T, 0)*10{,}000 \tag{15}$$

Put options are priced using a version of the Black-Scholes formula adapted to use natural gas futures prices as the underlying asset [21] (see Appendix 3 for details). Put option prices are simulated for the entire 300-year test period on a 12-month-ahead basis for a range of strike values under low, average historical and high natural gas price volatility. Payouts from individual put options are scaled by a factor of 10,000 to reflect the contract size of natural gas futures traded on the Chicago Mercantile Exchange [22].

A search algorithm is employed to identify strike levels and purchase amounts of insurance and natural gas put options that collectively replicate the cost-effectiveness of contracts based on index $i(1)_T$. It is important to note that to match the performance of contracts based on $i(1)_T$, the search algorithm is

limited to selecting a fixed volume of insurance and put options to buy for each year of the 300-year test period, and the algorithm must likewise identify strike levels for each contract type that remain constant for the entire 300-year test period (the premiums of the natural gas put options, however, change each year depending on the price of natural gas). This constraint prohibits selectively purchasing underpriced put-options (ones whose value are guaranteed to exceed their cost).

3. RESULTS

In the following section, testing results are presented for each of the four contract types ($i(1)_T$, $i(2)_T$, $i(3)_T$, and $i(4)_T$) as well as for the replicating portfolio of insurance based on inflows alone and natural gas put options.

3.1 Validation of the Reservoir Power System Model

Although the connection between peak prices and the marginal cost of electricity production at natural gas plants is a well-established phenomenon [17], the extent to which these values are correlated on a daily, seasonal and annual basis can depend on specific system characteristics. For the system considered in this paper (i.e., the Dominion Zone of PJM Interconnection), linear regression of seasonal peak electricity prices simulated by the reservoir-power system model and synthetically generated natural gas prices yields an R^2 value of 0.94 under historical levels of natural gas price volatility. Actual historical peak electricity prices for the system on which the model is based (obtained from PJM Interconnection for the period 2005-2012) show less correlation with natural gas prices ($R^2 = 0.73$). This difference suggests that the reservoir-power system model overestimates the extent to which natural gas prices (as opposed to other factors, such as changes in electricity demand) explain changes in peak prices. It is likely therefore that contracts designed for an actual hydropower producer in the Dominion Zone of PJM would also need to include consideration of electricity demand in the index (or some reasonable proxy for electricity demand, such as heating and cooling degree days).

81

3.2   Index Basis Risk

A first, critical step in minimizing the basis risk of index insurance contracts (i.e., maximizing the correlation between contract payouts and actual damages experienced by the policyholder) is selecting an underlying index that accurately predicts seasonal hydropower revenues.

At each level of natural gas price volatility, index $i(1)_T$ demonstrates the highest correlation with seasonal revenues at Kerr Dam. This is a strong indication that contracts structured around $i(1)_T$ will trigger payouts that correspond most closely in timing and magnitude to periods of low revenues for dam operators. The index $i(2)_T$, which incorporates a static assumption of the historical median price of natural gas, generally demonstrates the weakest correlation to revenues, although there is little difference in terms of R^2 values among index $i(2)_T$ and the indices $i(3)_T$ and $i(4)_T$, which make dynamic estimates of the price of natural gas based on the current spot price.

Table 2 shows R^2 values between seasonal hydropower revenues simulated by the reservoir-power system model and estimates produced using the four indices. The level of volatility in natural gas prices significantly affects the correlation between indices $i(2)_T$, $i(3)_T$, and $i(4)_T$ and hydropower revenues, with low volatility increasing correlations and high volatility having the opposite effect. Correlations between hydropower revenues and values of index $i(1)_T$, however, are immune to changes in natural gas price volatility. This further suggests that explicitly accounting for natural gas prices is a critical element in the design of reliable and cost-effective index insurance for hydropower producers, and indicates that doing so is even more important during periods of high volatility in fuel prices.

Table 2. Strength of correlation (R^2 values) between index values and simulated hydropower revenues at Kerr Dam.

Index	Natural Gas Price Volatility	Seasonal Coverage Period			
		Spring	Summer	Fall	Winter
$i(1)_T$	LOW	0.9387	0.8916	0.95	0.9063
	AVERAGE	0.9276	0.906	0.9294	0.9203
	HIGH	0.9399	0.9256	0.9563	0.9384
$i(2)_T$	LOW	0.6429	0.4557	0.7042	0.4707
	AVERAGE	0.5331	0.2283	0.5412	0.2719
	HIGH	0.4772	0.2277	0.5493	0.2636
$i(3)_T$	LOW	0.7246	0.55	0.7249	0.6428
	AVERAGE	0.5831	0.2924	0.5141	0.471
	HIGH	0.3861	0.2744	0.6176	0.261
$i(4)_T$	LOW	0.7437	0.5856	0.7486	0.6173
	AVERAGE	0.5969	0.3501	0.5723	0.4693
	HIGH	0.4863	0.3364	0.6455	0.3213

The indices $i(2)_T$, $i(3)_T$, and $i(4)_T$ also generally demonstrate a diminished ability to reproduce the tails (more extreme events) in empirical probability distributions of seasonal revenues. Since protecting against extremely low revenue values is the primary objective the contracts, this is a significant weakness.

Figure 16 illustrates the basis risk (i.e., the correlation between actual damages experienced by the operators of Kerr Dam and contract payouts) of a contract based on index $i(1)_T$ (panel A) and one based on index $i(2)_T$ (panel B) under average natural gas price volatility. Both contracts assume a seasonal revenue strike level of $2.7M and are written for the winter season (December – February). The x-axis of

each panel measures damages experienced by operators of Kerr Dam (defined here as the degree to which seasonal hydropower revenues fall below the chosen contract strike of $2.7M).

$$Damages_T = \max(\$2.7M - R_T, 0)\tag{16}$$

The y-axis of each panel measures the size of corresponding contract payouts. Payouts made by the contract based on index $i(1)_T$ are highly correlated ($R^2 = 0.87$) to actual damages experienced by the dam operator, while payouts from the contract based on index $i(2)_T$ exhibit considerably less correlation with actual damages ($R^2 = 0.42$).

In addition, panel B indicates that the contract based on index $i(2)_T$ results in many more incidences in which the dam operator experiences damages ($x > 0$) but receives no payout ($y = 0$), and in several of these cases damages exceed $1M without any insurance compensation. Panel B also indicates that the contract based on index $i(2)_T$ results in many more instances in which the dam operator experiences no damages ($x = 0$) but receives a payout ($y > 0$). Although less problematic from the perspective of operators at Kerr Dam, these errors likewise indicate a higher degree of basis risk inherent in the index $i(2)_T$. Comparison of damages vs. payouts for the other two contract types (i.e., those based on indices $i(3)_T$ and $i(4)_T$) generally yield levels of basis risk similar to that of index $i(2)_T$.

As will be shown in the following sections, the significantly lower levels of basis risk demonstrated here by index $i(1)_T$ contribute to a vastly improved effectiveness of index insurance contracts.
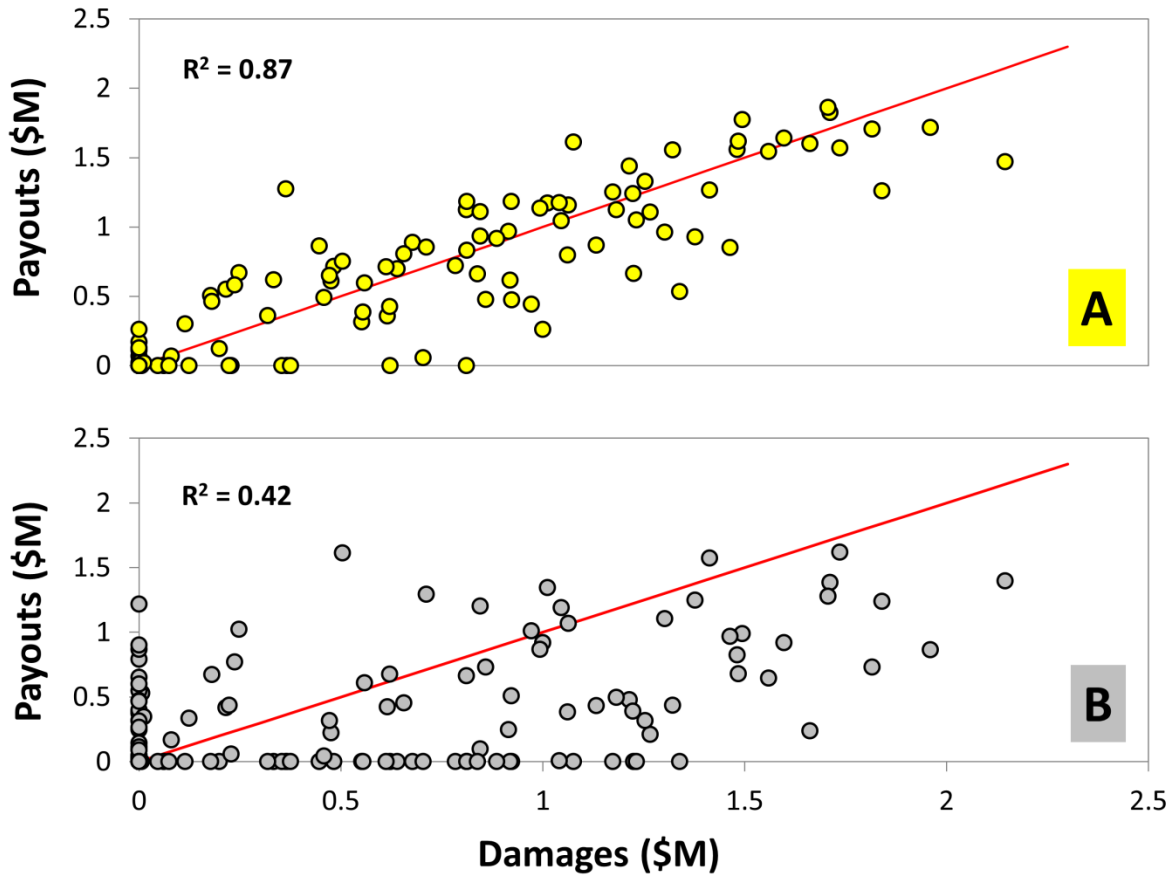
Figure 16. Correlation between actual damages experienced by operators of Kerr Dam (revenues less than $2.7M) and payouts from contracts based on the indices i(1)$_T$ (panel A) and i(2)$_T$ (panel B) under historical average natural gas price volatility. Data shown is for winter season.

3.3   Contract Performance

The performance of the four contracts ($i(1)_T$, $i(2)_T$, $i(3)_T$, and $i(4)_T$) over the 300-year testing period was assessed at multiple strike levels in terms of several factors, including:

- Annual premiums

- Net cost, or the difference between mean annual hydropower revenues with and without index insurance, expressed as both $ and % (Equations 10 and 11, respectively)

- Risk mitigation (Equation 12), or the difference between the minimum allowable revenue levels (or "floors") with and without insurance

- Risk mitigation factor (RMF) (Equation 13), defined as the ratio of the floor with insurance over the floor without insurance

Tables 21-28 in Appendix 3 display these values for each contract type, assessed under three different levels of natural gas price volatility (low, average and high) for each season (spring, summer, fall, and winter). For each volatility level, the minimum allowable revenue level without insurance (i.e., the old "floor") is specified. The new "floor" can be determined for each contract and at each strike level by adding the dollar-value extent of risk mitigation to the old floor.

3.3.1 Annual Premiums

Results for each contract type show that as the strike level is increased (i.e., as the hydropower producer's tolerance for risk is lowered), annual premiums and net cost increase monotonically. Figure 17 shows the increase in premiums and net cost for contracts based on index $i(1)_T$ implemented for the spring season under low, average, and high natural gas price volatility. Insurance premiums, or the amount of money paid up-front on an annual basis by a policyholder in order to receive insurance coverage, are shown to be distinct (and generally much larger) than the net cost of insurance, which takes into account payouts made by the insurer. Also note that both insurance premiums and net cost increase as a function of natural gas price volatility.
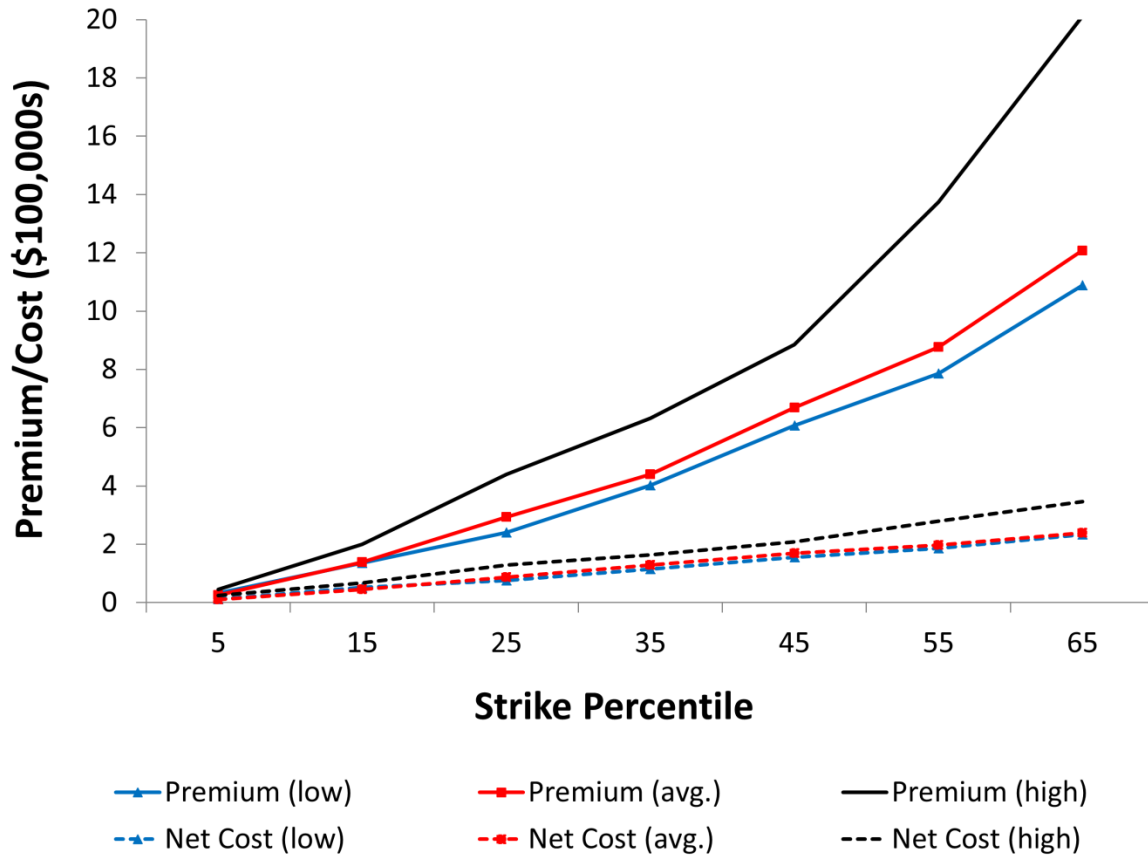
Figure 17. Increase in premiums and net cost for contracts based on index $i(1)_T$ implemented for the spring season under low, average, and high natural gas price volatility.

3.3.2 Identification of Non-dominated Index

A primary goal of this study is to identify whether any contract type is "non-dominated" (i.e., can consistently achieve a higher degree of risk mitigation for the same (or lower) net cost as other options). In order to facilitate identification of such a non-dominated contract type, cost effectiveness curves that plot RMF values as a function of net cost (%) are used.

Figure 18 shows cost effectiveness curves for each contract type implemented for the spring season under average natural gas price volatility. Except at very low net cost levels (i.e., strike levels <4%) contracts based on index $i(1)_T$ result in significantly larger increases in the revenue floor (i.e., higher

RMF values) for the same cost as other indices. Figure 18 also shows that contracts based on the indices (i.e., $i(2)_T$, $i(3)_T$, and $i(4)_T$) exhibit more discontinuous behavior (RMF values fluctuate, increasing then decreasing and increasing again, as a function of net cost (strike level)). This type of behavior is caused by the inability of contract indices to consistently recognize low-revenue years and trigger insurance payments (i.e., high basis risk).

Results for other seasons (see Tables 21-28 in Appendix 3) also show that contracts based on index $i(1)_T$ generally demonstrate significantly higher RMF values for the same net cost (%) than contracts based on the indices $i(2)_T$, $i(3)_T$, and $i(4)_T$. Results also demonstrate that the degree to which contracts based on $i(1)_T$ outperform other contract types is affected by natural gas price volatility (with higher volatility resulting in a much wider performance gap). This confirms findings from the basis risk analysis (see section 3.2) and further suggests that explicitly accounting for changes in natural gas prices in indices is critical during periods of high price volatility.

.
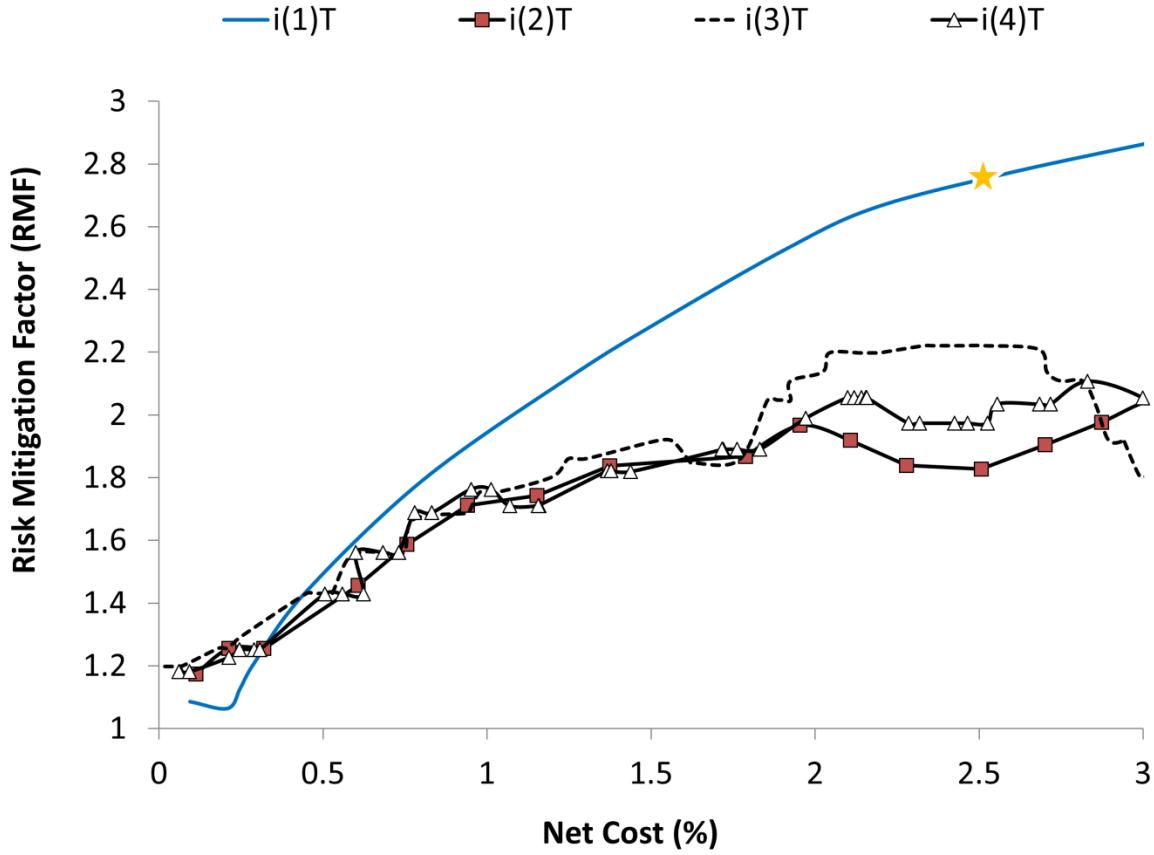
Figure 18. Cost-effectiveness curves for contracts in spring season under average natural gas price volatility. The placement of the star on the curve of $i(1)_T$ corresponds to the performance of the contract shown in Figure 19.

Adjusted revenues (a_R_T) (i.e., total revenues with insurance in place) under contract $i(1)_T$ are plotted alongside hydropower revenues without insurance (R_T) in Figure 19. Results displayed are for the spring season under average natural gas price volatility. The contract based on index $i(1)_T$ is implemented using a strike of 35% and entails net cost of 2.6%. Note that the performance of this particular contract is also represented by the star on the curve for $i(1)_T$ shown in Figure 18.
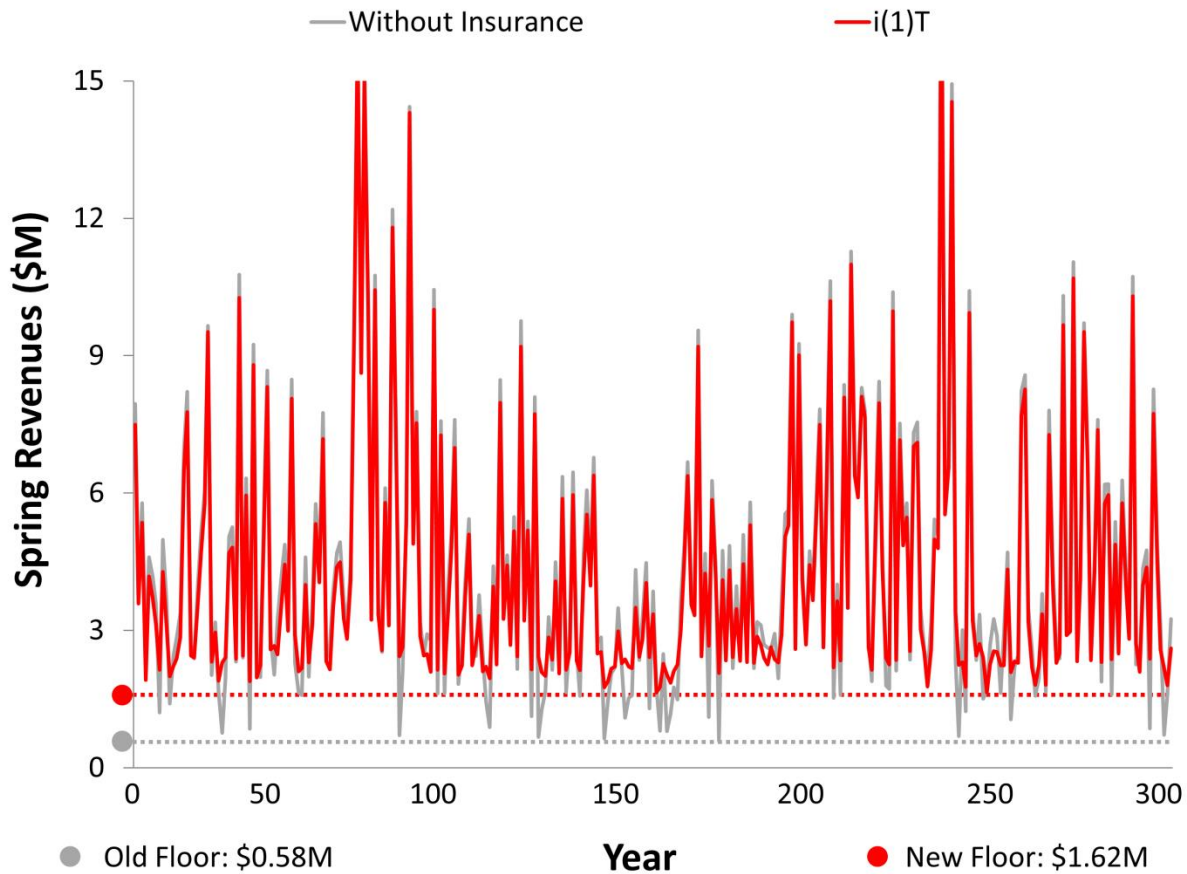
Figure 19. Spring revenues over 300-year testing period without insurance (gray) and with contract based on index $i(1)_T$ (red), assuming a strike of 35% (net cost of 2.6%). Insurance is shown to increase the seasonal revenue floor from $0.58M to $1.62M (an RMF of 2.8).

The contract based on index $i(1)_T$ is associated with an average annual premium of $382,000 and a net cost of $113,000 (i.e., mean annual spring revenues over the 300-year testing period are reduced by $113,000 from $4,369,812 to $4,256,812, a 2.6% percent decrease). In exchange, the minimum allowable spring revenue level (i.e., the floor) is raised from $583,332 to $1,616,765 (an RMF of 2.8). To give some perspective on how this compares to the performance of contracts based on other indices, for the same net cost ($113,000, or 2.6%) a contract based on index $i(2)_T$ only increases the revenue floor by $482,735 to $1,066,067 (an RMF of 1.8) This is due largely to basis risk in index $i(2)_T$, which results in the contract failing to make adequate payouts in several low revenue years.

3.4   Replicating Portfolio

Results discussed so far strongly suggest that the use of an index like $i(1)_T$ (i.e., one that explicitly accounts for changes in the price of natural gas) yields index insurance contracts for hydropower producers that are significantly more cost-effective than ones based around the indices $i(2)_T$, $i(3)_T$, or $i(4)_T$. Nonetheless, it is conceivable that under certain circumstances (e.g., following periods of high natural gas volatility caused by extreme weather or economic disturbances, or in systems in which natural gas prices and hydrological conditions are not statistically independent (as is assumed in this paper)) a single insurer may be hesitant to assume both hydrological risk and natural gas price risk from a hydropower producer.

In an attempt to present a viable alternative to the use of the index insurance contracts based on index $i(1)_T$, the potential use of "replicating portfolios" comprising: 1) index insurance contracts based on inflows alone; and 2) natural gas derivatives (put options), is investigated. The premise of these portfolios is that the financial risks to hydropower producers posed by dry periods and low natural gas prices can be separated and mitigated using independent hedging instruments.

Using 300 years of synthetic calibration data, combinations of insurance contracts based on inflows alone and natural gas put options were identified that, when used in concert, replicate as closely as possible the shape of seasonal cost effectiveness curves for the index $i(1)_T$ under average natural gas price volatility. The replicating portfolios were then implemented for the 300-year testing period, and their cost-effectiveness was compared alongside results from contracts based on index $i(1)_T$.

Figure 20 shows cost-effectiveness curves calculated for each season under average natural gas price volatility for contracts based on the index $i(1)_T$ (blue lines) and the replicating portfolios of hydrological insurance and natural gas put options (blue dotted lines). For additional comparison, the performance of contracts based on the index $i(2)_T$ (red squares) is also shown. Table 29 in Appendix 3 lists details of the replicating portfolios identified using calibration data (i.e., the volume/strike levels of hydrological insurance and natural gas put options used for each level of net cost (%)).
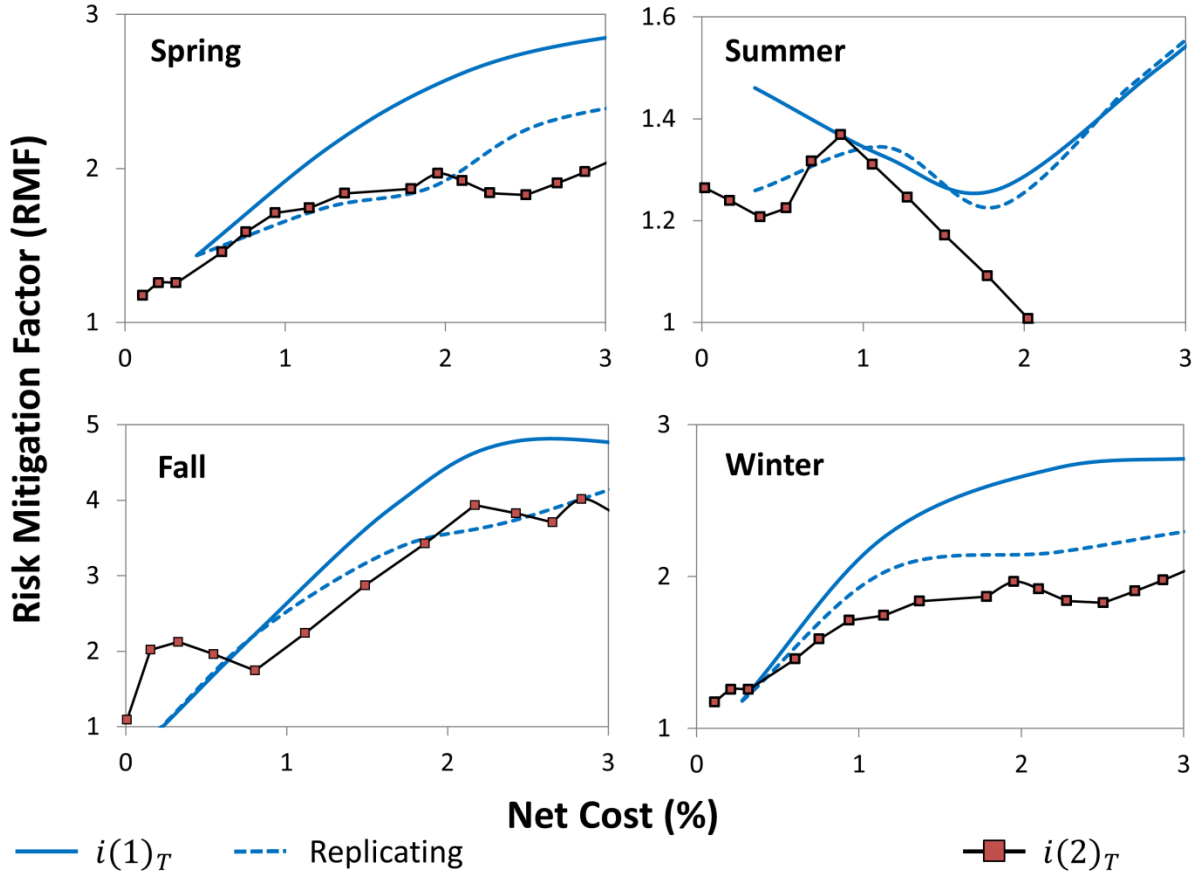
Figure 20. Comparison of cost-effectiveness curves for insurance contracts using i(1)ₜ (red lines) and replicating portfolio of hydrological insurance and natural gas put options (black dotted lines).

Figure 20 shows that only in a few cases do the replicating portfolios demonstrate a very high level of success at matching the performance of contracts based on $i(1)_T$. Part of the replicating portfolios' lack of success at matching the performance of contracts based on $i(1)_T$ is attributable to the fact that, similar to contracts based on the indices $i(3)_T$ and $i(4)_T$, they are associated with dynamically priced premiums that incorporate probabilistic assumptions about the future price of natural gas. In the case of natural gas put options, premiums are higher if the current 1-year futures price is close to or below the strike price, and they are lower if the futures price is well above the strike. This method of contract pricing is not inherently problematic; however, it can result in situations in which a hydropower producer

pays a very high premium for natural gas put options that do not pay-out (e.g., following an increase in the spot price of gas) in a moderately dry year. Even if payouts from hydrological insurance are made, they may be too modest to offset the substantial cost of natural gas put options, and total revenues can remain low.

Other drawbacks of the replicating portfolios used in this paper are that they are deliberately constrained in their purchase of a static volume of put options and insurance contacts (and likewise, static strike levels for each) for the entire 300-year testing period. This was done to prohibit the search algorithm from basing prospective replicating portfolios only on "sure things" (insurance and options that are guaranteed, with foresight, to pay-out). It is possible that a more sophisticated approach to purchasing insurance and options could yield better results (one such approach might be to purchase natural gas options closer to the coverage period (e.g., 6 months out), which would likely incorporate more accurate price estimates into the put option contracts).

Despite the replicating portfolios' lack of success at emulating exactly the cost-effectiveness of contracts based on $i(1)_T$, they are in most instances at least as cost-effective as contracts based on the indices $i(2)_T$, $i(3)_T$, and $i(4)_T$. Thus, in the event that a single counterparty willing to take on both the hydrological and natural gas price risk of a hydropower producer could not be found, replicating portfolios of hydrological insurance and natural gas put options may be a viable alternative, particularly if more sophisticated knowledge of natural gas markets were available.

4. CONCLUSIONS

The central goal of this study was to investigate the need for integrating consideration of natural gas price volatility in the development of index insurance contracts designed to reduce the financial exposure of hydropower producers to drought. To this end, four contract indices ($i(1)_T$, $i(2)_T$, $i(3)_T$ and $i(4)_T$) that differ primarily in their treatment of natural gas prices were investigated.

Contracts were calibrated and tested under three different levels of historical natural gas price volatility: low (2010-2012); average (1997-2012); and high (2003-2005). Results show that the index

93

$i(1)_T$, which is structured as a linear combination of seasonal reservoir inflows and natural gas prices, demonstrates the highest correlation with seasonal hydropower revenues at Kerr Dam and the lowest basis risk. Accordingly, contracts that are structured around $i(1)_T$ consistently show a greater ability (at equivalent costs) to increase the minimum allowable revenue level (or floor) than contracts based on other indices. Increased natural gas volatility was generally found to increase the basis risk of indices $i(2)_T$, $i(3)_T$ and $i(4)_T$, but was found to have little effect on the basis risk of index $i(1)_T$. We thus find that increased natural gas volatility contributes to a wider performance gap between contracts built around $i(1)_T$ and the other indices, with contracts built around $i(1)_T$ becoming more even more preferable at high levels of natural gas price volatility.

We also investigated the potential use of "replicating portfolios", or combinations of insurance contracts based on inflows alone and natural gas put options. In theory, replicating portfolios would be used to separate a hydropower producer's hydrological risk and electricity price risk and deal with them independently using instruments that exist right now (this could also circumvent the challenge of finding a single counterparty willing to absorb all of a hydropower producer's financial risk). In particular, there was interest in determining whether a portfolio of smaller hydrological insurance contracts and natural gas options could reduce a hydropower producer's overall financial exposure to the same extent (and for the same cost) as contracts based on index $i(1)_T$.

The results from this analysis were mixed: rarely are replicating portfolios shown to perfectly mimic the cost-effectiveness of contracts that use $i(1)_T$ (in most cases there is some performance gap between the two, and in some cases this gap can be considerable). Nonetheless, the use of replicating portfolios compares favorably to the performance of contracts based on other indices ($i(2)_T$, $i(3)_T$, and $i(4)_T$), i.e., most of the time they are at least as cost-effective. As such, we suggest that replicating portfolios may yet represent a viable (albeit more complex) alternative to the use of index insurance based on the index $i(1)_T$ (particularly if more sophisticated strategies for purchasing natural gas options can be employed), and we recommend this topic as an area for more detailed future research.

It is also important to note that although contracts were evaluated under different levels of natural gas price volatility, stationarity in system hydrology (i.e., reservoir inflows) is assumed throughout. Climatic changes that result in more frequent or severe dry periods (increased financial risk for hydropower producers) over extended periods of time would likely make hedging strategies more expensive (increase premiums) by: 1) increasing insurers' expected costs; and/or 2) increasing the largest occurring payout (increasing the amount of capital reserves that a potential insurer would need to keep in a liquid state). It is also possible that an insurer may perceive additional, unquantifiable hydrological uncertainty in future inflows and increase premiums simply in anticipation of an altered hydrological cycle.

Another important subject not considered here is contract duration. All contracts evaluated in this analysis are assumed to be signed 1-year out from the coverage period and cover a hydropower producer for one 3-month season. In principle, contracts could also be designed to cover much longer periods (e.g., the summer season over a consecutive 5 or 10-year period). There may be some advantages in doing so for a hydropower producer, namely the ability to lock-in a fixed premium. However, increased contract duration may increase premiums overall, since a longer time horizon exposes the insurer to unforeseen changes in natural gas prices. Longer duration contracts may likewise be subject to reduced effectiveness if changes in system hydrology yield reservoir inflows that are inconsistent with the historical record on which contracts were based.

Ultimately, a hydropower producer wishing to pursue one or the other of the index insurance contracts described here must weigh any internal tradeoffs presented by three things: 1) annual premiums (i.e., the up-front liquidity required to be able to purchase insurance; 2) net cost (the percentage of mean annual revenues that will be forfeit to the insurer over the long term); and 3) the desired level of risk mitigation. Strategies for balancing these three areas is not a concept that is explored in significant detail in this paper, but it is one that, considering the strong potential of index insurance to reduce the exposure of hydropower producers, deserves close attention in future work.

REFERENCES

[1] United States Bureau of Reclamation. 2005. "Hydropower." Website.
http://www.usbr.gov/power/edu/pamphlet.pdf

[2] National Energy Technology Laboratory. 2009. "An Analysis of the Effects of Drought Conditions on Electric Power Generation in the Western United States." Laboratory. DOE/NETL-2009/1365

[3] Harto, C.B., and Yan, Y.E. 2011. "Analysis of Drought Impacts on Electricity Production in the Western and Text Interconnections of the United States." Argonne National Laboratory. ANL/EVS/R-11/14

[4] Minton, B. A., & Schrand, C. (1999). The impact of cash flow volatility on discretionary investment and the costs of debt and equity financing. Journal of Financial Economics, 54(3), 423-460.

[5] Weare, C. 2003. "The California Electricity Crisis: Causes and Policy Options. Public Policy Insitute of California.

[6] Turvey, C.G. 2001. "Weather derivatives for specific event risks in agriculture." Review of Agricultural Economics. 23(3), pp. 333-351.

[7] Stoppa, A., and Hess, U. 2003. Design and use of weather derivatives in agricultural policies: the case of rainfall index insurance in Morocco. In International Conference: Agricultural Policy Reform and the WTO: Where are We Heading. pp. 23-26.

[8] Barrett, C., Barnett, B., Carter, M., Chantarat, S., Hansen, J., Mude, A., Osgood, D., Skees, J., Turvey, C., Ward, M. "Poverty Traps and Climate Risk: Limitations and Opportunities of Index-Based Risk Financing." Working Paper. The International Research Institute for Climate and Society. 2007. IRI Technical Report Number 07-02.

[9] Collier, B., Skees, J., and Barnett, B. 2009. "Weather Index Insurance and Climate Change: Opportunities and Challenges in Lower Income Countries." The Geneva Papers. Volume 34, 401-424. The International Association for the Study of Insurance Economics 1018-5895/09.

[10] Manfredo, M.R., and Richards, T.J. 2009. Hedging Yield with Weather Derivatives: A Role for Options in Reducing Basis Risk. Applied Financial Economics, 19(2), pp. 87-97.

[11] Brown, C., and Carriquiry, M. 2007. Managing hydroclimatological risk to water supply with option contracts and reservoir index insurance. Water Resources Research, 43(11).

[12] Zeff, H.B., and Characklis, G.W. 2013. Managing water utility financial risks through third-party index insurance contracts. Water Resources Research. No. 49. pp 4939-4951.

[13] Foster, B. and Characklis, G. 2014. "Managing Water Supply Related Financial Risk in Hydropower Production with Index-Based Financial Instruments."

[14] Khalil, A.F., Kwon, H.-H., Lall, U., Miranda, M.J., and Skees, J. 2007. El Nino-Souther Oscillation-based index insurance for floods: Statistical risk analyses and application to Peru. Water Resources Research. No. 43.

[15] Cao, M., Li, A., & Wei, J. 2004. Precipitation modeling and contract valuation: a frontier in weather derivatives. The Journal of Alternative Investments, 7(2), 93-99.

[16] SwissRe. 2012. "Swiss Re Corporate Solutions receives award for Weather Risk Management Transaction of the Year 2012". Website. http://www.swissre.com/corporate_solutions/swiss_re_corporate_solutions_receives_award_for_weather_risk_management_transaction_of_the_year_2012.html

[17] Energy Information Administration. 2013. "Natural gas-fired combustion turbines are generally used to meet peak electricity load." Website. http://www.eia.gov/todayinenergy/detail.cfm?id=13191. Accessed Jan. 6, 2014.

[18] Kern, J.D., Patino-Echeverri, D., Characklis, G.W. ""An Integrated Reservoir – Power System Model for Evaluating the Impact of Wind Power Integration on Hydropower Resources." Renewable Energy. Submitted

[19] Nowak, K., Prairie, J., Rajagopalan, B., Lall, U. 2010. "A nonparametric stochastic approach for multisite disaggregation of annual to daily streamflow." Water Resource Research. Vol. 46, W08529, doi: 10.1029/2009WR008530.

[20] Wang, S. 2002. "A Universal Framework for Pricing Financial and Insurance Risks." ASTIN Bulletin. Vol. 32, No. 2. pp. 213-234.

[21] Hull, J. 2011. "Options, Futures, and Other Derivatives. 8th Edition." Prentice Hall.

[22] Chicago Mercantile Exchange. Website. http://www.cmegroup.com/trading/energy/natural-gas/natural-gas_contractSpecs_options.html. Accessed March 1, 2014.

[23] Haugh, L. 1976. "Checking the Independence of Two Covariance-Stationary Time Series: A Univariate Residual Cross-Correlation Approach." Journal of the American Statistical Association. Vol. 71, No. 354. pp. 378-385.

[24] Energy Information Administration. 2013. "Natural Gas Explained: Factors Affecting Natural Gas Prices." Website. http://www.eia.gov/energyexplained/index.cfm?page=natural_gas_factors_affecting_prices. Accessed Jan. 6, 2014.

[25] Kogan, L., Livdan, D., Yaron, A. 2009. "Oil Futures Prices in a Production Economy with Investment Constraints." The Journal of Finance. Vol. 64. pp. 1345-1375

CHAPTER 4: THE IMPACTS OF CHANGES IN NATURAL GAS PRICES AND HYDROLOGIC VARIABILITY ON THE COST OF RAMP RATE RESTRICTIONS AT HYDROELECTRIC DAMS

1. INTRODUCTION

The financial optimization of hydropower projects relies heavily on the practice of hydropower "peaking," in which dams produce electricity (release water) at maximum rates during high demand hours and release much less water during other, less valuable hours. However, the large fluctuations in sub-daily river flows that occur as a result of this practice can cause significant environmental impacts downstream, including: habitat loss, altered physicochemical properties, changes in sediment dynamics, stranding of fish and other organisms, and/or the disruption of life cycle processes [1,2,3,4,5]. Policymakers' understanding of these negative externalities has developed alongside an increasing awareness of the economic benefits of healthy river ecosystems [6,7,8,9]. As a result, efforts to protect downstream ecosystems from the effects of hydropower peaking have become more widespread, particularly as part of the Federal Energy Regulatory Commission's dam relicensing process [10]. Jager and Bevelhimer [11] found that of the 223 dams whose licenses were renewed between 1988 and 2000, 23 (13%) were converted from peaking to "run-of-river" (ROR) operations, a distinction that means reservoir output is set equal to inflows on a daily (and sometimes hourly) basis. Nonetheless, the high value of hydropower as a peaking resource persists as a barrier to restoring natural sub-daily variability in river flows.

Efforts to restore sub-daily flow patterns below dams commonly include the use of "ramp rate" restrictions, or limits on the magnitude of hour-to-hour changes in reservoir discharge, which force a fraction of total hydropower production to be shifted away from periods of peak electricity demand towards less valuable off-peak hours. The financial penalty that dam owners incur as a result of these

restrictions is a function of two factors: 1) the "spread" (difference) between peak and off-peak electricity prices; and 2) the total amount of generation that is shifted from peak to off-peak hours (this amount, in turn, depends on the availability of water for hydropower production) [8,12,13,14].

In recent years, a handful of studies have estimated the annualized cost of ramp rate restrictions for dam owners. Harpman [13] found that implementing ramping restrictions at Glen Canyon Dam (Arizona, USA) for a single representative water year would result in a reduction in hydropower revenues of $6.17 million (8.8%). Kotchen et al. [8] found the mean annual cost of implementing ROR operations at two dams in Michigan over a 12-year period to be $310,000. More recent work by Jager and Bevelhimer [11] noted lower bound cost estimates of between $2,500 and $93,000 per year, depending on the size of the project.

These previous research efforts give very little consideration, however, to the extent to which the cost of ramp rate restrictions at dams may vary on a seasonal and year-to-year basis due to fluctuations in the price spread and hydrologic variability. A more comprehensive quantitative understanding of how uncertainty in each of these factors contributes to changes in the cost of restrictions at dams would allow more realistic long-term projections of these costs to be included in dam relicensing—an important consideration given the typical length of FERC operating licenses (30 years).

For example, in the last decade, the spread between peak and off-peak electricity prices has fluctuated significantly, rising in numerous months to more than $100/MWh and at other times falling to around $20/MWh (Figure 21). A primary cause of this historical variability may be volatility in natural gas markets. Natural gas power plants are typically used in a similar manner to hydroelectric dams (i.e., as peaking plants) and they generally set the market price of electricity during peak hours [15]. As a consequence, increases and decreases in peak electricity prices often reflect changes in the price of natural gas. More recently, however, horizontal hydraulic fracturing, or "fracking", has led to a surge in domestic (U.S. and Canadian) gas supply, and contributed to an extended period of low natural gas prices [16]. As a consequence, the spread between peak and off-peak prices is at a relative low point, and the implementation of ramp rate restrictions at hydroelectric dams may be less costly than in the past.
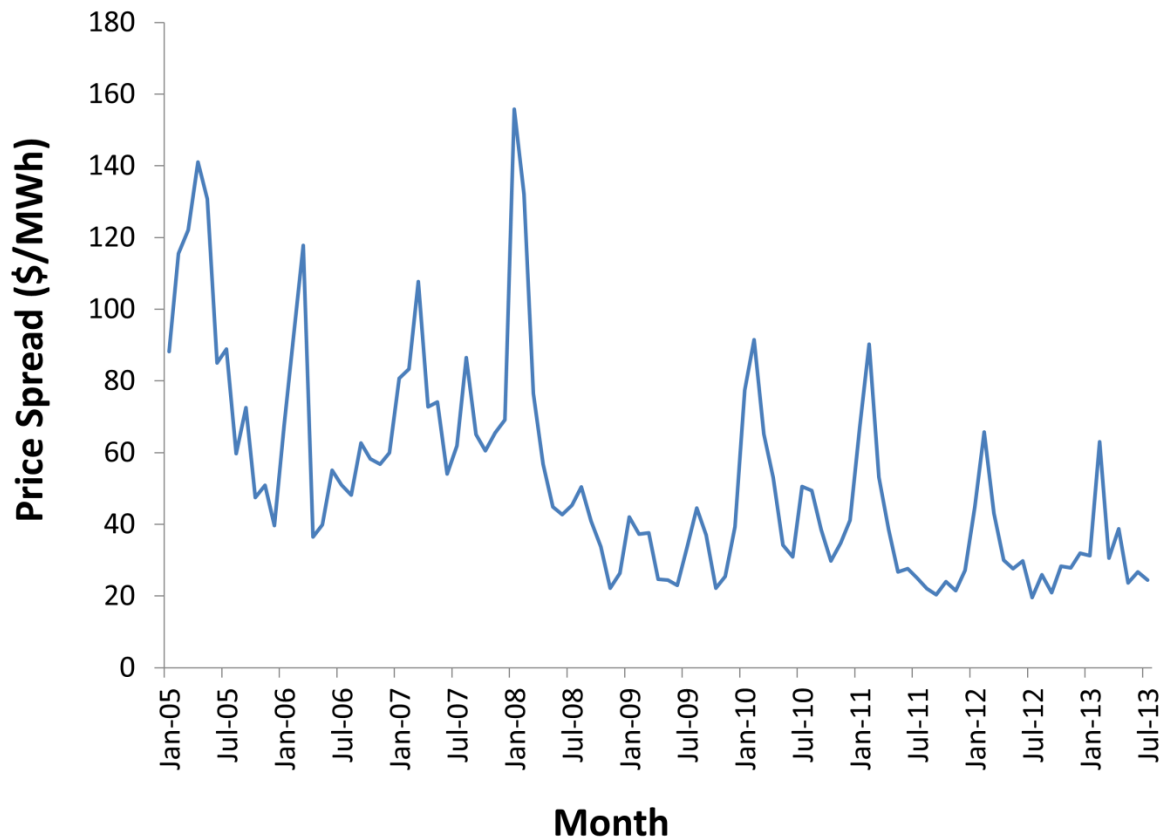
Figure 21. Average monthly price spread in Dominion Zone of PJM Interconnection (2005-2013).

Collectively, variability in the price spread and reservoir inflows may cause large swings in the cost of ramp rate restrictions on a seasonal and annual basis. This variability may be particularly problematic for downstream stakeholders (e.g., conservation trusts, non-profits, and charitable organizations) interested in "purchasing" operational changes at upstream dams in order to restore sub-daily variation in river flows to natural levels. There is significant precedent for this type of arrangement, in which downstream stakeholders agree to send "make whole" payments to upstream water users in return for the implementation of conservation practices that improve downstream river conditions [17]. The potential for large year-to-year fluctuations in the cost of ramp rate restrictions may, however, preclude downstream stakeholders from engaging dam owners in this type of exchange. As a result,

financial hedging strategies capable of significantly reducing this uncertainty may be of value to prospective buyers of ramp rate restrictions at dams. One such strategy could be the use of "collar" agreements between a downstream stakeholder and a third party insurer that compensate the downstream stakeholder in high cost periods and require a pay-out to the insurer in low cost periods, yielding net costs that approximate the long-term mean.

In this paper, we characterize the effects of water availability and the spread between peak and off-peak prices on the cost of ramp rate restrictions at a hydroelectric dam over the period 2005-2013. Of particular interest is determining whether recent low natural gas prices (partly attributable to improvements in oil and gas extraction technology) have reduced the cost of implementing operating restrictions. The historically observed costs of ramp rate restrictions are also used to calibrate a model for estimating the seasonal cost of restrictions based on price spread and total hydropower generation. This seasonal cost model is then used to price collar agreements designed to help prospective purchasers of environmental flow benefits make constant payments in exchange for the implementation of operational restrictions at dams.

2. METHODS

2.1. Modeling Platform and Study Area

This analysis builds on previous research involving the development of a hydrologic-economic model adapted from previous work by the authors [18] that simulates the operation of a series of hydroelectric dams in the Lower Roanoke River basin (Virginia and North Carolina, U.S.) (Figure 22). The model uses historical hydrological inputs of run-off, precipitation and evaporation, along with existing reservoir operating guidelines, to drive water balance equations and allocate daily volumes of water for release (hydropower production) at dams. Daily volumes of water available for hydropower production are then scheduled for release on an hourly basis using a mixed integer optimization program that maximizes revenues from the sale of electricity using historical market prices.

This paper focuses on the operation of Roanoke Rapids Dam, a 100MW project that is owned and operated by Dominion Energy. As the furthest downstream dam in the Roanoke River basin, the operations of Roanoke Rapids Dam have been the subject of considerable scrutiny in the past, particularly with regard to its impacts on the downstream environment. Downstream of Roanoke Rapids Dam are extensive areas of un-fragmented bottomland hardwood forest considered by The Nature Conservancy, the U.S. Fish and Wildlife Service, and the State of North Carolina to be highly valuable ecological resources [19]. In addition, the Roanoke River downstream of Roanoke Rapids Dam provides estimated recreational fishing benefits of $4.2M (million) per year [20].
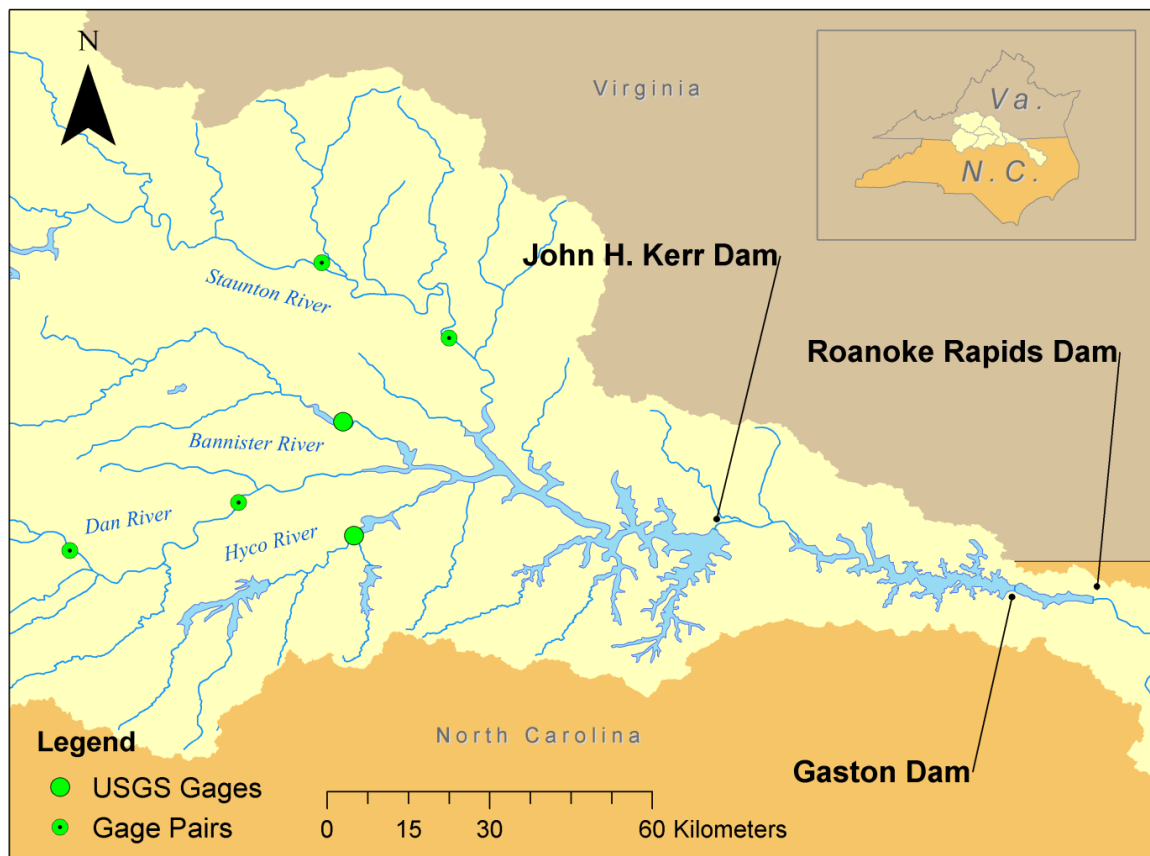
Figure 22. The Lower Roanoke River Basin, featuring John. H. Kerr Dam (US Army Corps of Engineers) and Gaston and Roanoke Rapids dams (Dominion).

2.2. Study Framework

Figure 23 shows a schematic of the study framework used in this paper. First, the seasonal cost of restrictions at Roanoke Rapids Dam over the period 2005-2013 is determined by comparing simulated hydropower revenues at the dam under two different operational scenarios that, respectively, represent the lowest and highest degree of sub-daily operational restrictions typically found at hydroelectric dams in the U.S.

- *Unrestricted*: dam owners are free to employ hydropower peaking (i.e., schedule power production in a manner that maximizes profits) and make hourly reservoir releases up to maximum turbine capacity (20,000 cfs). Hourly releases from Roanoke Rapids Dam are, however, subject to instantaneous minimum release requirements (325 cubic feet per second (cfs).

- *Restricted*: in this scenario, operations at Roanoke Rapids Dam are converted to "run-of-river" (ROR), with daily reservoir discharge at Roanoke Rapids Dam set equal to reservoir inflows and hourly flows re-regulated to remove peaking effects from upstream Gaston Dam (e.g., if total reservoir inflows for a given day equal 240,000 cfs, then the dam releases 10,000 cfs in each hour).

Hydropower revenues at Roanoke Rapids Dam are maximized for both scenarios over the period 2005-2013, subject to dam operating constraints and water availability, using a moving 4-day planning horizon and historical day-ahead electricity prices obtained for the Dominion Zone of PJM Interconnection, a large deregulated electricity market in the Mid-Atlantic region of the U.S. [21]. The operations of upstream dams (Gaston and John H. Kerr) are simulated in an identical manner under each scenario according to existing guidelines for these projects. As a result, daily inflows to Roanoke Rapids

Dam are the same for each scenario, and differences in revenues between the two scenarios can be attributed solely to the implementation of operating restrictions at the dam.

The cost of restrictions at Roanoke Rapids Dam is calculated on a seasonal (cumulative 3-month) basis as the difference in hydropower revenues between the unrestricted scenario and restricted scenario.

$$C_T = U_T - R_T \qquad\qquad (1)$$

where, $T =$ season (Spring, Summer, Fall, or Winter)

$U_T =$ cumulative unrestricted revenues in season T ($\$$)

$R_T =$ cumulative restricted revenues in season T ($\$$)
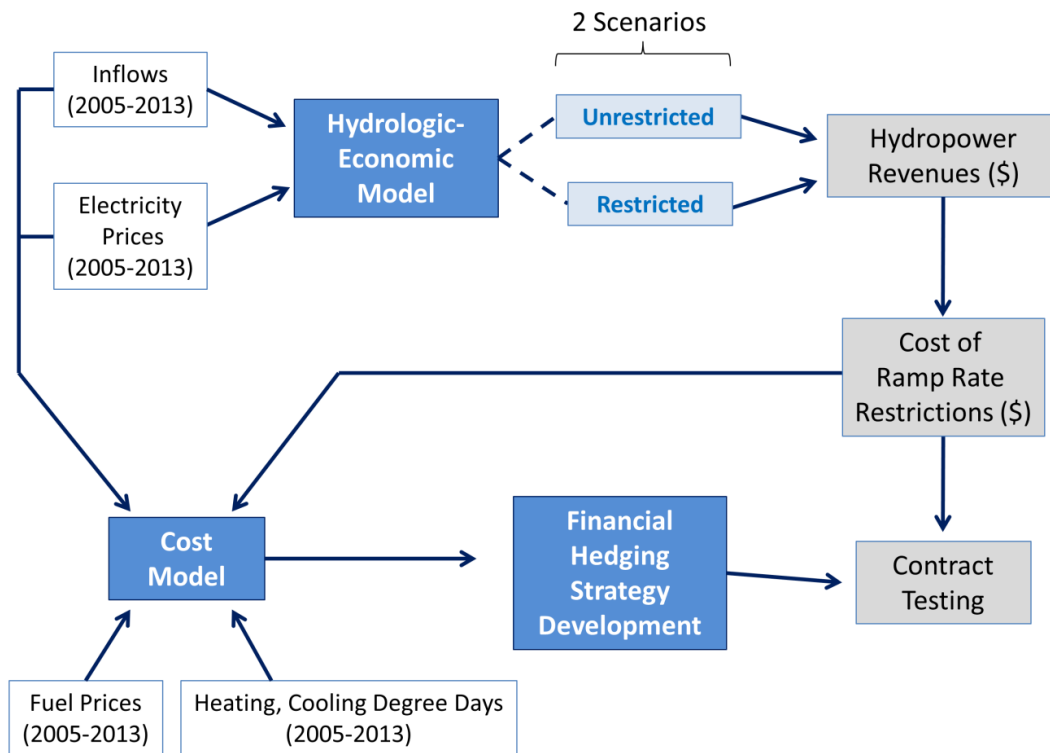
Figure 23. Study framework.

104

Historically observed seasonal cost data (C_T) are then evaluated for linear correlation with price spread, hydropower generation (water availability), and natural gas prices. In particular, we assess whether low natural gas prices in recent years have contributed to: 1) a narrower spread between peak and off-peak electricity prices; and 2) a decline in the cost of restrictions at Roanoke Rapids Dam.

2.2.1. Cost Model

Seasonal cost data (C_T) calculated for the period 2005-2013 are used to calibrate a mathematical model for estimating the cost of restrictions at Roanoke Rapids Dam based on seasonal price spread and hydropower generation. Estimated seasonal costs $(\hat{C}_T)$ are assumed by the model to be linearly dependent on price spread (the higher the price spread, the higher the cost of ramp-rate restrictions) and non-linearly dependent on hydropower generation, as shown in Equation 2.

$$\hat{C}_T = (a * G_T{}^3 + b * G_T{}^2 + c * G_T) * \gamma * S_T \tag{2}$$

where, $\hat{C}_T$ = estimated cost of restrictions in season T

$\{a, b, c\}$ = multiplication coefficents

G_T = total generation at Roanoke Rapids Dam in season T (MWh)

γ = multiplication coefficient for price spread

S_T = average spread between peak and off peak electricity prices in season T ($\frac{\$}{\text{MWh}}$)

Values for the parameters a, b, c, d, and γ in Equation 2 are identified using a non-linear optimization algorithm, the objective of which is to find a model that yields a non-dominated linear

correlation (R^2 value) and mean squared error when compared with actual seasonal costs (C_T) over the period 2005-2013.

The rationale for using a non-linear relationship to describe the effect of seasonal hydropower generation on the cost of restrictions (shown in Figure 24) is based on results from a preliminary analysis in which seasonal costs were calculated across a range of inflow levels while keeping electricity prices constant. For any given season, the lowest possible cost of restrictions is $0 (no difference in revenues between the restricted and unrestricted operating scenarios). Although rare, this circumstance can occur as a result of either: 1) very high reservoir inflows that force dam operators to release water at maximum turbine capacity in every hour for an entire season; or 2) very low reservoir inflows that result in the dam making only the FERC-required minimum release in every hour for an entire season.

As seasonal generation is increased from the FERC-required minimum level, the cost of restrictions increases because the marginal value ($/MWh) of hydropower generation is higher under the unrestricted scenario than it is under the restricted scenario. Costs increase until they reach an inflection point (maximum), which occurs when the marginal value of hydropower generation is equal for both the restricted and unrestricted scenarios (this point is associated with high inflows that force a peaking dam to produce substantial amounts of electricity in off-peak hours). As seasonal generation increases further, costs decrease (and eventually reach zero), because the marginal value of generation in the unrestricted scenario is below that of the restricted scenario.
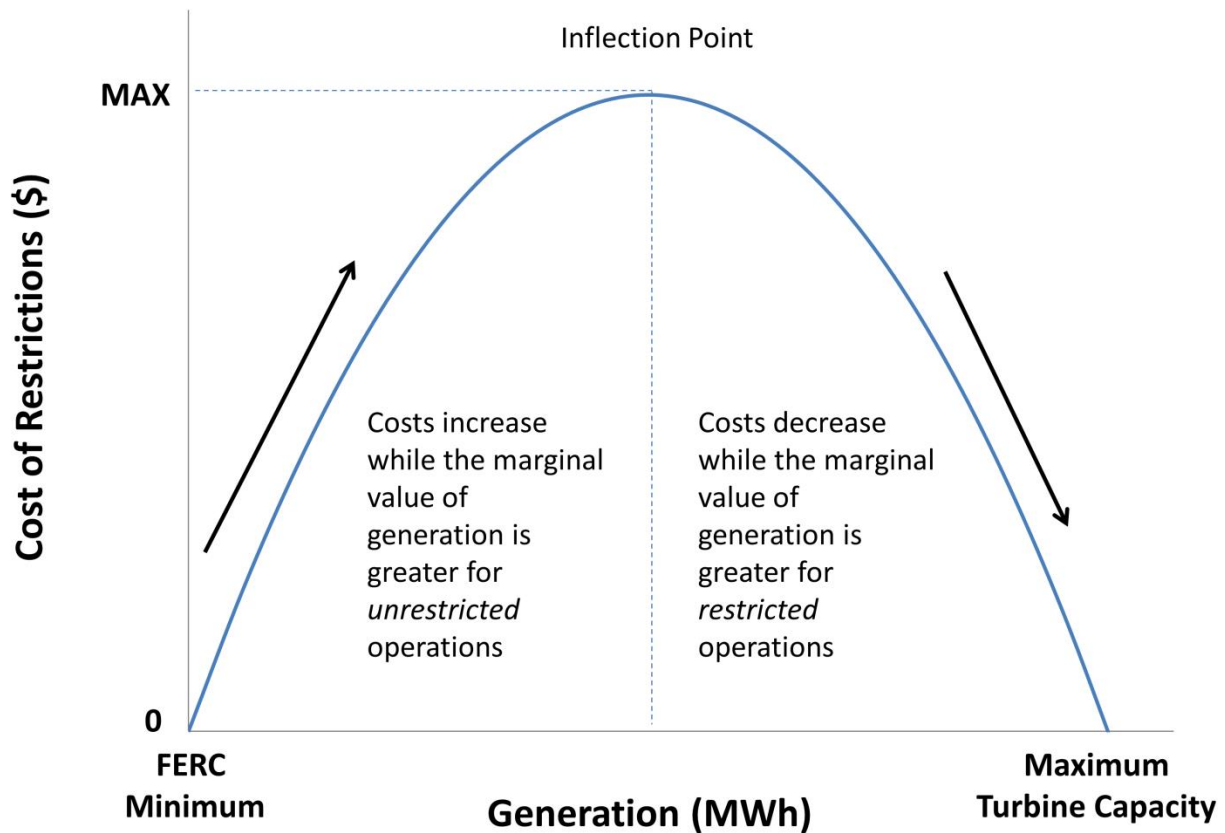
Figure 24. Non-linear relationship between seasonal generation and the cost of restrictions at a hydroelectric dam, assuming a fixed spread between peak and off-peak electricity prices.

2.2.2. Financial Hedging Strategy

We also explore the potential for financial hedging strategies to help achieve constant costs for downstream stakeholders interested in purchasing operational limits at dams in order to restore sub-daily variability in river flows.

There is significant precedent for financial exchanges in which conservation organizations agree to compensate upstream agricultural water users in exchange for implementing conservation practices that augment in-stream flows. For example, since 2005 the Freshwater Trust in Oregon (U.S.) has administered a program in which upstream agricultural water users are compensated by the trust for

reducing their water consumption. This reduced consumption then helps maintain increased river flows for salmon spawning downstream [17].

An analogous arrangement structured to reduce the impacts of hydropower peaking on sub-daily variation in river flows would entail a downstream stakeholder sending "make-whole" payments to compensate a dam owner for implementing ramp rate restrictions. In principle, payments sent from the downstream stakeholder to the dam owner would be equivalent to the "spot" cost of restrictions at the dam, i.e., the difference in hydropower revenues between the restricted and unrestricted scenarios in each period (C_T). To the extent that this value changes on a seasonal and/or annual basis, a downstream stakeholder may also wish to engage in a financial hedging agreement that allows them to make constant payments rather than pay the spot cost of restrictions.

One option for doing so could be multi-year bilateral agreements in which the downstream stakeholder pays the expected spot cost of restrictions ($E[C_T]$) to the dam owner. In most years, payments made by the downstream stakeholder would either be too large ($E[C_T] > C_T$) or too small ($E[C_T] < C_T$). Over a longer period, however, the average payment made by the downstream stakeholder would approximate the expected spot cost of operational restrictions.

Nonetheless, dam owners may be unwilling to engage in such a payment scheme and, rather, require that payments from the downstream stakeholder in each period equal the spot cost of restrictions (C_T). This research develops an alternative approach that would allow the downstream stakeholder to achieve constant conservation payments by engaging a third party insurer in a financial "collar" agreement [22] (see Figure 25).

In a collar agreement, the downstream stakeholder pays a premium to a third party insurer, who, in return, agrees to make payments in period T to the downstream stakeholder equal to:

$$Collar_T = \max (C_T - E[C_T],0) - \max(E[C_T] - C_T,0) \tag{3}$$

When $C_T < E[C_T]$, the value of $\boldsymbol{Collar_T}$ is negative and a contract pay-out is made from the downstream stakeholder to the insurer. Alternatively, when $C_T > E[C_T]$ the value of $\boldsymbol{Collar_T}$ is positive and a contract pay-out is made from the insurer to the downstream stakeholder (if $C_T = E[C_T]$ no exchange of funds occurs). Thus, in high cost periods (i.e., whenever $C_T > E[C_T]$) the collar agreement is a source of funds for the downstream stakeholder that can be used to defray any portion of make-whole payments to the dam owner in excess of $E[C_T]$. In low cost periods, however, (i.e., whenever $C_T < E[C_T]$) the downstream stakeholder must make a payment to the insurer equal to $(E[C_T] - C_T)$.

Net payments made by the downstream stakeholder in each period equal the sum of three components (Equation 4): 1) the spot cost of restrictions (C_T); 2) the risk premium associated with the collar agreement (P_T); and 3) the collar payoff function (Equation 3).

$$Net\ Payment_T = C_T + P_T + Collar_T \tag{4}$$

In principle, this type of arrangement allows the downstream stakeholder to make a payment of $(E[C_T] + P_T)$ in each period. The only fluctuation in this value comes as a result of relatively minor fluctuations in the risk premium.

$$Conservation\ Payment_T = \mathrm{E}[C_T] + P_T$$
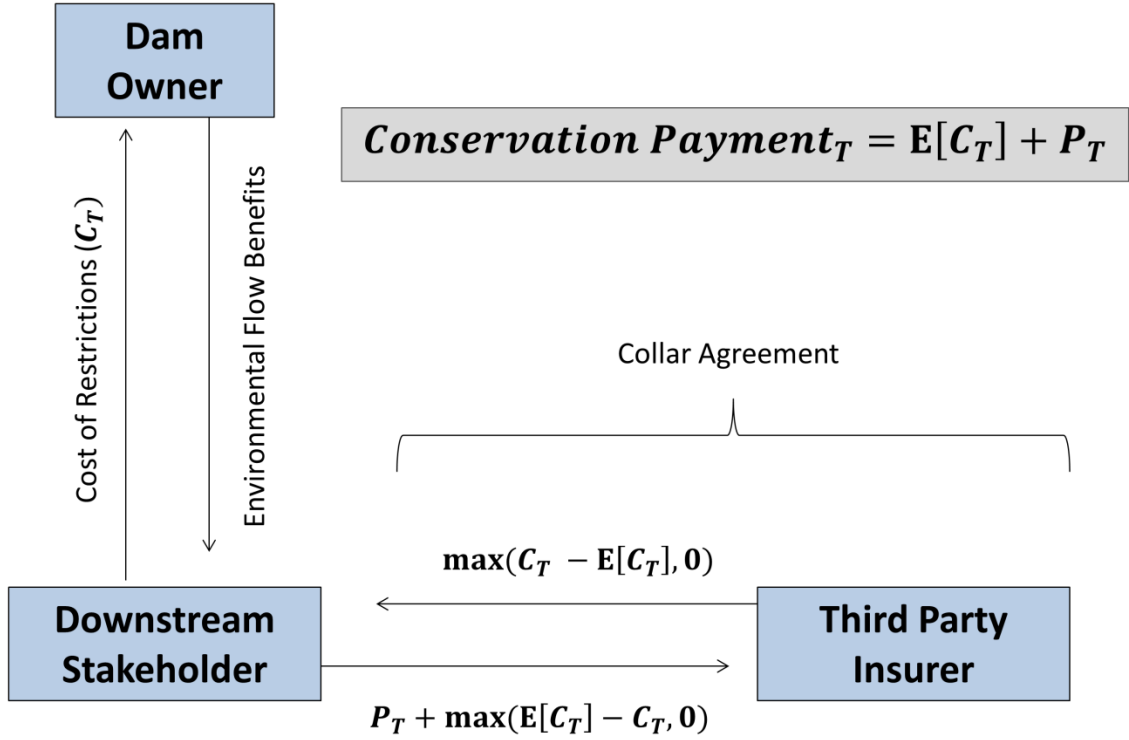
Figure 25. Schematic of financial risk management strategy for achieving constant conservation payments.

Contract premiums are calculated on a rolling, seasonal basis one year prior to period T using a method outlined in Wang et al. [23], in which an empirical probability distribution for $Collar_T$ derived from 300 years of synthetic input data is transformed (see Equation 5) in order to account for the "market price of risk". This transform assigns more weight to the risk posed by positive collar payouts (instances when the insurer is paying the downstream stakeholder). Seasonal contract premiums (P_T) are then calculated as the expected value of the net collar payment function after its density function has been altered by the Wang transform (Equation 6).

$$F^*(Collar_T) = Q[\varphi^{-1}(F(Collar_T)) + \lambda] \qquad (5)$$

where, $F^*(Collar_T)$ = risk adjusted probability density function (pdf) of payout function

Q = student T test with n degrees of freedom (n = sample size)

φ = standard normal cumulative distribution function

$F(Collar_T)$ = original pdf of payout function $Collar_T$

λ = market price of risk

$$P_T = E[F^*(Collar_T) *]^* Collar_T \tag{6}$$

Premiums calculated in this manner are said to equal the expected net collar payment plus an additional risk premium determined by the market price of risk (λ). Similar to previous studies that have employed the Wang transform to price index-based insurance products and weather derivatives [23,24,25], here λ is assumed to equal 0.25. For a detailed description of methods used to calculated contract premiums, please refer to Appendix 4, section 2.

3. RESULTS

Results are presented in three sections. In section 3.1, historical changes in the cost of restrictions at Roanoke Rapids Dam are analyzed for the period 2005-2013. In particular, we determine whether recent years of low natural gas prices have resulted in lower costs. In section 3.2, a model for estimating the seasonal cost of restrictions based on the spread between peak and off-peak electricity prices is validated; and in section 3.3, we explore the potential for third party collar agreements to achieve constant conservation payments for purchasers of environmental flow benefits.

3.1. Historical Changes in Cost of Restrictions

Seasonal costs of restrictions at Roanoke Rapids Dam (C_T) were calculated over the period 2005-2013 (Figure 26). The mean trend (fitted via ordinary least squares) decreases from approximately $1.9M/season in early 2005 to around $0.5M/season at the end of 2013. In particular, a decrease in the mean and volatility of the cost of restrictions occurs in late 2008/early 2009 and is shown to persist throughout the remainder of the time series. This shift coincides with a decline in natural gas prices caused by: 1) a global financial crisis that significantly reduced worldwide economic productivity; and 2) a surge in supply from increased domestic (U.S. and Canadian) production from underground shale deposits, made possible by horizontal hydraulic fracturing [16].
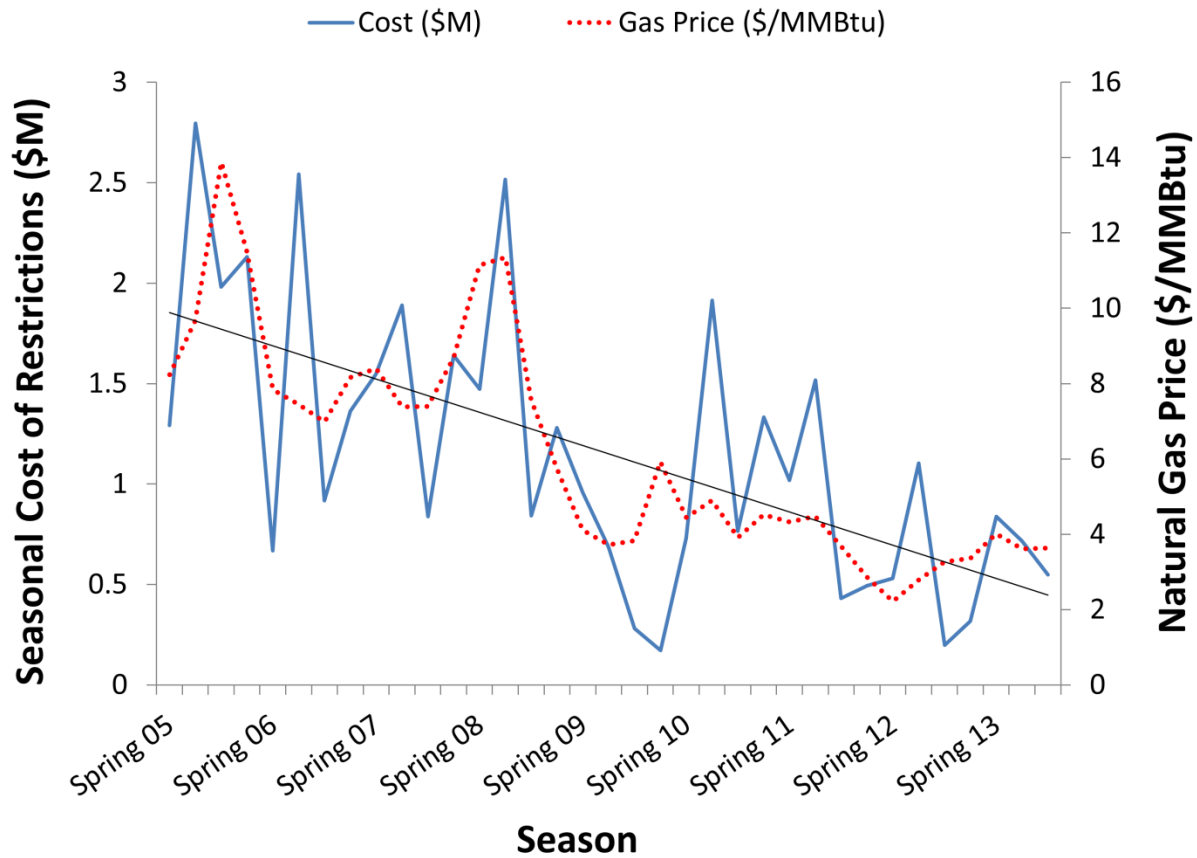
Figure 26. General decline in seasonal cost of restrictions at Roanoke Rapids Dam and natural gas prices over the period 2005-2013.

Clearly, however, the seasonal cost of restrictions at Roanoke Rapids Dam also depends on factors other than natural gas prices, since the cost of restrictions fluctuates significantly around the mean trend and at no point corresponds on a 1:1 basis with changes in natural gas prices. In order to quantify the extent to which gas prices (as well as other factors, such as total hydropower generation (i.e., water availability)) impact the cost of restrictions at Roanoke Rapids Dam, Pearson correlation coefficients were calculated between seasonal costs and several relevant variables (Table 3).

Table 3. Matrix of Pearson correlation coefficients (R) describing relationship between the seasonal cost of restrictions and fuel prices, peak demand, electricity prices, hydropower production at Roanoke Rapids Dam, and price spread.

	Gas Price ($/MMBtu)	Demand (MWh)	Hydro Generation (MWh)	Peak Price ($/MWh)	Spread ($/MWh)	Cost of Restrictions ($)
Gas Price ($/MMBtu)	*1.00*					
Demand (MWh)	0.03	*1.00*				
Hydro Generation (MWh)	0.05	-0.07	*1.00*			
Peak Price ($/MWh)	0.86	0.47	-0.13	*1.00*		
Spread ($/MWh)	0.79	0.54	-0.20	0.97	*1.00*	
Cost of Restrictions ($)	0.70	0.53	-0.13	0.89	0.90	*1.00*

Table 3 highlights a series of linked statistical dependencies that connect changes in gas prices to fluctuations in the cost of restrictions at Roanoke Rapids Dam. First, changes in the price of natural gas are strongly linked to movements in the peak price of electricity ($R = 0.86$). Changes in peak prices in turn act as the primary driver of fluctuations in the spread between peak and off-peak prices ($R = 0.97$); and the price spread is shown to be a critical factor in determining the seasonal cost of restrictions at Roanoke Rapids Dam ($R = 0.90$). The direct correlation between natural gas prices and the cost of restrictions is shown to be $R = 0.70$ (we thus estimate that natural gas prices explain roughly $R^2 = 49\%$ of the seasonal variability in the cost of restrictions). This result strongly suggests that lower natural gas prices, driven in part by advances in drilling technology, have caused a reduction in the cost of implementing ramp rate restrictions at dams.

Table 3 also shows that, in addition to natural gas prices, seasonal variability in electricity demand is an important driver of the price spread ($R = 0.54$), and thus also the overall cost of restricted

operations at the dam (R = 0.53), with higher costs more likely to occur in high demand seasons (i.e., winter and summer). Although water availability (i.e., seasonal hydropower generation) is a critical contributing factor to the cost of restricted operations at the dam, the non-linear relationship between hydropower generation and the cost of restricted operations (described in section 2.2.1) leads to a very weak linear relationship between these two variables.

Figure 27 maps the seasonal cost of restrictions (C_T) over the period 2005-2013 according to price spread (x-axis) and seasonal generation at Roanoke Rapids Dam (y-axis). This figure reaffirms the linear relationship found between the cost of restrictions and price spread, with costs at a given generation level increasing as a function of price spread. The non-linear quality of the relationship between seasonal hydropower generation and the cost of restrictions is also evidenced somewhat by the lowest costs at each price spread generally occurring at higher or lower generation levels, and the highest costs at each price spread occurring at intermediate generation levels.
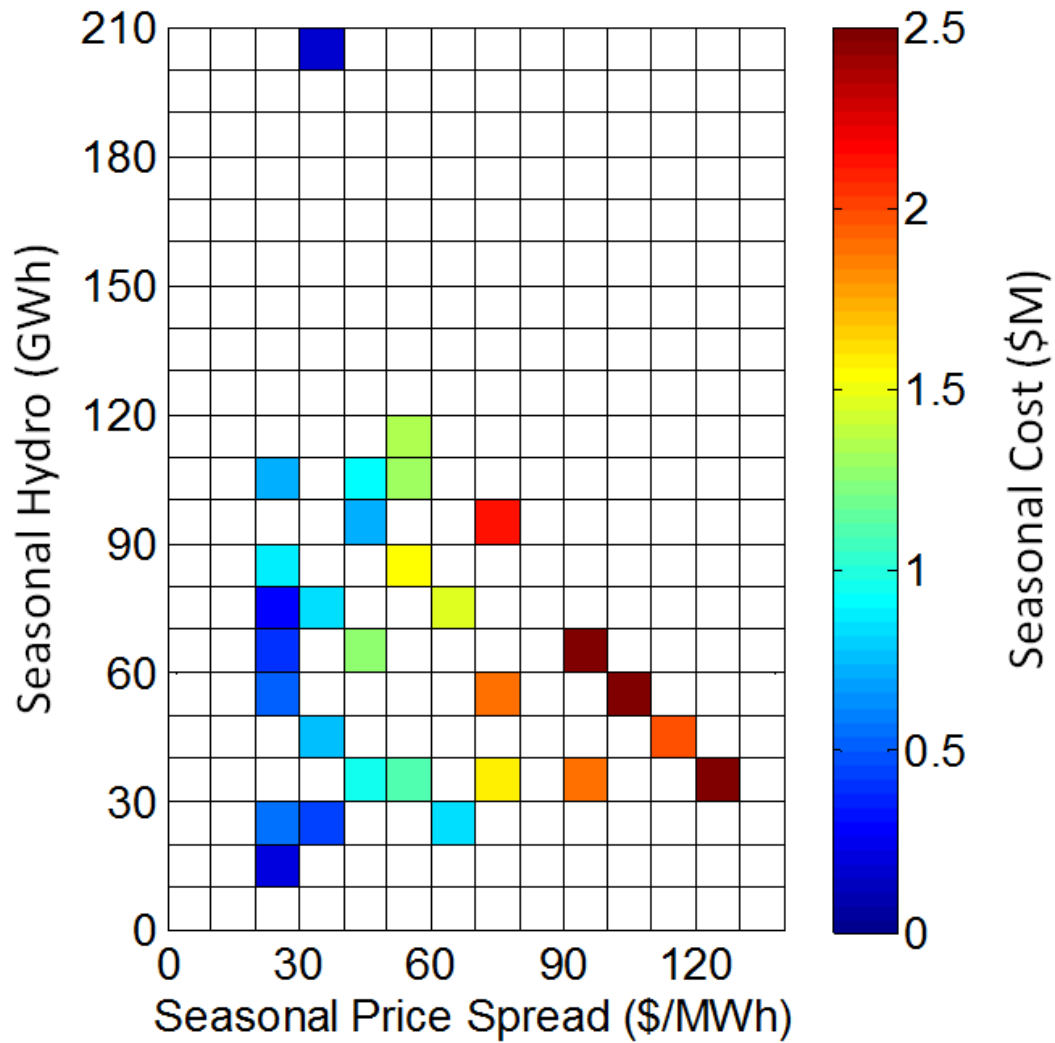
Figure 27. Seasonal cost of restricted operations as a function of total hydropower generation (GWh) and spread between peak and off-peak electricity prices ($/MWh) for the period 2005-2013.

3.2. Cost Model

Cost data for the period 2005-2013 was used to calibrate a model that estimates the seasonal cost of restrictions at Roanoke Rapids Dam based on total hydropower generation and the price spread (see Equation 2). Figure 28 shows a three dimensional representation of the calibrated model. For any given price spread, estimates of seasonal cost ($\widehat{C}_T$) change as a function of total hydropower generation in a non-linear manner: the lowest cost values occur at high and low generation levels, while the highest cost

values occur at intermediate generation levels (i.e., when total hydropower generation is around 95GWh). Maximum possible costs increase as a function of price spread, as does the sensitivity of seasonal costs to different levels of hydropower generation. Likewise note that hydrologic conditions regulate the sensitivity of seasonal costs to the price spread (for example, during extremely wet or dry hydrological conditions, price spread has little influence on costs).
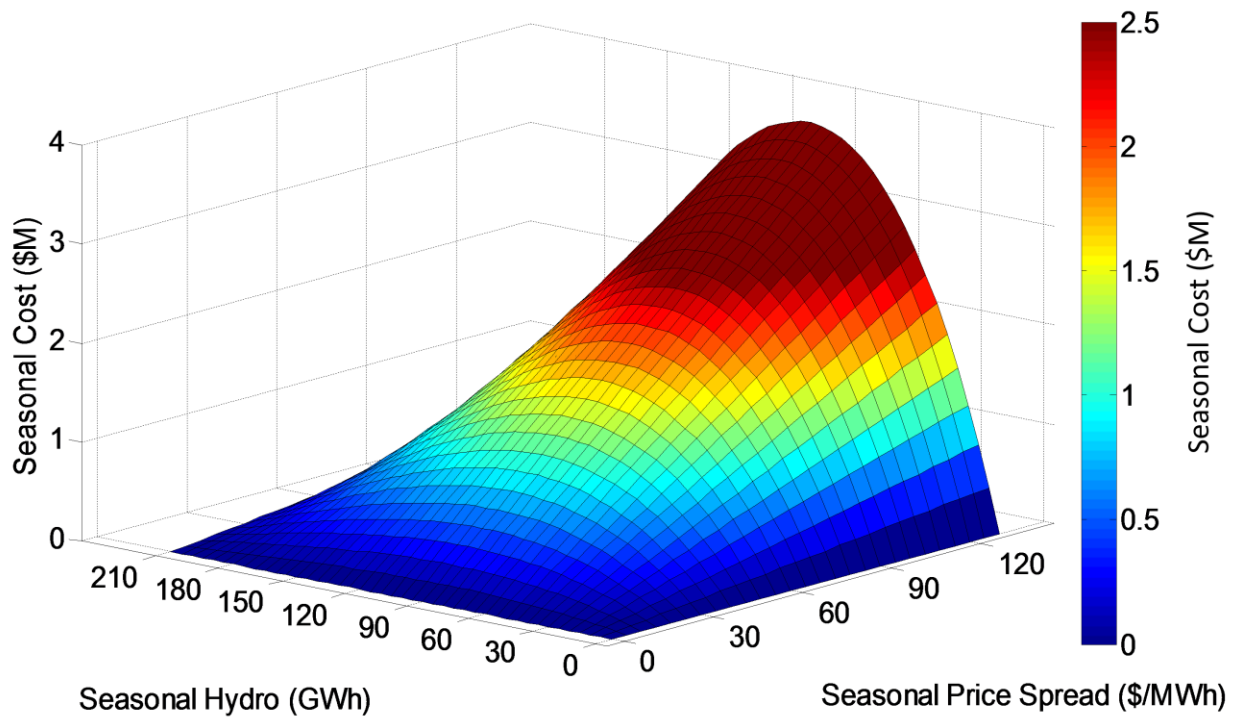
Figure 28. Model of seasonal cost of restricted operations at Roanoke Rapids Dam as a function of total hydropower generation and price spread.

Figure 29 compares historical seasonal costs (C_T) for the period 2005-2013 alongside estimates produced using the cost model; results suggest that the cost model has a high capacity for reproducing the historical times series of seasonal costs, with $R^2 = 0.91$ and MSE of \$158,000/season (13% of $E[C_T]$).
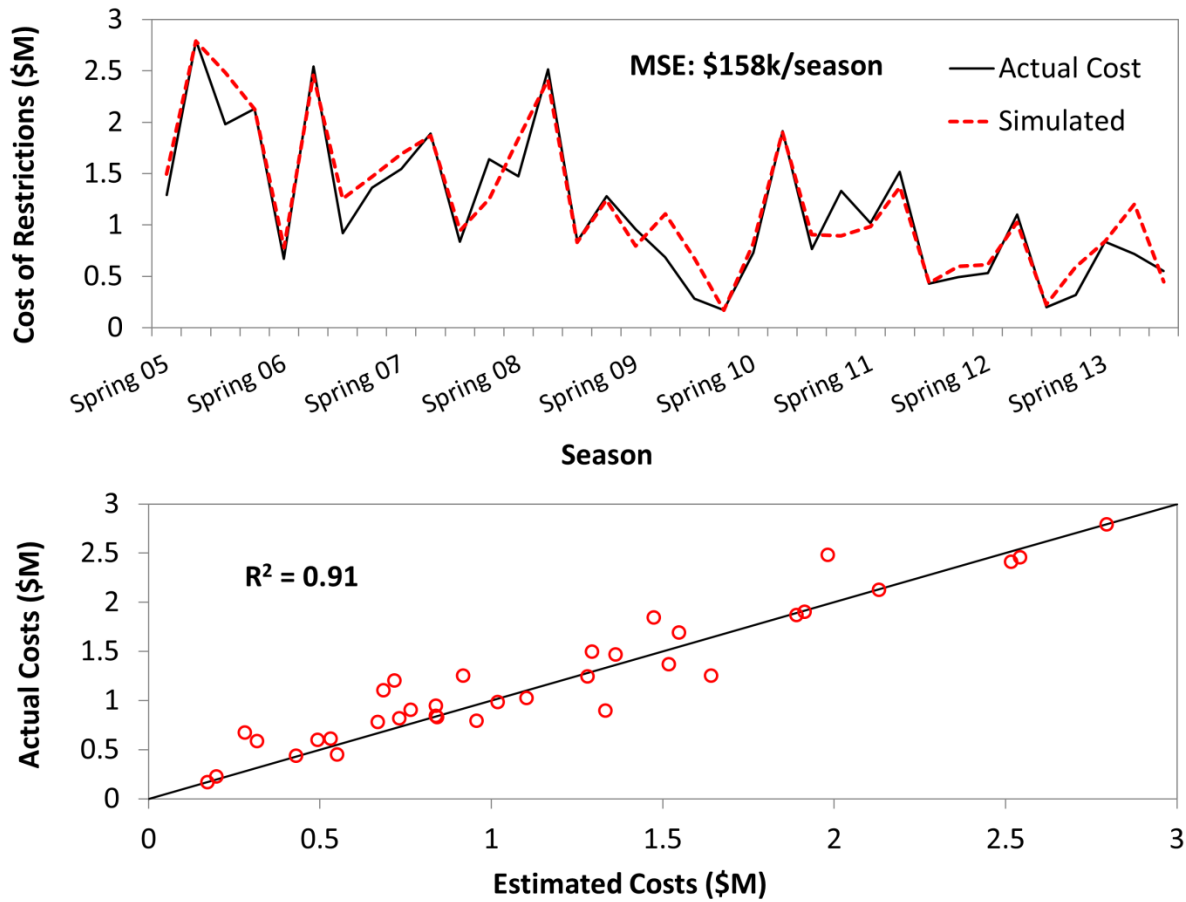
Figure 29. Actual and estimated seasonal costs of restricted operations using cost model calibrated with historical hydropower generation and price spread data from 2005-2013.

3.3. Financial Hedging Strategy

The financial hedging strategy shown in Figure 25 (i.e., a collar agreement between a downstream stakeholder and a third party insurer) was implemented over the period 2005-2013, with collar payments triggered by fluctuations in the seasonal (or "spot") cost of restrictions at Roanoke Rapids Dam (C_T) (see Equation 3). Table 4 shows the results of this arrangement in terms of the mean and standard deviation of net payments (see Equation 4) made by a hypothetical downstream stakeholder who has agreed to send make-whole payments to the dam owner in exchange for the implementation of

restricted operations. Results shown are for contracts "signed" one year prior to season T that entail coverage for one full calendar year (four consecutive seasons).

Note that since the use of third party insurance requires the downstream stakeholder to pay a premium regardless of the net exchange of funds in the collar agreement, the average net seasonal payment under the third party contract ($1.34M) is higher than the expected spot cost of restrictions ($E[C_T]$) ($1.15M). The average seasonal premium associated with the collar agreement was calculated to be $190,000, or about 16.5% of the expected spot cost of restrictions. In exchange for this premium, however, the collar agreement provides to the downstream stakeholder a significant decrease in the seasonal variability of net payments (the standard deviation is reduced from $0.69M to $0.19M). The collar agreement also reduces the downstream stakeholder's exposure to very large single season payments (the maximum payment falls from $2.8M to $1.58M).

Table 4. Effect of collar agreement on net seasonal payments paid by downstream stakeholder over the period 2005-2013.

	Mean ($M)	Standard Deviation ($M)	Min ($M)	Max ($M)
Without Collar	1.15	0.69	0.17	2.80
With Collar	1.34	0.19	0.99	1.58

Figure 30 shows net seasonal payments for the downstream stakeholder with and without the collar agreement over the period 2005-2013. The collar agreement enables the downstream stakeholder to make lower net payments when C_T is high (collar payments are used to defray costs above $E[C_T]$); but it increases net payments for the downstream stakeholder when C_T is low.
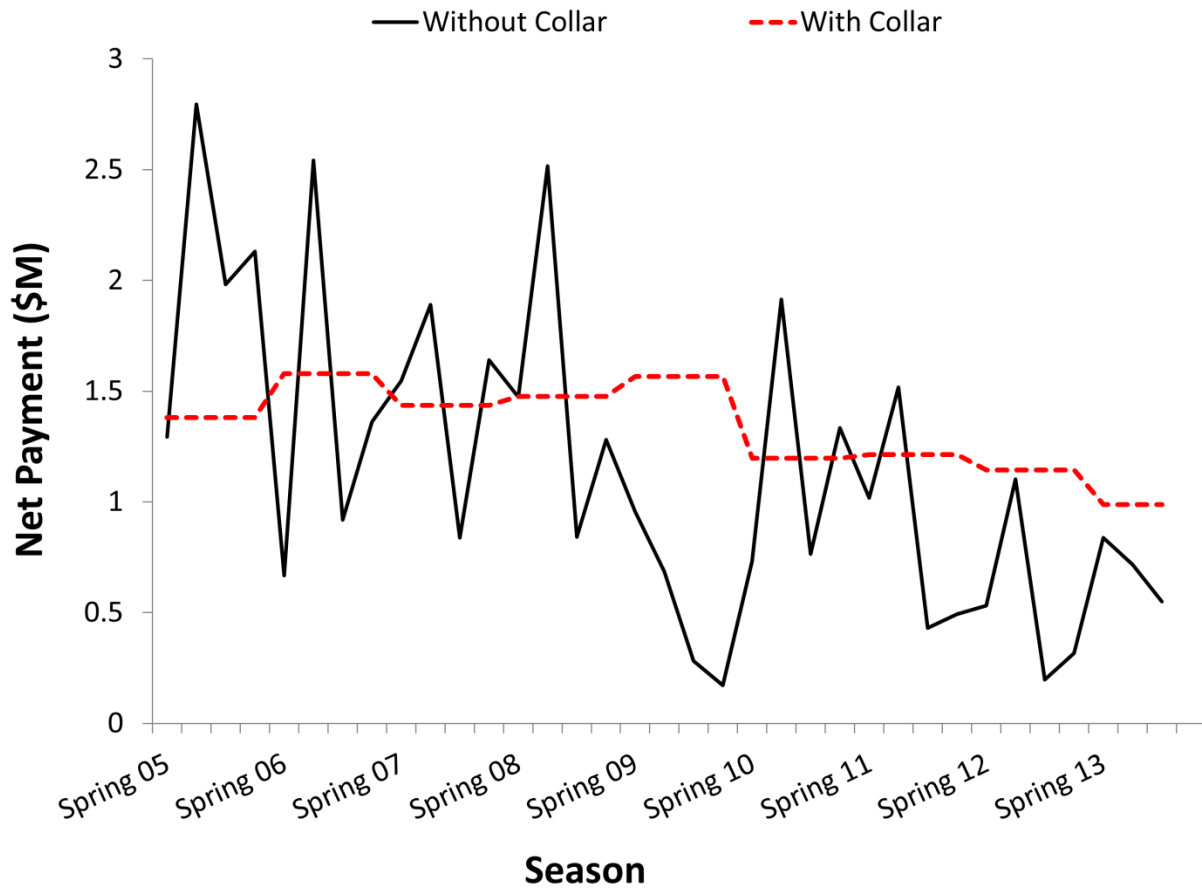
Figure 30. Seasonal net payments with and without a collar agreement for the period 2005-2013.

4. CONCLUSIONS

Findings from this study confirm that the mean cost of restricted operations at Roanoke Rapids Dam decreased over the period 2005-2013, and that this decrease is strongly associated with a narrower spread between peak and off-peak electricity prices caused by low natural gas prices. In addition to the price spread, year-to-year changes in hydropower generation at the dam are also identified as a primary factor driving fluctuations in the cost of restrictions. Although natural gas prices have in recent years been near a 20-year low point, we suggest that, based on historical variability in gas prices and hydrological conditions in this region, the cost of restrictions at the dam is susceptible to large year-to-year fluctuations in the future.

With this in mind, we also evaluated the use of third party hedging agreements to help a hypothetical downstream stakeholder reduce year-to-year financial uncertainty associated with the purchase of environmental flow benefits (operational restrictions) from an upstream dam owner. Results suggest that for a relatively small premium (16.5% of expected costs), the downstream stakeholder can dramatically reduce fluctuations in net payments and eliminate their risk of having to make very large payments in any given year. Although this type of hedging strategy increases mean net payments for the dam stakeholder, the corresponding improvement in financial certainty may be important in setting up multi-year exchanges between conservation organizations and dam owners.

In considering prospective sites for the implementation of exchanges between dam owners and downstream stakeholders, it is important to note that the costs of ramp rate restrictions at large dams are likely to be much greater than those of smaller dams. In addition, third party insurers may be reluctant to engage in collar agreements if seasonal reservoir inflows (hydropower production) are subject to manipulation by the dam owner or a different upstream water user. As a result, the best sites for the implementation of exchanges (along with third party collar agreements) may be smaller headwater projects, where the cost of restrictions is reduced and inflows can be considered unregulated.

Results from this analysis represent an improved understanding of how different underlying factors contribute to variability in the cost of ramp rate restrictions at dams and provide a framework for making more accurate estimates of the long-term costs of these restrictions that can be included in dam relicensing discussions. In addition, the demonstrated potential of collar agreements in reducing financial uncertainty for purchasers of environmental flow benefits provides the basis of another viable pathway (outside of the FERC relicensing process) for the restoration of sub-daily variability in river flows.

REFERENCES

[1] Cushman, R.M. 1985. Review of ecological effects of rapidly varying flows downstream from hydroelectric facilities. North American Journal of Fisheries Management 5: 330–339.

[2] Blinn, W., Shannon, JP., Stevens, LE., Carder, JP. 1995. Consequences of fluctuating discharge for lotic communities. Journal of the North American Benthological Society 14: 233–248.

[3] Freeman, M.C, Bowen, Z.H, Bovee, K.D, and Irwin, E.R. 2001. Flow and habitat effects on juvenile fish abundance in natural and altered flow regimes. Ecological Applications 11: 179–190.

[4] Grand, T.C, Railsback, S.F, Hayse, J.W, and Lagory, K.E. 2006. A physical habitat model for predicting the effects of flow fluctuations in nursery habitats of the endangered Colorado pikeminnow (Ptychocheilus lucius). River Research and Applications 22: 1125–1142.

[5] van Looy K, Jochems H, Vanacker S, Lommelen E. 2007. Hydropeaking impact on a riparian ground beetle community. River Research and Applications 23: 223–233.

[6] Duffield, J.W., C. J. Neher, and T. C. Brown. 1992. ''Recreational Benefits of Insteam Flow: Application to Montana's Big Hole and Bitterroot Rivers.'' Water Resources Research 28 (9): 2169–81.

[7] Loomis, J. B. 1996. ''Measuring the Economic Benefits of Removing Dams and Restoring the Elwha River: Results of a Contingent Valuation Survey.'' Water Resources Research 32 (2): 441–47.

[8] Kotchen, M., Moore, M., Lupi, F., and Rutherford, E. "Environmental Constraints on Hydropower: An Ex Post Benefit-Cost Analysis of Dam Relicensing in Michigan." Land Economics. Vol. 82, No. 3. August, 2006. pp. 384 – 403.

[9] Berrens, R., A. Bohara, H. Jenkins-Smith, C. Silva, P. Ganderton, andD. Brookshire. 1998. ''A Joint Investigation of Public Support and Public Values: Case of Instream Flows in New Mexico.'' Ecological Economics 27 (2): 189–203.

[10] DeShazo, J.R., Freeman, J. 2005. "Public agencies as lobbyists. Columbia Law Review. 105:2217-2309.

[11] Jager, H.I. and M.S. Bevelhimer. 2007. How run-of-river operation affects hydropower generation. Environmental Management 40: 1004-1015

[12] Edwards, B.K., Flaim, S.J., and Howitt, R.E. "Optimal Provision of Hydroelectric Power under Environmental and Regulatory Constraints." Land Economics. Vol. 75, No. 2., May, 1999. pp. 267-283

[13] Harpman, D. "Assessing the Short-Run Economic Cost of Environmental Constraints on Hydropower Operations at Glen Canyon Dam." Land Economics. Vol. 75, No. 3. August, 1999. pp. 390-401.

[14] Palmer, S.C., Burbidge, C., and Patno, H. "The Financial Impacts of the Low Summer Steady Flow Experiment at Glen Canyon Dam." Western Area Power Administration. June, 2004.

[15] US Energy Information Administration. Website. "Natural gas-fired combustion turbines are generally used to meet peak electricity load." http://www.eia.gov/todayinenergy/detail.cfm?id=13191. Accessed January 2014.

[16] McElroy, M., and Lu, Xi. 2013. "Fracking's Future". Harvard Magazine. January-February 2013.

[17] Freshwater Trust. 2014. Website. http://www.thefreshwatertrust.org/projects/. Accessed February 14, 2014.

[18] Kern, J.D., Characklis, G., Doyle, M., Blumsack, S., and Whisnant, R. 2011. "Influence of Deregulated Markets on Hydropower Generation and Downstream Flow Regime." Journal of Water Resources Planning and Management. 138(4). pp. 342-355.

[19] Pearsall, S., McCrodden, B., and Townsend, P. 2005. "Adaptive management of flows in the lower Roanoke River, North Carolina, USA." Environmental Management. 35(4), pp. 353-367.

[20] Whisnant, R., Characklis, G., Doyle, M., Flatt, V., Kern, J. 2009. "Operating policies and administrative discretion at the John H. Kerr projects." A component of a study of operations at the John H. Kerr Project pursuant to Section 216 of Public Law 91-611, University of North Carolina at Chapel Hill, Chapel Hill, NC.

[21] PJM Interconnection. 2013. Website. http://www.pjm.com/markets-and-operations/energy/day-ahead.aspx. Accessed February 2014.

[22] Hull, J. 2005. *Fundamentals of Futures and Options Markets*, 5th ed. Upper Saddle River, NJ: Prentice Hall

[23] Wang, S. 2002. "A Universal Framework for Pricing Financial and Insurance Risks." ASTIN Bulletin. Vol. 32, No. 2. pp. 213-234

[24] Foster, B. and Characklis, G. 2014. "Managing Water Supply Related Financial Risk in Hydropower Production with Index-Based Financial Instruments."

[25] Kern, J.D., Characklis, G.W., Foster, B. Working. "Natural Gas Prices and the Success of Financial Hedging Strategies for Hydropower Producers."

[26] Nowak, K., Prairie, J., Rajagopalan, B., Lall, U. 2010. "A nonparametric stochastic approach for multisite disaggregation of annual to daily streamflow." Water Resource Research. Vol. 46, W08529, doi: 10.1029/2009WR008530

[27] US Energy Information Administration. Website. http://www.eia.gov/naturalgas/data.cfm. Accessed October 2012.

APPENDIX 1: CHAPTER 1

1. Electricity Market Model

The actual generating portfolio in the system of interest (i.e., the Dominion Zone of PJM Interconnection) was modeled using the Environmental Protection Agency's (EPA) 2010 eGrid database, with each generator in the utility's footprint was catalogued by generating capacity (MW), age, fuel type, prime mover and average heat rate (MMBtu/MWh). Specific operating constraints parameters were estimated for each size and type of plant using a range of industry, governmental and academic sources (Table 5). The exact generation portfolio used to simulate wind integration results is shown in Table 6.

1.1 Plant Costs

1.1.1 Electricity

The cost of electricity production at each size and type of thermal power plant in the system was estimated from average heat rates reported in the EPA's eGrid database, as well as information taken from previous industry and academic studies. For illustrative purposes, an example calculation of fixed and variable costs of electricity production at a 254MW coal plant is presented below.

For each type of thermal power plant in the system, applicable heat rate data from previous studies were standardized in terms of an independent variable (percentage of maximum plant output) and a dependent variable (a multiplier of maximum plant efficiency); then, a single, standardized heat rate curve was estimated using a power law or polynomial function. Figure 31 plots heat rate data for coal plants of different sizes from three different sources [25,26,27] along with the standardized heat rate curve determined for all coal plants.

$$y = 0.9796x^{-0.204}$$
$$R^2 = 0.5227$$
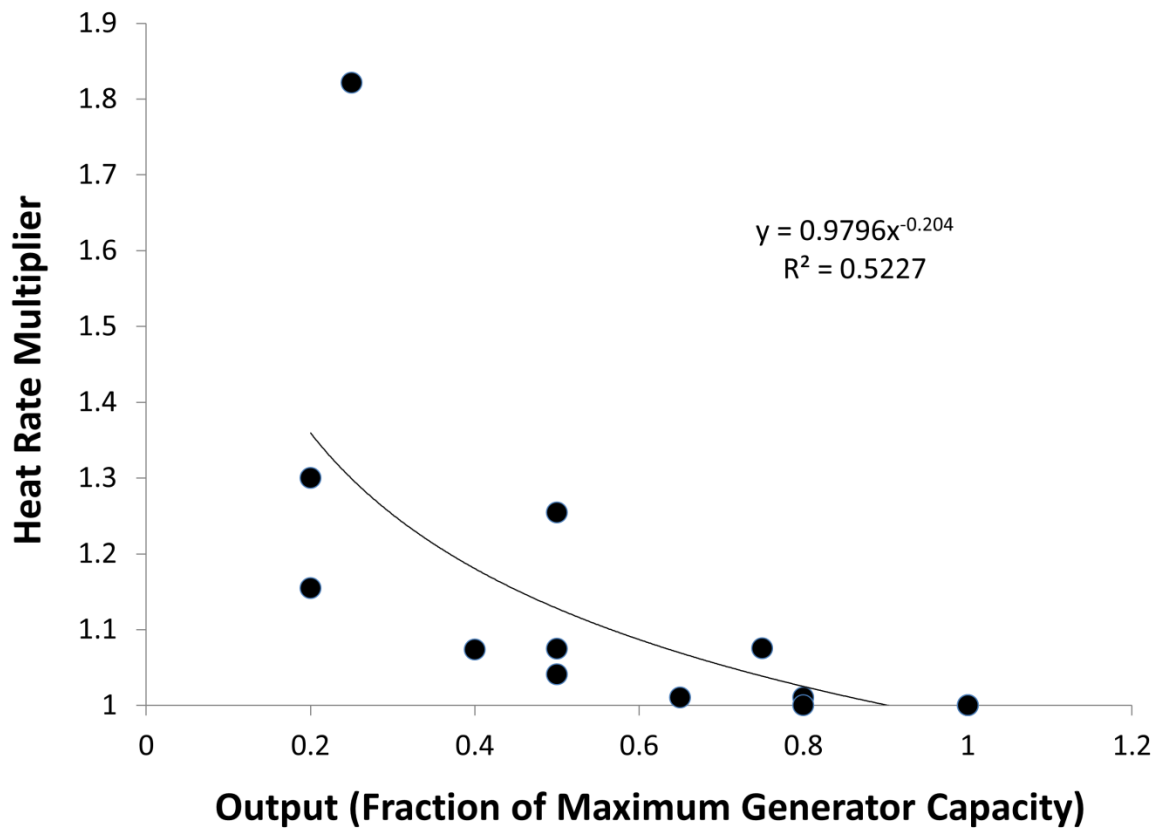
Figure 31. Standardized heat rate curve for all modeled coal plants.

Heat rate curves for each individual thermal plant in the system were then established by multiplying each plant's reported heat rate from the EPA eGrid database times the appropriate standardized curve. For example: the reported average heat rate for the 254 MW coal plant is 10.27 MMBtu/MWh; in order to calculate the heat rate curve for this plant, the standardized curve calculated for all coal plants (shown in Figure 31) was multiplied by 10.27 MMBtu/MWh. Table 7 shows the standardized heat rate curve for all coal plants, as well as the individual heat rate and fuel cost curve for the example 254 MW coal plant, assuming a delivered 2010 cost of coal of $1.62/MMBtu [24].

Since there is great interest in simulating hourly market prices over an entire year for many different wind development scenarios, achieving reasonable solution times for a single iteration of the

electricity market model (i.e., hourly prices for a single 24-hour period) is critical. In order to reduce the number of binary variables in model's sub programs, linear regression was used to represent fuel cost functions for each individual plant ($r^2 > 0.98$ in all cases), yielding constant variable fuel costs. Fixed fuel costs were represented by the y-intercept of the linear cost models. Fixed and variable operations and maintenance (O&M) costs were estimated by plant type using reported information from investor owned utilities [28]. Start costs were estimated from a number of previous academic studies [29,25,26,30].

1.1.2 Reserves

Two costs of power plants' providing reserves were considered: 1) the additional O&M costs associated with ramping activities, which applies to both spinning and non-spinning reserves; and 2) the heat rate penalty associated with producing power at a lower efficiency, which applies only to spinning reserves. For the former, median costs of cycling for thermal plants of different sizes and types were taken from a report funded by the NREL completed by Intertek Aptec [30].

The heat rate penalty that a thermal power plant experiences as a result of providing spinning reserves is a dynamic value that depends on the amount of reserves offered and where the generator is operating along its heat rate curve (i.e., how much electricity it is already producing). For each power plant in the system, the expected value of this dynamic cost was approximated using a matrix (an example for the 254 MW coal plant is shown in Table 8) with the value in each cell equaling:

$$Heat\ Rate\ Penalty_{i,j} = C(i) - \frac{C(i+j)i}{(i+j)} \tag{8}$$

where $C(x) =$ plant fuel costs of producing x MWh

$i =$ electricity production (MWh) specified by row i

$j =$ reserve offer (MW) specified by column j

Equation 8 represents the additional fuel costs associated with producing i MWh of electricity at a higher heat rate, C(i)—i.e., a lower efficiency, because of a j MW reserve offer. The expected value of each column j of Table 8 is the estimated heat rate penalty associated with a reserve offer of that amount. Using similar matrices for each individual thermal plant, cost functions describing reserve offer (MW) vs. heat rate penalty ($) were estimated using linear regression ($r^2 > 0.96$ for all plants). This yielded constant variable heat rate penalties ($/MW), and fixed penalties set by the y-intercept. Total variable costs of spinning reserves were calculated by adding variable heat rate penalties and variable O&M costs ($/MW) attributable to cycling.

1.2 Simplifying Assumptions
1.2.1 Portfolio Clustering

In order to reduce the computational complexity of the EM model's problems, the generation portfolio for the system of interest (i.e., Dominion Zone of PJM) was clustered. In this process, the full portfolio of 68 generators was sorted by fuel type and prime mover into eight categories; each of these eight groups was then partitioned by fixed and variable costs of electricity and reserves using a geometric clustering method, with each cluster of similar generators forming a 'composite' plant. In this manner, the total number of power plants represented (and concurrently, the computational burden of the model) was reduced to a manageable, yet representative, quantity (24)—while total system wide generating capacity remained the same. The number of clusters used was determined heuristically by contrasting results and solution times from the full generating portfolio with those of simplified portfolios. Moreover, nuclear and biomass plants in the system (totaling 4118 MW generating capacity) were assumed to be 'must take resources' for the system and incorporated as demand reduction in the day-ahead electricity market.

1.2.2 Transmission Constraints

Transmission constraints can introduce a critical bottleneck in unit commitment problems that limits the flow of power from one point to another. However, incorporating these limits into a power system model can dramatically increase its computational complexity. Previous studies employing unit commitment problems to investigate the impacts of wind integration on power systems have omitted consideration of transmission constraints, forgoing some level of model detail to enhance its explorative power [31]. Likewise, the electricity model described in this paper disregards transmission constraints and physical power flows among wind sites, power plants and demand centers, in the interest of achieving solution times short enough to simulate hourly results over long periods for multiple scenarios.

1.3 Stochastic Real-time Electricity Demand Model

Real-time electricity demand in each hour is simulated using as the sum of three different factors: 1) unexpected ('forced') outages of scheduled generation capacity; 2) demand forecast errors in the day-ahead electricity market; and 3) positive and negative wind forecast errors:

$$RTDemand_{s,t} = \max(DemErr_t + \sum_j^J OutGen_{t,j} - WindErr_{s,t}, 0) \qquad (9)$$

where, $DemErr_t = $ demand error (actual minus forecasted)in hour t (MWh)

$OutGen_{t,j} = $ Forced capacity outage at generator j in hour t (MW)

$WindErr_{s,t} = $ day ahead wind error in hour t in scenario s (MWh)

$s = $ wind scenario (given region and market penetration)

$t = $ hour in simulation period

$j = $ generator in system portfolio

A stochastic model for simulating demand forecast error in the day-ahead electricity market ($\textbf{\textit{DemErr}}_t$) was constructed using a discrete Markov Chain Monte Carlo method and historical information from PJM regarding day-ahead demand forecast errors. Historical hourly demand forecast error data were converted to histogram form (Table 9)*;* for each bin, sample populations were built describing the 't+1' (next period) error. Normal conditional probability density functions were calculated using the sample means and standard deviations of these t+ 1distributions. Then a Markov Chain model employing truncated versions of the 't+1' probability distributions was used with a random number generator to create a time series simulation of day-ahead demand forecast error in the modeled system. Special consideration was given to accurate reproduction of the standard moments of historical demand forecast errors (Figure 32), as well as their time series characteristics, e.g., autocorrelation (Figure 33). Results show the model does well in both respects.
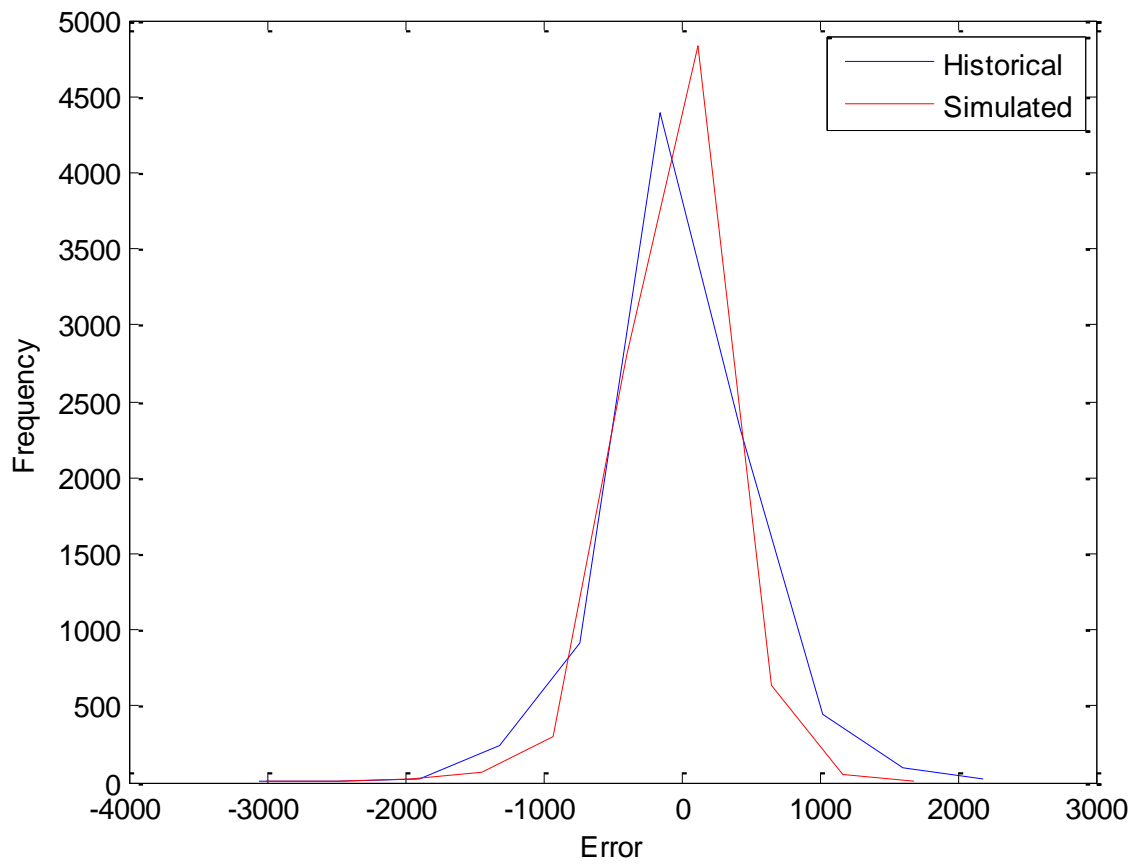
Figure 32. Histograms of historical and simulated day-ahead demand forecast error.
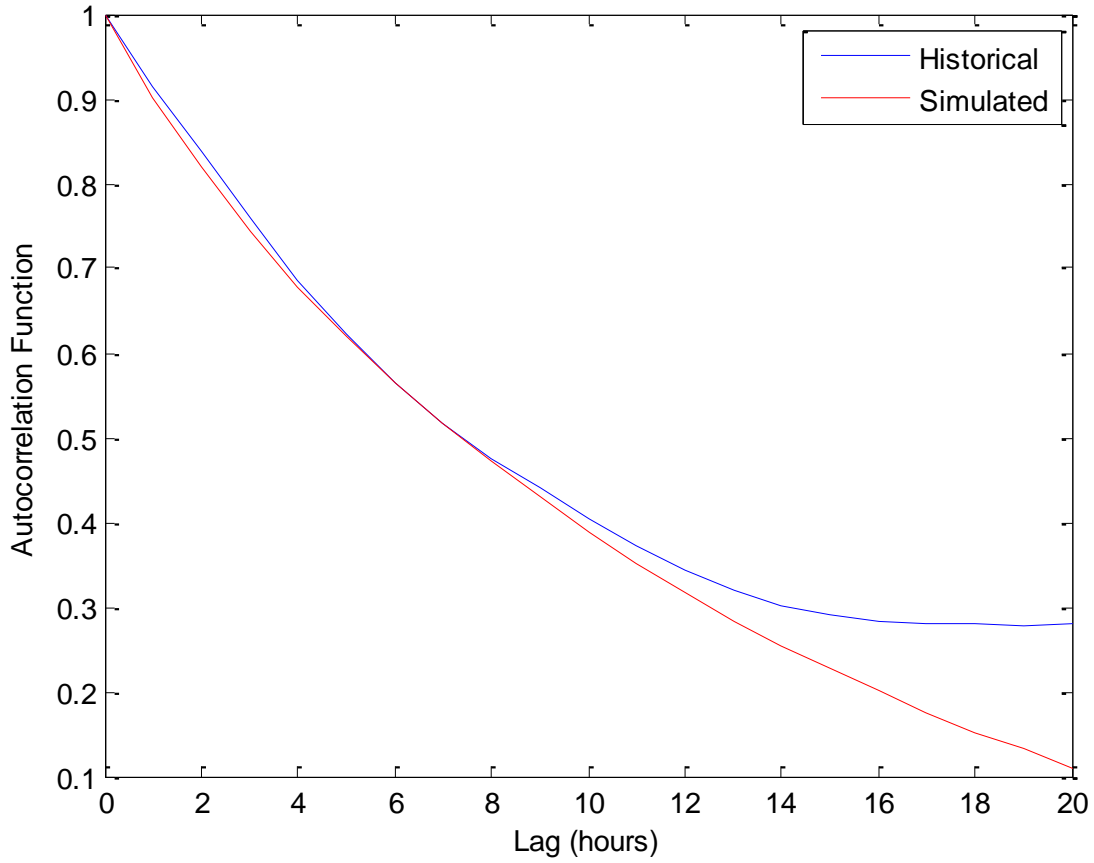
Figure 33. Autocorrelation functions for historical and simulated day-ahead demand forecast error.

In order to simulate forced outage events at power plants in the system (***OutGen**$_{t,j}$*), hourly forced

outage probabilities for each plant are determined using reported rates from the North American Electric

Reliability Corporation [32]. Forced outage rates for each size and type of plant (i.e., # of outages per

1000 service hours) were weighted by lognormal hourly electricity demand, such that the likelihood of a

forced outage event increases during periods of higher plant usage. Time series of weighted outage

probabilities for each plant were then converted to outage signals using Monte Carlo sampling over the

uniform distribution $U(0,1)$, with 24 hour plant maintenance periods assumed when an outage occurs. In

order to isolate the effects of wind energy, the same time series of forced plant outages and historical demand forecast errors are used to calculate real-time electricity demand in each wind scenario.

1.4 Calculation of System Reserve Requirements

Allocating too few generating reserves can expose a system to more frequent and more severe economic losses from 'loss of load'; on the other hand, allocating too many generating reserves can result in higher system costs without any associated increases in reliability [33]. Methods for determining hourly reserve requirements vary by system; but, a general rule is the so called 'N minus 1' criterion, which stipulates that a system operator should reserve enough hourly generating capacity to cover the potential loss of its largest power plant [34]. This level of reserves may suffice to protect a system from loss of load in most contingencies; but due to the variability and unpredictability of wind speeds, maintaining system reliability while integrating wind energy will require utilities to reserve generating capacity beyond current levels [35].

An approach similar to those of [20] and [21] is used to determine hourly reserve requirements under wind development. Each scenario tested assumes a static base level reserve requirement (consistent with an N minus1 criterion). In addition, each wind scenario includes an additional dynamic reserve component beyond the N minus 1 criterion, set as a fixed percentage of forecasted wind energy in each hour. The total hourly system reserve requirement for each scenario is calculated as:

$$Reserve_{s,t} = NM1 + \alpha_s * WindFor_{s,t} \tag{10}$$

where, $s =$ a given wind scenario

$t =$ hour in simulation

$NM1 =$ static N $-$ 1 reserve requirement

$\alpha_s =$ Fixed percentage specified for scenario s

$WindFor_{s,t}$ = wind energy forecasted for hour t in scenario s

Fixed percentages for each respective wind scenario ($\boldsymbol{\alpha_s}$) are determined using the stochastic model for real-time electricity demand described in section 1.3 of this Appendix. For each wind scenario tested, hourly real-time electricity demand is simulated over 300 discrete, year long periods. Then, a value of $\boldsymbol{\alpha_s}$ is identified that yields a loss of load probability (LOLP) equivalent to that of baseline conditions (i.e., a system with no wind capacity).

$$LOLP = \frac{\sum_{t=1}^{T} \gamma_{s,t}}{T} \tag{11}$$

where, $\gamma_{s,t} = \begin{cases} 1, & if\ Reserve_{s,t} < RTDemand_t \\ 0, & otherwise \end{cases}$

t = hour in simulation

T = number of hours in simulation period

Wind reserve requirements ($\boldsymbol{\alpha_s}$) generally increase with greater installed wind power capacity, because negative wind forecast errors become more severe and require higher levels of reserves to maintain baseline reliability. Values of $\boldsymbol{\alpha_s}$ calculated using the EM model and EWITS data from five separate geographical regions suggest that an average daily wind market penetration of 5% would require additional reserves equivalent to 7 to 10% of forecasted wind energy (i.e., $\boldsymbol{\alpha_s}$ = 0.07 to 0.10); while a market penetration of 25% would require additional reserves equivalent to 10 to 25% of forecasted wind energy (i.e., $\boldsymbol{\alpha_s}$ = 0.10 to 0.25), depending on source region and geographical distribution.

1.5 Unit Commitment Problem

The solution of a single iteration of the unit commitment (UC) problem, which co optimizes the provision of day-ahead electricity and reserves to meet forecasted demand in each market, is bound by a number of system wide and plant specific constraints. Most of the constraints imposed by the UC problem on individual generators reflect plant specific operating parameters. These include: maximum generating capacity, minimum ('turn down') generating capacity, ramp rate, and minimum up and down times. Another important constraint that applies to the day-ahead problem concerns its use of a single market for allocating both spinning and non-spinning reserves. In reality, a system may distinguish between reserves used to meet real-time electricity demand occurring as a result of demand forecast error (e.g., spinning reserves) and reserves used to respond within minutes to the sudden loss of generating capacity (non-spinning reserves) [35]. Although a single market for reserves is represented in this study, the UC problem is bound by a constraint that 50% of hourly demand for reserves must be met by spinning reserves, i.e., unused capacity that is already online in the day-ahead electricity market or hydropower, a rule shared by other large electric power systems [36].

The provision of reserves by an individual power plant is limited by its ramp rate. In addition, startup times affect a power plant's ability to provide non-spinning reserves. Coal fired and natural gas combined cycle generators, both of which are assumed to have start up times longer than one hour, can only provide reserves if they are already online [37]. Natural gas and oil combustion turbines have quicker start up times and are able to provide spinning or non-spinning reserves; hydropower is also able to provide either type of reserve.

1.5.1 Full Mathematical Formulation

Time series parameters and decision variables for the UC problem are described in Tables 10 and 11, respectively. Constraints are described in Table 12.

Objective Function:

$$\text{Minimize } Z_{DayAheadCosts} \sum_{t=1}^{96} \sum_{j}^{J} [(DAMWh_{t,j} * VC_j) + (ON_{t,j} * FC_j)$$

$$+ (SRVMW_{t,j} * VCSR_j) + (SRVON_{t,j} * FCSR_j) + (NRVMW_{t,j} * VCNR_j)$$

$$+ (START_{t,j} * SC_j)]$$

$where$, t = hour in planning horizon $\in \{1,2,\dots 96\}$

j = generator in system portfolio

Subject to Constraints:

1. $ON_{t,j} = InitialON_j$
2. $DAMWh_{t,j} = InitialMWh_j$
3. $\sum_{j}^{J} DAMWh_{t,j} \geq DADemand_t$
4. $DAMWh_{t,j} \leq ON_{t,j} * MaxCap_j$
5. $DAMWh_{t,j} \geq ON_{t,j} * MinCap_j$
6. $\sum_{j}^{J} SRVMW_{t,j} + \sum_{j}^{J} NRVMW_{t,j} \geq RVDemand_t$
7. $\sum_{j}^{J} SRVMW_{t,j} \geq 0.5 * RVDemand_t$
8. $SRVMW_{t,j} + NRVMW_{t,j} \leq RRate_j$
9. $SRVMW_{t,j} \leq SRVON_{t,j} * RRate_j$
10. $NRVMW_{t,j} \leq NRVON_{t,j} * RRate_j$
11. $DAMWh_{t,j} \geq SRVON_{t,j} * MinCap_j$
12. $DAMWh_{t,j} \geq NRVON_{t,j} * MinCap_j$
13. $DAMWh_{t,j} + SRVMW_{t,j} + NRVMW_{t,j} \leq MaxCap_j - PlannedOutage_{t,j}$
14. $DAMWh_{t,j} - DAMWh_{t-1,j} \leq RRate_j$
15. $DAMWh_{t-1,j} - DAMWh_{t,j} \leq RRate_j$
16. $ON_{t,j} - ON_{t-1,j} \leq ON_{k,j}$
17. $ON_{t-1,j} - ON_{t,j} \leq 1 - ON_{k,j}$
18. $START_{t,j} \geq ON_{t,j} - ON_{t-1,j}$

19. $\sum_{t}^{T} \frac{DAMWh_{t,j} + SVMW_{t,j} + NVMW_{t,j}}{TurbineEfficiency_j} + \sum_{t}^{T} ReservoirSpill_{t,j} \leq Available\ Storage$

$20. \sum_{t}^{t+23} \frac{DAMWh_{t,j}+SVMW_{t,j}+NVMW_{t,j}}{TurbineEfficiency_j} \leq Available\ Storage$

1.6 Economic Dispatch Problem

The primary constraint on the solution of the economic dispatch problem is that the system must exhaust its hourly supply of reserves before selecting other resources to help meet real-time electricity demand. In addition, the amount of real-time electricity provided by any plant in a given hour must be less than or equal to its concurrent offer in the reserves market.

1.6.1 Full Mathematical Formulation

Time series parameters and decision variables for the economic dispatch problem are described in Tables 13 and 14, respectively. Constraints are described in Table 15.

Objective Function:

$$Minimize\ Z_{RealTimeCosts}: \sum_{t=1}^{24} \sum_{s}^{S}(RTMWh_{t,s} * VC_s)$$

$$+ \sum_{t=1}^{24} \sum_{n}^{N}[(RTMWh_{t,n} * VC_n) + (RTON_{t,n} * FC_n) + (START_{t,n} * SC_n)]$$

where, $t =$ hour in planning horizon $\in \{1, 2, \dots 24\}$

$p =$ generator in spinning reserves portfolio

$n =$ generator in non-spinning reserves portfolio

Subject to Constraints:

21. $rtON_{t,n} = InitialON_n$
22. $\sum_{n}^{N} RTMWh_{t,n} + \sum_{s}^{S} RTMWh_{t,s} \geq RTDemand_t$
23. $RTMWh_{t,n} \leq rtON_{t,n} * NRVMW_{t,n}$

24. $RTON_{t,n} \geq rtON_{t,n} - ON_{t,n}$

25. $RTSWITCH_{t,n} \geq RTON_{t,n} - RTON_{t-1,n}$

26. $RTMWh_{t,s} \leq SRVMW_{t,s}$

2. Reservoir System Model

2.1 Hourly Natural Flow Model

The hourly river flow model uses cross correlation functions calculated for pairs of subsequent (upstream and downstream) United States Geological Survey (USGS) stream gages to estimate expected travel times (and likewise, flow speeds) for river segments throughout the Roanoke River basin. Average flow speeds are then used to extrapolate hourly inflows to John H. Kerr Reservoir, as well as natural flows at the present day site of Roanoke Rapids Dam.

Given simultaneous hourly flow records at a pair of successive (upstream and downstream) gages on the same river, their sample cross correlation function $r_{xy}(k)$ can be calculated as follows:

$$r_{xy}(k) = \frac{c_{xy}(k)}{s_x s_y} \qquad\qquad (12)$$

where, $c_{xy}(k) = \frac{1}{n}\sum_{t=1}^{n-k}(x_t - \bar{x})(y_{t+k} - \bar{y})$

$s_x = \sqrt{c_{xx}(0)}$

$s_y = \sqrt{c_{yy}(0)}$

$k = \{0, 1, \dots \text{hours}\}$

$x = $ upstream gage

$y = $ downstream gage

$n = $ length of hourly time series

137

The hourly lag (member of k) yielding the highest sample cross correlation ($r_{xy}(k)$) between the two flow records approximates t_{xy}, or the average time required for water to flow from the upstream (x) to downstream (y) site. The average flow speed for the gage pair (sp_{xy}) can then be calculated as d_{xy} (measured stream length from x to y) divided by t_{xy}. Assuming a constant flow speed and a Lagrangian frame of reference in which individual parcels of hourly flow experience no inter blending, flows at a downstream location in future time period (f_t) are estimated using recorded flows from an upstream gage.

$$f_t = g_{t-\tau} \tag{13}$$

where, g_t = recorded flow at an upstream gage site in hour t

$\tau = \dfrac{d}{sp_{xy}}$, travel time for water to flow from upstream gage site (hours)

d = distance between gage site x and downstream simulation site (km)

The methodology described above is used by the hourly natural flow model to simulate inflows to John H. Kerr reservoir, as well as pre-dam flows at the present day site of Roanoke Rapids Dam. Pairs of successive US Geological Survey (USGS) gages were selected for the Staunton and Dan Rivers, which collectively contribute 90% of the inflows reaching upstream John H. Kerr Reservoir from the upper basin. Hourly flow records for the period 2005 to 2010, as well as stream distances measured in ArcGIS, were used to estimate flow speeds for both rivers. Figure 34 shows historical hourly flows at the furthest downstream USGS stream gage on the Staunton River (#2066000) alongside simulated flows at the same site, which were extrapolated using cross correlation analysis from a second USGS gage 42km upstream (#2062500). Linear regression of the two time series for the period 2005 to 2010 yields an $r^2 = 0.92$. Results for the gage pair selected on the Dan River reveal a similarly high level of predictive capacity ($r^2 = 0.89$). No pairs of gages are available for the Bannister or Hyco Rivers, so flow speeds for these rivers

are assumed to be an average of values for the Staunton and Dan Rivers, weighted by contributing flow volume.
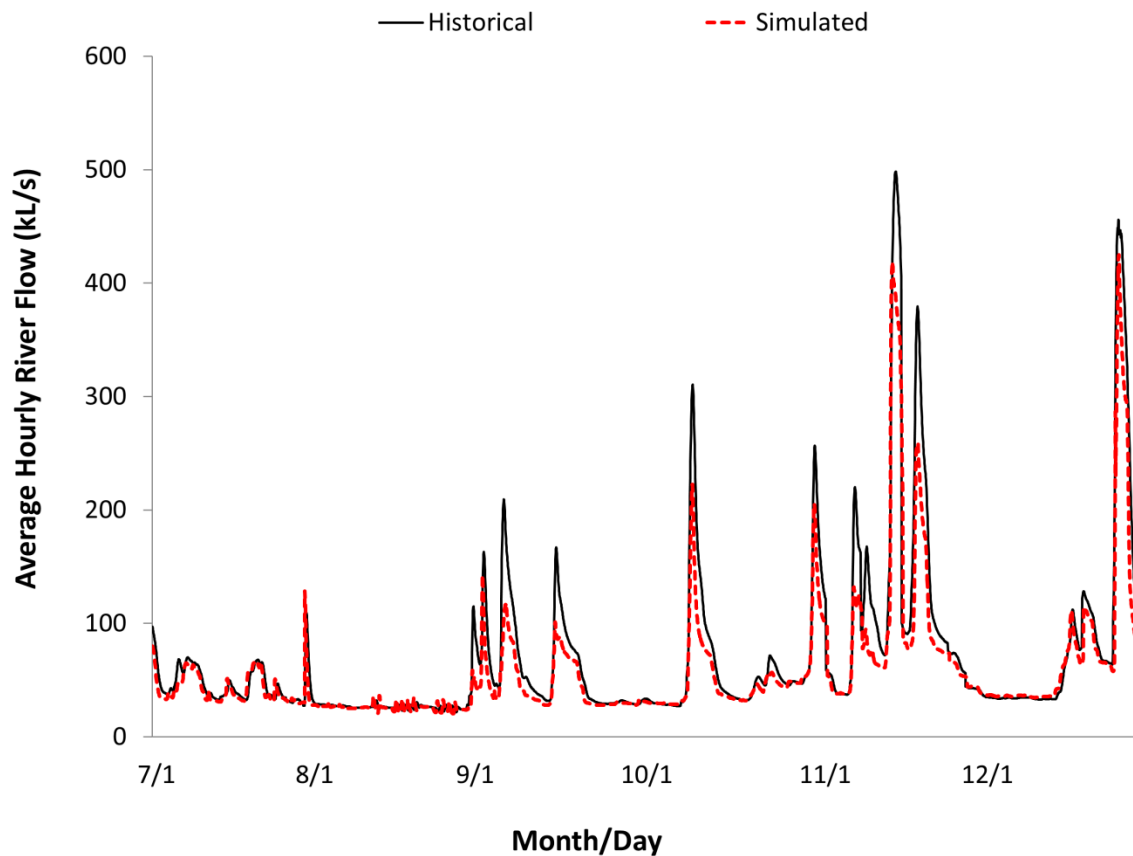
Figure 34. Historical vs. Simulated Hourly Flows at USGS gage 2066000, for the period 7/1/2006 – 12/31/2006. Simulated flows are extrapolated from USGS gage 2062500 (42km upstream) using cross correlation analysis.

Hourly flows at the confluence of the four rivers are estimated, employing: 1) one USGS gage for each river, located just upstream of the confluence; 2) calculated flow speeds for each individual river; and 3) stream distances measured in ArcGIS. Pre dam flows at the present day site of Roanoke Rapids Dam are simulated in a similar manner, using the weighted average flow speed of the Staunton and Dan Rivers.

It is important to note that this technique does not incorporate runoff from floodplain areas adjacent to the river or the contribution of unrecorded downstream tributaries. As a result, the model underestimates flows at downstream sites, particularly during high magnitude flow events. Although linear regression of historical and simulated weekly inflows to Kerr Reservoir show an $r^2 = .95$, total annual inflows are underestimated by 11%. It is likely, therefore, that the hourly flow model under predicts the magnitude of pre dam flows at the site of Roanoke Rapids Dam. Nonetheless, cross correlation analysis provides an accurate representation of natural flow dynamics (i.e., hourly and daily variability) for present day dam sites. If characterizing flow dynamics under a variety of wind development scenarios were a central modeling focus, relatively small errors in flow volume would be deemed an acceptable cost.

2.2 Hourly Hydropower Dispatch Model

The hydropower dispatch model's core optimization program has perfect foresight regarding day-ahead electricity and reserve prices within each discrete planning horizon, i.e., for hours $t = 1,2,...96$, as well as perfect foresight regarding real-time electricity prices for hours $t = 1,2,...24$. In general, forecasts of day-ahead electricity prices in wholesale markets demonstrate mean absolute error of (3 to 20%) [38]. Real-time electricity prices, which depend on stochastic elements like forced outages and forecast errors, are more difficult to predict. A result of assigning the hydropower dispatch model enhanced foresight regarding real-time market prices is that reservoir release schedules simulated by the hydropower dispatch model may not always reflect decisions that a dam operator would make under uncertainty. Rather, they should be viewed as an upper bound on a dam operator's ability to respond to financial incentives.

2.1.1   Full Mathematical Formulation

Detailed lists of time series parameters, decision variables and constraints for the hourly hydropower dispatch model are contained in Tables 16, 17, and 18.

Objective Function:

$$\text{Maximize Profits: } \sum_{t=1}^{96}(DAMWh_t * DAP_t) + (RVMW_t * RVP_t)$$

$$+ (RTMWh_t * RTP_t) - (ON_t * \text{Fixed Cost}) - (START_t * \text{Start Cost})$$

where, t = hour of operating horizon

Subject to:

1. $ON_t = InitialON$

2. $DAMWh_t + RVMW_t \leq MaxCap$

3. $\sum_{t=1}^{96}(\frac{DAMWh_t + RVMW_t}{\delta} + Reservoir\ Spill_t) \leq \text{Available Storage}$

4. $RTMWh_t \leq RVMW_t$

5. $DAMWh_t + RTMW_t \leq MaxCap * ON_t$

6. $START_t \geq ON_t - ON_{t-1}$

Table 5. List of plant specific operating parameters with descriptions and source material.

Parameter	Description	Source
Minimum Generating Capacity (MW)	Minimum generating capacity that can be sustained by a unit before it must be shut off.	[25,26,39,41]
Minimum Up Time (hrs)	Minimum number of consecutive hours that a unit must run if it is turned on.	[25,26,29,43,47]
Minimum Down Time (hrs)	Minimum number of consecutive hours that a unit must rest if it is turned off.	[25,26,30,39,45,47]
Ramp Rate (MWh/hr)	Maximum hour to hour change in plant electricity output.	[26,39,40,41,44,45,46]
Forced Outage Rate	Probability of unplanned outage at power plant.	[32]
Planned Outage Rate	Probability of planned outage at power plant.	[32]
Start Up Cost ($)	Cost ($) of starting a plant that is off.	[25,26,29,30]
Heat Rate Curves	Plant heat rate (MMBtu/MWh) as function of plant electricity output.	[25,26,27]
Fixed O&M Cost ($)	Fixed operations and maintenance costs accruing while plant is on.	[25]
Variable O&M Cost ($/MWh)	Operations and maintenance costs accruing as a function of plant energy output.	[25,30,42]
Fuel Prices ($/MMBtu)	Price of fuel feedstocks for thermal plants.	[24]

Table 6. Reference generation portfolio based on Dominion Zone of PJM (assuming 2010 prices of coal and natural gas of $1.62/MMBtu and $4.86/MMBtu, respectively).

	$MaxCap_i$ (MW)	$MinCap_j$ (MW)	$MinUp_i$ (hours)	$MinDown_i$ (hours)	$RRate_i$ (MW/h)	VC_i ($/MWh)	$FC_{j/n}$ ($)	$SC_{j/n}$ ($)	$VCSR_i$ ($/MW)	$FCSR_i$ ($)	$VCNR_n$ ($/MW)	$VC_{n/s}$ ($/MWh)
HYD1	208.0	1.0	1	1	208	0.00	1224	400	0.00	0.00	0.00	0.00
HYD2	178.0	1.0	1	1	178	0.00	1306	400	0.00	0.00	0.00	0.00
PSH1	1637.0	1.0	1	1	1637	8.11	5300	450	0.00	0.00	0.00	8.11
COAL1	1918.4	226.0	9	15	226	19.76	6991	84800	5.25	51.87	n/a	17.19
COAL2	440.5	73.5	9	15	88	17.51	2092	22960	5.18	21.08	n/a	14.17
COAL3	3480.4	180.0	24	24	180	18.90	13375	264526	5.39	12.76	n/a	16.94
COAL4	483.8	81.3	17	20	94	18.00	3019	37367	5.26	25.15	n/a	14.66
COAL5	1257.0	180.0	24	24	180	18.88	31397	184779	5.15	20.00	n/a	16.92
COAL6	439.3	58.3	9	15	64	16.60	1372	18230	5.06	14.36	n/a	13.26
COAL7	99.4	18.5	12	17	21	14.58	366	5780	4.77	4.47	n/a	11.24
NGCT1	1462.7	44.7	2	2	536	68.48	13369	22576	2.68	193.98	1.10	67.38
NGCT2	1943.9	10.0	2	2	1944	51.96	9132	200221	2.14	473.50	1.10	50.86
NGCT3	509.1	46.0	2	2	509	75.13	25171	16291	2.79	199.00	1.10	74.03
NGCT4	1813.5	46.0	2	2	676	68.60	18594	91927	2.61	231.00	1.10	67.50
NGCC1	399.0	45.0	4	6	399	29.54	6068	31521	7.28	682.00	n/a	28.90
NGCC2	330.0	42.7	4	6	330	34.77	6867	26070	8.60	676.00	n/a	34.13
NGCC3	480.4	41.2	4	6	255	31.77	4941	23731	7.85	478.71	n/a	31.13
NGCC4	1885.1	35.9	4	6	943	30.93	14428	74741	8.28	1856.02	n/a	30.29
OIL1	104.2	1.0	4	3	104.2	308.73	2191	2649	18.81	283.59	0.60	308.13
OIL2	131.2	1.0	1	1	131.2	229.74	2878.47	768.00	13.99	44.59	0.60	229.14
OIL3	130.4	1.0	4	2	130.4	369.79	2105.54	2649.60	22.59	353.01	0.60	369.19
NUC1	1695											
NUC2	1944											
BIOM1	463											

Key:
HYD = Conventional Hydropower
PSH = Pumped Storage Hydropower
NGCT = Combustion Turbine Natural Gas
NGCC = Combine Cycle Natural Gas
BIOM = Biomass
NUC = Nuclear

Table 7. Calculation of heat rate and fuel cost curves for a 254 MW coal plant with reported eGrid efficiency of 10.27 MMBtu/MWh, assuming a delivered fuel price for coal of $1.62/MMBtu.

Fraction of Maximum Plant Capacity	Individual Plant Output (MWh)	Standardized Heat Rate Multipliers for All Coal Plants	Individual Plant Heat Rate (MMBtu/MWh)	Individual Plant Fuel Costs ($)
0.1	25.4	1.568	16.1	662.48
0.2	50.8	1.361	13.98	1150.50
0.3	76.2	1.253	12.87	1588.72
0.4	101.6	1.181	12.13	1996.50
0.5	127	1.129	11.59	2384.53
0.6	152.4	1.088	11.17	2757.74
0.7	177.8	1.054	10.82	3116.55
0.8	203.2	1.026	10.53	3466.31
0.9	228.6	1.001	10.28	3807.01
1	254	1	10.27	4225.90

Table 8. Expected heat rate penalties associated with provision of reserves for example 254 MW coal plant with minimum generating capacity of 101.6 MW and a ramp rate of 127MW/h.

(i,j)	Reserve Offer (MW)									
	12.7	25.4	38.1	50.8	63.5	76.2	88.9	101.6	114.3	127
101.6	$46.77	$87.68	$123.95	$156.46	$185.87	$212.68	$237.28	$259.99	$281.06	$300.68
127	$45.34	$85.97	$122.74	$156.25	$187.00	$215.39	$241.72	$266.25	$289.20	$310.74
152.4	$44.11	$84.33	$121.23	$155.30	$186.89	$216.33	$243.87	$269.72		
177.8	$43.06	$82.80	$119.66	$154.00	$186.13	$216.29				
203.2	$42.13	$81.38	$118.10	$152.57						
228.6	$41.31	$80.08								
E[]	*$43.79*	*$83.71*	*$121.14*	*$154.92*	*$186.47*	*$215.17*	*$240.96*	*$265.32*	*$285.13*	*$305.71*

Table 9. Historical Day-ahead Demand Forecast Error Probabilities

Period *t* Frequency Histogram			Period *t+1* Conditional Distribution $N(\mu,\sigma)$	
Bins		Frequency	Mean	Variance
3400	3200	5	3222.6	20620.96
3200	3000	5	2808.6	545529.96
3000	2800	2	2938	43222.41
2800	2600	4	2732.5	114446.89
2600	2400	2	2469.5	34077.16
2400	2200	8	2117.9	536263.29
2200	2000	3	1994	109627.21
2000	1800	6	1813.3	99351.04
1800	1600	20	1517.2	232131.24
1600	1400	53	1372.9	109759.69
1400	1200	70	1286.4	73495.21
1200	1000	123	1039.5	106536.96
1000	800	192	827.9	95976.04
800	600	314	612.9	96783.21
600	400	562	455.3	45582.25
400	200	861	248.9	40320.64
200	0	1482	90	25953.21
0	200	2209	53.7	30102.25
200	400	1024	261.6	31612.84
400	600	664	454	44436.64
600	800	390	626.2	70649.64
800	1000	228	759.9	110556.25
1000	1200	98	913.1	166953.96
1200	1400	70	1224	94310.41
1400	1600	20	1415.6	99225
1600	1800	27	1487.4	105820.09
1800	2000	13	1749.9	334199.61
2000	2200	10	1799.3	383037.21
2200	2400	5	2117.4	121452.25
2400	2600	2	2385	510.76

Table 10. UC problem time series parameters.

Parameter	Description
Planned Outage$_{t,j}$ (MW)	Planned outage or derating of generator.
Turbine Efficiency$_{t,j}$ (MWh/km^3)	Water to electricity conversion efficiency of hydroelectric turbine; function of reservoir elevation.
Available Storage$_j$ (km^3)	Available reservoir storage for hydroelectric power production at plant j (dynamic value).
DADemand$_t$ (MWh)	Net hourly electricity demand in day-ahead market.
RVDemand$_t$ (MW)	Hourly demand in reserves market (spinning + non-spinning).
InitialON$_j$ {0,1}	Initial plant status conditions determined from previous iteration of UC model.
InitialMWh$_j$ (MWh)	Initial plant status conditions determined from previous iteration of UC model.

Table 11. UC problem decision variables

Variable	Description	Range
DAMWh$_{t,j}$	Day-ahead electricity production in hour t at generator j	>= 0
NRVMW$_{t,j}$	Non-spinning reserve provided in hour t by generator j	>= 0
SRVMW$_{t,j}$	Spinning reserve provided in hour t by generator j	>= 0
On$_{t,j}$	Binary state variable indicating production in day-ahead electricity market	{0,1}
NRVON$_{t,j}$	Binary state variable indicating provision of non-spinning reserves	{0,1}
SRVON$_{t,j}$	Binary state variable indicating provision of spinning reserves	{0,1}
START$_{t,j}$	Binary state variable indicating plant start in day-ahead market	{0,1}
Reservoir Spill$_{t,j}$	Reservoir release that does not produce electricity	>= 0

Table 12. Unit commitment problem constraints.

Constraint	Description	Scope
1	Unit 'on/off' initial conditions.	$for\ t = 0$
2	Unit production initial conditions.	$for\ t = 0$
3	Total day-ahead electricity generation must meet forecasted hourly demand.	$\forall\ t$
4	Forces ON variable = 1 if scheduled generation > 0.	$\forall\ t, j$
5	Minimum or 'turn off' generating capacity.	$\forall\ t, j$
6	Cumulative system supply of spinning and non-spinning reserves must meet hourly demand.	$\forall\ t$
7	Spinning reserves must supply at least half of total reserves.	$\forall\ t$
8	Total supply of reserves at a generator is limited by unit's maximum ramp rate.	$\forall\ t, j$
9	Forces SRON variable = 1 if scheduled spinning reserves > 0.	$\forall\ t, j$
10	Forces NRON variable = 1 if scheduled non-spinning reserves > 0.	$\forall\ t, j$
11	Spinning reserves can only be supplied by thermal units that are already online, or hydropower.	$\forall\ t, j$
12	Non-spinning reserves can only be supplied by quick start units (hydropower, combustion turbine natural gas, and oil).	$\forall\ t,$ $j \in \{coal,\ CCNG\}$
13	Maximum turbine capacity constraint with planned outages and deratings.	$\forall\ t, j$
14	Ramp rate restriction.	$\forall\ t\ \in \{2,3, \dots T\},$ j
15	Ramp rate restriction.	$\forall\ t\ \in \{2,3, \dots T\},$ j
16	Minimum up time.	$\forall\ t\ \in \{2,3, \dots T - 1\},\ j,$ k $\in \{t + 1,\ t$ $+ 2,\ \dots \min(t$ $+ MinUp_j - 1,\ T)\}$

17	Minimum down time.	$\forall\, t\,\in\{2,3,\dots T-1\},\, j,$ k $\in \{t+1,\, t$ $+\,2,\;\dots \min\big(t$ $+\, MinDown_j\, -\, 1,\, T\big)\}$
18	Forces START variable = 1 if unit is started in hour t.	$\forall\, t, j$
19	Water balance equation for conventional hydroelectric dams.	$\forall\, t,$ $j \in \{conventional$ $hydropower\}$
20	Water balance equation for pumped storage hydroelectric dams.	$\forall\, t\,\in\{1,25,49,$ $\dots T-23\},$ $j \in \{pumped\ storage$ $hydropower\}$

Table 13. ED problem time series parameters.

Parameter	Description
RTDemand$_t$ (MWh)	Hourly electricity demand in real-time market.
InitialON$_n$ {0,1}	Plant status condition determined by UC model.

Table 14. ED problem decision variables.

Variable	Description	Range
RTMWh$_{t,n}$	Real-time electricity production from non-spinning reserves in hour t at generator n	>= 0
RTMWh$_{t,p}$	Real-time electricity production from spinning reserves in hour t at generator s	>= 1
rtON$_{t,n}$	Binary state variable indicating production real-time production	{0,1}
RTON$_{t,n}$	Binary state variable indicating real-time (but not day-ahead) production	{0,1}
START$_{t,n}$	Binary state variable indicating plant start in real-time market	{0,1}

Table 15. Economic dispatch problem constraints.

Constraint	Description	Scope
21	Unit 'on/off' initial conditions for non-spinning reserve.	$\forall\, n,\ t = 0$
22	Real-time electricity demand constraint.	$\forall\, t$
23	Real-time electricity production from non-spinning reserves must be less than or equal to reserve offering; forces rtON variable = 1 if real-time electricity production is > 0	$\forall\, t$
24	Forces RTON variable = 1 if real-time electricity production is > 0 and day-ahead electricity production = 0.	$\forall\, t,\ n$
25	Forces RTSWITCH variable = 1 if plant start occurs in real-time.	$\forall\, t$
26	Real-time electricity production from spinning reserves must be less than or equal to reserve offering.	$\forall\, t,\ s$

Table 16. Time series parameters for hourly hydropower dispatch model.

Parameter	Description
σ (MWh/km^3)	Water to electricity conversion efficiency of hydroelectric turbine; function of beginning of period reservoir elevation.
Available Storage (km^3)	Available reservoir storage for hydroelectric power production (dynamic value).
DAP$_t$ ($/MWh)	Hourly electricity price in day-ahead market.
RTP$_t$ ($/MWh)	Hourly electricity prices in real-time market.
RVP$_t$ ($/MW)	Hourly price in reserves market (spinning + non-spinning).
InitialON {0,1}	Initial plant status conditions determined from previous iteration of dispatch model.

Table 17. Decision variables in hourly hydropower dispatch model.

Variable	Description	Range
DAMWh$_t$	Day-ahead electricity production in hour t	$>= 0$
RVMW$_t$	Non-spinning reserve provided in hour t	$>= 0$
On$_t$	Binary state variable indicating production in day-ahead electricity market	{0,1}
START$_t$	Binary state variable indicating plant start in day-ahead market	{0,1}
Reservoir Spill$_t$	Reservoir release that does not produce electricity	$>= 0$
RTMWh$_t$	Real-time electricity production in hour t	$>= 0$

Table 18. Constraints for hourly hydropower dispatch model.

Constraint	Description	Scope
1	Unit 'on/off' initial conditions.	$t = 0$
2	Turbine capacity constraint.	$\forall\, t$
3	Reservoir water balance equation.	$\forall\, t$
4	Limits production of real-time electricity by reserve offer.	$\forall\, t$
5	Forces ON variable = 1 if electricity production in the day-ahead or real-time markets > 0.	$\forall\, t$
6	Forces START variable = 1 if electricity production > 0 in hour t and equal to zero in hour t 1.	$\forall\, t$

Table 19. Proportionality constants (α) used to calculated hourly reserve requirements for each wind scenario. Please refer to [*21*] for detailed description of methodology used to simulate hourly dynamic reserve requirements.

		Installed Wind Power Capacity		
		LOW	MED	HIGH
Geographical Source Region	Northern Plains	8	7.7	10.17
	Southern Plains	7.83	7.71	9.29
	Midwest	10.82	15.69	28.75
	Mid-Atlantic	8.33	10.7	19.13
	Offshore	7.69	11.09	15.44

Table 20. The 15 wind development scenarios tested in this study. Please refer to [21] for detailed description of algorithm used to select wind sites for each scenario.

<table>
<tr><td colspan="2"></td><td colspan="5">Geographical Source Region</td></tr>
<tr><td colspan="2"></td><td>*Northern Plains*</td><td>*Southern Plains*</td><td>*Midwest*</td><td>*Mid-Atlantic and Appalachia*</td><td>*Offshore Atlantic Coast*</td></tr>
<tr><td colspan="2"></td><td>MT, ND, SD, NE, MN, IA, MI, KS, CO</td><td>NM, OK, TX, KS, MI, AK, CO</td><td>IL, IN, OH</td><td>NC, VA, WV, PA, MD</td><td>NC, VA</td></tr>
<tr><td colspan="2"></td><td>Installed Capacity *(Avg. Capacity Factor)*</td><td>Installed Capacity *(Avg. Capacity Factor)*</td><td>Installed Capacity *(Avg. Capacity Factor)*</td><td>Installed Capacity *(Avg. Capacity Factor)*</td><td>Installed Capacity *(Avg. Capacity Factor)*</td></tr>
<tr><td rowspan="3">Installed Wind Capacity</td><td>LOW</td><td>1.21 GW *(.469)*</td><td>1.36 GW *(.464)*</td><td>1.61 GW *(.339)*</td><td>1.53 GW *(.357)*</td><td>1.20 GW *(.442)*</td></tr>
<tr><td>MED</td><td>3.82 GW *(.452)*</td><td>3.62 GW *(.451)*</td><td>4.78 GW *(.335)*</td><td>4.98 GW *(.323)*</td><td>3.62 GW *(0.439)*</td></tr>
<tr><td>HIGH</td><td>6.49 GW *(.441)*</td><td>6.37 GW *(.444)*</td><td>8.87 GW *(.333)*</td><td>8.81 GW *(.303)*</td><td>6.04 GW *(.438)*</td></tr>
</table>

APPENDIX 3: CHAPTER 3

1.   Synthetic Model Inputs

1.1   Weather Data

An approach developed by Nowak et al. [19] for disaggregating annual to daily streamflow across multiple sites was used to generate synthetic hydrological inputs (precipitation, evaporation and runoff) for the reservoir model. This method simulates daily flow data at multiple locations from historical annual flow values using K-nearest neighbor resampling of historical daily flow proportion vectors (all historical flows were obtained from the North Carolina Department of Natural Resources). The approach produces daily synthetic flow data that exhibits identical time-series characteristics as the historical record (e.g., it maintains historical daily, weekly and seasonal precipitation patterns) and provides for the potential occurrence of daily flow values outside (lower or higher than) historical occurrences. Each calendar year (365 days) of synthetic hydrological data is constructed as the algebraic product of: 1) a scalar equal to an annual flow value ($\mathbf{Z}_a$) selected at random from a year ($y = a$) in the historical record; and 2) a daily flow proportion vector ($\vec{\boldsymbol{p}}_b$) resampled from a different year ($y = b$) in the historical record.

In order to maintain the connection between the occurrence of precipitation and changes in mean daily temperature, each year of synthetic hydrological data produced was paired with historical temperature data collected from the Richmond International Airport (Virginia) obtained from the National Climatic Data Center from year b (the year from which the proportion vector ($\vec{\boldsymbol{p}}_b$) was obtained). Daily temperature data was then used to estimate daily peak electricity demand using a Markov Chain Monte Carlo model. Since the co-generation of synthetic hydrological and temperature (electricity demand) data in this manner requires concurrent historical records of each input, historical daily data from the period (1947-2012) served as the basis for the creation of synthetic temperature (electricity demand) and hydrological inputs.

Historical data for the period 1993-2012 were then assessed for statistical dependence between temperature and inflows and Henry Hub natural gas prices taken from the Energy Information Administration. A method developed by Haugh [23] for checking the dependence of stationary time series was used to evaluate each pair of inputs (i.e., temperature and gas prices, reservoir inflows and gas prices), with the null hypothesis in each case being that monthly values of one input (e.g., cumulative inflows to Kerr Reservoir) are independent of monthly values of another input (e.g., average natural gas price). Autoregressive (AR) models were fit to log-transformed historical data for each input, and the cross correlation function (Equation 1) of model residuals were used to calculate a test statistic, $\mathbf{S_M}^*$ (Equation 2), described by a chi-square distribution. Results from this test failed to reject the null hypothesis (statistical independence) for each input pairing at a significance level of $\boldsymbol{\alpha} = 0.05$.

$$r_{gx}(k) = \frac{c_{gx}(k)}{s_g s_x} \qquad (1)$$

where, $c_{gx}(k) = \frac{1}{N}\sum_{t=1}^{N-k}(g_t - \bar{g})(x_{t+k} - \bar{x})$

$s_g = \sqrt{c_{gg}(0)}$

$s_x = \sqrt{c_{xx}(0)}$

$k = $ time lag $\{0,1,\dots \text{months}\}$

$g_t = $ natural gas price in month t $(\frac{\$}{\text{MMBtu}})$

$x_t = $ cumulative monthly inflows (km^3) or average temperature $(°\text{F})$ in month t

$N = $ length of monthly time series

$t = $ month

$$S_M* = N^2 \sum_{k=-M}^{M} (N - |k|)^{-1} * r_{gx}(k)^2 \tag{2}$$

where, M = total number of lags considered

Although Haugh's test suggests that natural gas prices are relatively independent of localized temperature and inflows in Roanoke River basin, seasonal changes in temperature (electricity demand) are known to increase demand for natural gas in many systems, and extreme weather (e.g., hurricanes) can have significant short term impacts on supply [24]. It is thus important to recognize that the independence of natural gas prices from temperature and reservoir inflows may not hold in other systems, and if a significant relationship were to exist between gas prices and other model inputs, that relationship would need to be accounted for in the generation of synthetic data.

1.2 Natural Gas Prices

Synthetic natural gas prices were generated using an Ornstein-Uhlenbeck (OU) stochastic difference model (Equation 3). In order to replicate the statistical characteristics of the historical record, model parameters (volatility, mean, and mean reversion rate) were estimated using a least squares polynomial fit to a time-series of historical natural gas prices (1997-2012).

$$dx_t = \theta(\mu - x_t)dt + \sigma dW_t \tag{3}$$

where, x_t = natural gas price in week t ($/MMBtu)

μ = historical mean price of natural gas ($/MMBtu)

θ = mean reversion rate

σ = natural gas price volatility

W_t = Brownian motion

t = week

Synthetic natural gas prices simulated by the fitted model demonstrate a high degree of success and replicating historical time-series characteristics and statistical moments of average monthly natural gas prices. Figure 35 shows that the OU model is adept at reproducing the historical time-series autocorrelation of monthly gas prices at lags up to one year (12 months), an important consideration for the contracts developed in this paper, which are assumed to apply to seasonal coverage periods 12 months after contract inception. Figure 36 shows that the OU model also reproduces the log-normal shape of the historical distribution of natural gas prices, as well as the mean (historical: $5.60/MMBtu; simulated: $5.52/MMBtu).
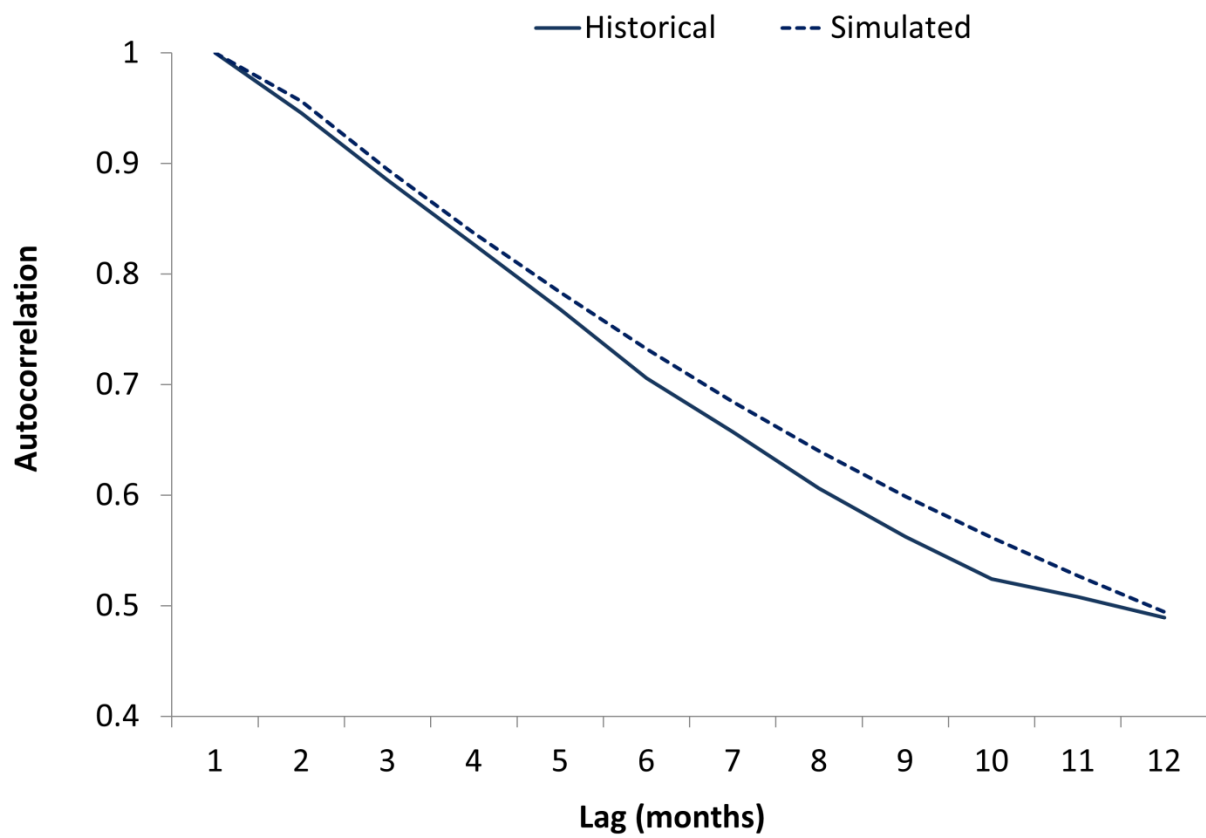
Figure 35. Time-series autocorrelation of historical and simulated monthly natural gas prices.
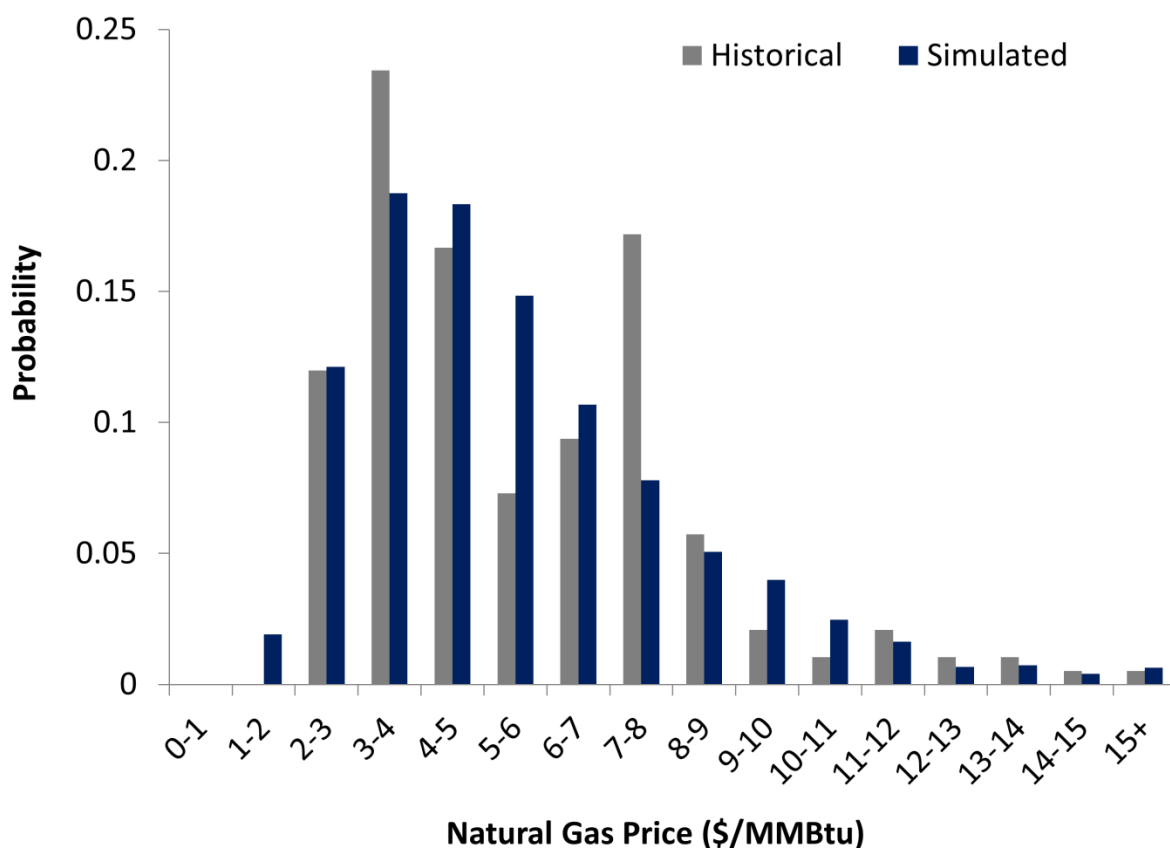
Figure 36. Probability distributions for historical and simulated natural gas prices.

The OU model was also used to simulate natural gas prices assuming lower and higher levels of volatility than the historical average. "Low" volatility was calculated as the lowest volatility level for any consecutive three-year section in the historical record (years selected were 2010-2012, a period of very low natural gas prices brought on by reduced economic activity and the recent increase in natural gas supply, largely attributable to advances in horizontal hydraulic fracturing). Likewise, "high" volatility was calculated as the highest volatility level for any three-year period (years selected were 2003-2005, a period in which the price of natural gas spike on multiple occasions due to Gulf occurring hurricanes disrupting refinery activity).

1.2.1 Natural Gas Derivatives

Natural gas put options are priced on a monthly basis using a version of the Black-Scholes formula adapted to use natural gas futures prices as the underlying asset [21].

$$PutPrice\ (\$) = e^{-r(\tau-t)}(X * \varphi(-d_2) - U * \varphi(-d_1)) \tag{4}$$

$$d_1 = \frac{\ln\left(\frac{U}{X}\right) + \frac{1}{2}\sigma^2(\tau-t)}{\sigma\sqrt{\tau-t}} \tag{5}$$

$$d_2 = d_1 - \sigma\sqrt{\tau-t} \tag{6}$$

where, $\tau - t$ = time to maturity

U = current futures price ($\frac{\$}{\text{MMBtu}}$)

K = strike price ($\frac{\$}{\text{MMBtu}}$)

φ = standard normal cumulative distribution function

σ = annualized volatility of log returns

Monthly futures prices (U) were simulated in a manner similar to that employed by Kogan et al. [25], as the risk-neutral conditional expectation of natural gas prices one year into the future, given the current spot price (Equation 7).

$$U = E[S(t + \tau)|S(t)] * (1 + r)^{\tau-t} \tag{7}$$

where, $S(t)$ = current spot price of natural gas $\left(\frac{\$}{\text{MMBtu}}\right)$

$S(t + \tau)$ = spot price of natural gas at time $(t + \tau)$ ($\frac{\$}{\text{MMBtu}}$)

1.3 Additional Results

Table 21. Contract cost effectiveness measures for contracts i(1)$_T$ and i(2)$_T$ for spring coverage period (March, April, May). Note that premiums listed for contracts based on the index i(1)$_T$ are averages for the 300-year testing period (in reality, premiums for these contracts fluctuate on an annual basis, depending on the spot price of natural gas).

| | Strike (%) | $i(1)_T$ | | | | | $i(2)_T$ | | | | |
		Premium ($)	Net Cost ($)	Net Cost (%)	Risk Mitigation ($)	RMF	Premium ($)	Net Cost ($)	Net Cost (%)	Risk Mitigation ($)	RMF
Low Volatility Old floor: $614,328	5	2.76E+04	1.10E+04	0.25	1.94E+05	1.32	2.00E+04	-1.56E+03	-0.04	2.10E+05	1.34
	15	1.26E+05	4.57E+04	1.03	6.36E+05	2.04	1.10E+05	2.67E+04	0.60	5.90E+05	1.96
	25	2.37E+05	8.04E+04	1.82	8.99E+05	2.46	1.89E+05	4.96E+04	1.12	7.40E+05	2.20
	35	4.35E+05	1.31E+05	2.95	1.16E+06	2.89	3.81E+05	9.29E+04	2.10	6.70E+05	2.09
Average Volatility Old floor: $583,332	5	4.47E+04	1.95E+04	0.45	2.54E+05	1.43	1.79E+04	-1.67E+03	-0.04	4.18E+04	1.07
	15	1.34E+05	5.47E+04	1.25	6.53E+05	2.12	1.08E+05	2.65E+04	0.61	2.66E+05	1.46
	25	2.32E+05	8.36E+04	1.91	8.92E+05	2.53	1.90E+05	5.04E+04	1.15	4.33E+05	1.74
	35	3.82E+05	1.13E+05	2.59	1.03E+06	2.77	3.44E+05	8.54E+04	1.95	5.64E+05	1.97
High Volatility Old floor: $712,169	5	5.15E+04	2.54E+04	0.54	6.64E+05	3.11	2.35E+04	-1.94E+03	-0.04	4.61E+05	2.46
	15	1.84E+05	7.24E+04	1.54	8.90E+05	3.82	1.27E+05	3.05E+04	0.65	5.21E+05	2.65
	25	3.51E+05	1.19E+05	2.54	1.04E+06	4.29	2.32E+05	6.13E+04	1.30	5.59E+05	2.77
	35	6.44E+05	1.81E+05	3.86	1.22E+06	4.88	4.66E+05	1.12E+05	2.39	5.65E+05	2.79

Table 22. Contract cost effectiveness measures for contracts i(3)$_T$ and i(4)$_T$ for spring coverage period (March, April, May). Note that premiums listed for contracts based on the indices i(3)$_T$ and i(4)$_T$ are averages of the 300-year testing period (in reality, premiums for these contracts fluctuate on an annual basis, depending on the spot price of natural gas).

	Strike (%)	$i(3)_T$					$i(4)_T$				
		Premium ($)	Net Cost ($)	Net Cost (%)	Risk Mitigation ($)	RMF	Premium ($)	Net Cost ($)	Net Cost (%)	Risk Mitigation ($)	RMF
Low Volatility Old floor: $614,328	5	1.92E+04	-1.52E+03	-0.03	2.17E+05	1.35	1.92E+04	-1.37E+03	-0.03	2.12E+05	1.34
	15	1.13E+05	3.08E+04	0.69	5.13E+05	1.83	1.12E+05	2.86E+04	0.65	5.30E+05	1.86
	25	2.05E+05	5.81E+04	1.31	6.64E+05	2.08	2.04E+05	5.61E+04	1.27	7.41E+05	2.21
	35	3.98E+05	1.04E+05	2.34	7.74E+05	2.26	3.94E+05	9.86E+04	2.23	7.18E+05	2.17
Average Volatility Old floor: $583,332	5	1.91E+04	-2.74E+03	-0.06	4.69E+04	1.08	1.98E+04	-2.69E+03	-0.06	3.96E+04	1.07
	15	1.13E+05	1.97E+04	0.45	2.51E+05	1.43	1.17E+05	2.21E+04	0.50	2.50E+05	1.43
	25	2.05E+05	4.12E+04	0.94	4.00E+05	1.69	2.10E+05	4.67E+04	1.07	4.14E+05	1.71
	35	3.98E+05	7.74E+04	1.77	5.00E+05	1.86	4.08E+05	8.62E+04	1.97	5.77E+05	1.99
High Volatility Old floor: $712,169	5	2.10E+04	1.18E+03	0.03	4.42E+05	2.40	2.14E+04	-1.28E+03	-0.03	4.52E+05	2.43
	15	1.23E+05	2.66E+04	0.57	5.27E+05	2.67	1.25E+05	2.72E+04	0.58	5.53E+05	2.75
	25	2.23E+05	5.18E+04	1.10	6.53E+05	3.07	2.30E+05	5.65E+04	1.20	6.10E+05	2.93
	35	4.28E+05	8.88E+04	1.89	8.28E+05	3.63	4.44E+05	9.99E+04	2.13	7.78E+05	3.47

Table 23. Contract cost effectiveness measures for contracts $i(1)_T$ and $i(2)_T$ summer season (June, July, August). Note that premiums listed for contracts based on the index $i(1)_T$ are averages for the 300-year testing period (in reality, premiums for these contracts fluctuate on an annual basis, depending on the spot price of natural gas).

	Strike (%)	$i(1)_T$					$i(2)_T$				
		Premium ($)	Net Cost ($)	Net Cost (%)	Risk Mitigation ($)	RMF	Premium ($)	Net Cost ($)	Net Cost (%)	Risk Mitigation ($)	RMF
Low Volatility Old floor: $1,049,004	5	3.25E+04	1.70E+04	0.52	1.71E+05	1.16	6.36E+03	-1.72E+03	-0.05	1.17E+05	1.11
	15	8.46E+04	3.34E+04	1.01	1.68E+05	1.16	2.74E+04	1.17E+03	0.04	2.56E+05	1.24
	25	1.54E+05	5.23E+04	1.59	1.24E+05	1.12	9.88E+04	1.82E+04	0.55	1.95E+05	1.19
	35	2.70E+05	8.36E+04	2.54	1.52E+04	1.01	1.69E+05	2.94E+04	0.89	1.24E+05	1.12
Average Volatility Old floor: $738,409	5	2.17E+04	1.08E+04	0.33	3.40E+05	1.46	5.19E+03	-1.35E+03	-0.04	1.13E+05	1.15
	15	1.04E+05	3.73E+04	1.13	2.41E+05	1.33	4.24E+04	5.82E+03	0.18	1.77E+05	1.24
	25	1.95E+05	6.03E+04	1.83	1.93E+05	1.26	9.38E+04	1.74E+04	0.53	1.66E+05	1.22
	35	3.41E+05	9.30E+04	2.82	3.67E+05	1.50	1.64E+05	2.85E+04	0.86	2.72E+05	1.37
High Volatility Old floor: $607,546	5	3.09E+04	1.78E+04	0.52	4.39E+05	1.72	6.81E+03	-1.86E+03	-0.05	2.72E+05	1.45
	15	1.09E+05	5.27E+04	1.52	5.53E+05	1.91	4.34E+04	5.06E+03	0.15	3.69E+05	1.61
	25	2.49E+05	9.43E+04	2.73	6.14E+05	2.01	1.21E+05	2.20E+04	0.64	3.60E+05	1.59
	35	4.24E+05	1.25E+05	3.62	2.93E+05	1.48	1.93E+05	3.35E+04	0.97	2.88E+05	1.47

Table 24. Contract cost effectiveness measures for contracts i(3)$_T$ and i(4)$_T$ for summer season (June, July, August). Note that premiums listed for contracts based on the indices i(3)$_T$ and i(4)$_T$ are averages of the 300-year testing period (in reality, premiums for these contracts fluctuate on an annual basis, depending on the spot price of natural gas).

	Strike (%)	$i(3)_T$					$i(4)_T$				
		Premium ($)	Net Cost ($)	Net Cost (%)	Risk Mitigation ($)	RMF	Premium ($)	Net Cost ($)	Net Cost (%)	Risk Mitigation ($)	RMF
Low Volatility Old floor: $1,049,004	5	7.28E+03	-1.93E+03	-0.06	1.21E+05	1.12	6.59E+03	-1.97E+03	-0.06	1.19E+05	1.11
	15	3.77E+04	5.65E+03	0.17	2.10E+05	1.20	3.77E+04	4.44E+03	0.13	2.54E+05	1.24
	25	1.12E+05	2.09E+04	0.63	2.13E+05	1.20	1.12E+05	2.13E+04	0.65	2.03E+05	1.19
	35	1.96E+05	3.44E+04	1.05	1.37E+05	1.13	1.90E+05	3.28E+04	1.00	1.31E+05	1.13
Average Volatility Old floor: $738,409	5	7.29E+03	-3.62E+03	-0.11	1.51E+05	1.20	6.94E+03	-2.61E+03	-0.08	1.76E+05	1.24
	15	3.78E+04	-1.31E+03	-0.04	1.93E+05	1.26	3.74E+04	1.94E+03	0.06	1.82E+05	1.25
	25	1.11E+05	1.32E+04	0.40	1.81E+05	1.24	1.16E+05	1.87E+04	0.57	1.92E+05	1.26
	35	1.95E+05	2.49E+04	0.76	2.69E+05	1.36	1.99E+05	3.07E+04	0.93	2.54E+05	1.34
High Volatility Old floor: $607,546	5	7.89E+03	-3.02E+03	-0.09	2.76E+05	1.45	8.66E+03	-3.28E+03	-0.09	2.72E+05	1.45
	15	4.10E+04	9.53E+02	0.03	3.27E+05	1.54	4.07E+04	2.68E+03	0.08	3.41E+05	1.56
	25	1.20E+05	1.54E+04	0.45	3.70E+05	1.61	1.24E+05	2.09E+04	0.60	3.57E+05	1.59
	35	2.11E+05	2.28E+04	0.66	2.61E+05	1.43	2.17E+05	3.09E+04	0.89	2.44E+05	1.40

Table 25. Contract cost effectiveness measures for contracts i(1)$_T$ and i(2)$_T$ for fall season (September, October, and November). Note that premiums listed for contracts based on the index i(1)$_T$ are averages for the 300-year testing period (in reality, premiums for these contracts fluctuate on an annual basis, depending on the spot price of natural gas).

	Strike (%)	$i(1)_T$					$i(2)_T$				
		Premium ($)	Net Cost ($)	Net Cost (%)	Risk Mitigation ($)	RMF	Premium ($)	Net Cost ($)	Net Cost (%)	Risk Mitigation ($)	RMF
Low Volatility Old floor: $94,276	5	1.02E+04	6.22E+03	0.28	9.66E+04	2.02	5.45E+03	3.21E+03	0.14	8.44E+04	1.89
	15	4.05E+04	1.93E+04	0.86	1.32E+05	2.40	3.11E+04	1.17E+04	0.52	1.36E+05	2.45
	25	9.58E+04	3.70E+04	1.66	2.57E+05	3.72	7.94E+04	2.37E+04	1.06	1.52E+05	2.61
	35	1.98E+05	6.55E+04	2.93	3.76E+05	4.99	1.13E+05	3.16E+04	1.41	2.18E+05	3.31
Average Volatility Old floor: $101,954	5	8.07E+03	4.19E+03	0.19	-7.59E+03	0.93	5.74E+03	3.34E+03	0.15	1.04E+05	2.02
	15	4.36E+04	1.75E+04	0.81	1.26E+05	2.24	3.24E+04	1.19E+04	0.54	9.81E+04	1.96
	25	1.15E+05	3.61E+04	1.67	2.98E+05	3.93	8.21E+04	2.43E+04	1.11	1.26E+05	2.24
	35	1.96E+05	5.24E+04	2.42	3.85E+05	4.78	1.17E+05	3.24E+04	1.49	1.91E+05	2.87
High Volatility Old floor: $101,010	5	1.12E+04	6.24E+03	0.24	-1.50E+04	0.86	2.19E+03	1.46E+03	0.06	3.37E+04	1.32
	15	7.54E+04	2.29E+04	0.90	8.76E+04	1.83	3.71E+04	1.36E+04	0.53	9.10E+04	1.87
	25	1.61E+05	4.07E+04	1.59	1.85E+05	2.76	8.53E+04	2.56E+04	1.00	1.03E+05	1.98
	35	2.99E+05	6.45E+04	2.53	3.27E+05	4.12	1.58E+05	4.15E+04	1.62	2.28E+05	3.17

Table 26. Contract cost effectiveness measures for contracts i(3)$_T$ and i(4)$_T$ for fall season (September, October and November). Note that premiums listed for contracts based on the indices i(3)$_T$ and i(4)$_T$ are averages of the 300-year testing period (in reality, premiums for these contracts fluctuate on an annual basis, depending on the spot price of natural gas).

	Strike (%)	$i(3)_T$					$i(4)_T$				
		Premium ($)	Net Cost ($)	Net Cost (%)	Risk Mitigation ($)	RMF	Premium ($)	Net Cost ($)	Net Cost (%)	Risk Mitigation ($)	RMF
Low Volatility Old floor: $94,276	5	4.26E+03	2.30E+03	0.10	-1.38E+02	1.00	4.10E+03	2.94E+03	0.13	1.86E+04	1.20
	15	3.23E+04	1.18E+04	0.53	1.42E+05	2.50	2.99E+04	1.09E+04	0.49	1.41E+05	2.50
	25	8.77E+04	2.42E+04	1.08	1.35E+05	2.43	8.54E+04	2.42E+04	1.08	1.65E+05	2.75
	35	1.37E+05	3.26E+04	1.46	2.03E+05	3.15	1.36E+05	3.46E+04	1.55	2.29E+05	3.43
Average Volatility Old floor: $101,954	5	4.57E+03	1.41E+03	0.07	6.44E+04	1.63	4.71E+03	2.69E+03	0.12	7.70E+04	1.75
	15	3.29E+04	9.38E+03	0.43	1.05E+05	2.03	3.38E+04	1.24E+04	0.57	9.53E+04	1.94
	25	8.92E+04	2.26E+04	1.05	9.60E+04	1.94	9.29E+04	2.58E+04	1.19	1.10E+05	2.07
	35	1.40E+05	3.28E+04	1.52	1.55E+05	2.52	1.44E+05	3.67E+04	1.70	1.80E+05	2.76
High Volatility Old floor: $101,010	5	4.92E+03	2.36E+03	0.09	2.19E+04	1.21	5.04E+03	2.62E+03	0.10	4.36E+04	1.42
	15	3.66E+04	1.30E+04	0.51	9.60E+04	1.91	3.72E+04	1.38E+04	0.54	9.84E+04	1.94
	25	9.85E+04	2.99E+04	1.17	1.29E+05	2.23	9.95E+04	2.99E+04	1.17	1.01E+05	1.96
	35	1.54E+05	4.21E+04	1.65	1.92E+05	2.83	1.54E+05	4.01E+04	1.57	2.28E+05	3.17

Table 27. Contract cost effectiveness measures for contracts i(1)$_T$ and i(2)$_T$ for winter season (December, January, February). Note that premiums listed for contracts based on the index i(1)$_T$ are averages for the 300-year testing period (in reality, premiums for these contracts fluctuate on an annual basis, depending on the spot price of natural gas).

	Strike (%)	$i(1)_T$					$i(2)_T$				
		Premium ($)	Net Cost ($)	Net Cost (%)	Risk Mitigtation ($)	RMF	Premium ($)	Net Cost ($)	Net Cost (%)	Risk Mitigtation ($)	RMF
Low Volatility Old floor: $644,543	5	3.34E+04	1.17E+04	0.30	5.07E+05	1.79	2.68E+04	1.61E+03	0.04	2.33E+05	1.36
	15	1.36E+05	5.16E+04	1.30	6.36E+05	1.99	7.89E+04	1.03E+04	0.26	5.59E+05	1.87
	25	2.41E+05	7.59E+04	1.92	8.06E+05	2.25	1.82E+05	3.32E+04	0.84	6.34E+05	1.98
	35	4.03E+05	1.14E+05	2.89	9.93E+05	2.54	2.94E+05	5.48E+04	1.39	7.95E+05	2.23
Average Volatility Old floor: $554,868	5	2.53E+04	1.10E+04	0.28	1.02E+05	1.18	2.40E+04	1.60E+03	0.04	1.61E+05	1.29
	15	1.39E+05	4.57E+04	1.17	7.05E+05	2.27	7.34E+04	9.06E+03	0.23	4.11E+05	1.74
	25	2.94E+05	8.71E+04	2.22	9.53E+05	2.72	1.75E+05	3.17E+04	0.81	4.48E+05	1.81
	35	4.40E+05	1.28E+05	3.28	9.99E+05	2.80	2.86E+05	5.35E+04	1.36	6.37E+05	2.15
High Volatility Old floor: $712,169	5	4.47E+04	2.49E+04	0.58	2.72E+05	1.38	2.87E+04	1.93E+03	0.04	9.13E+03	1.01
	15	1.99E+05	6.70E+04	1.55	4.88E+05	1.69	9.21E+04	1.21E+04	0.28	1.21E+05	1.17
	25	4.39E+05	1.28E+05	2.97	6.12E+05	1.86	1.92E+05	3.37E+04	0.78	3.64E+05	1.51
	35	6.32E+05	1.64E+05	3.79	7.52E+05	2.06	3.80E+05	6.95E+04	1.61	3.55E+05	1.50

Table 28. Contract cost effectiveness measures for contracts i(3)$_T$ and i(4)$_T$ for winter season (December, January, February). Note that premiums listed for contracts based on the indices i(3)$_T$ and i(4)$_T$ are averages of the 300-year testing period (in reality, premiums for these contracts fluctuate on an annual basis, depending on the spot price of natural gas).

	Strike (%)	$i(3)_T$					$i(4)_T$				
		Premium ($)	Net Cost ($)	Net Cost (%)	Risk Mitigtation ($)	RMF	Premium ($)	Net Cost ($)	Net Cost (%)	Risk Mitigtation ($)	RMF
Low Volatility Old floor: $644,543	5	2.92E+04	4.66E+03	0.12	2.51E+05	1.39	2.88E+04	3.29E+03	0.08	2.55E+05	1.40
	15	8.25E+04	1.62E+04	0.41	5.11E+05	1.79	8.24E+04	1.37E+04	0.35	5.17E+05	1.80
	25	1.88E+05	4.26E+04	1.08	6.38E+05	1.99	1.87E+05	3.71E+04	0.94	6.53E+05	2.01
	35	3.29E+05	7.27E+04	1.84	7.64E+05	2.19	3.26E+05	6.48E+04	1.64	7.95E+05	2.23
Average Volatility Old floor: $554,868	5	2.97E+04	-1.97E+03	-0.05	1.86E+05	1.33	3.09E+04	-7.89E+02	-0.02	1.63E+05	1.29
	15	8.45E+04	4.58E+03	0.12	3.61E+05	1.65	8.91E+04	6.65E+03	0.17	4.16E+05	1.75
	25	1.94E+05	2.13E+04	0.54	4.66E+05	1.84	1.98E+05	2.79E+04	0.71	4.73E+05	1.85
	35	3.40E+05	4.28E+04	1.09	5.90E+05	2.06	3.48E+05	5.35E+04	1.37	5.97E+05	2.08
High Volatility Old floor: $712,169	5	3.25E+04	-1.09E+03	-0.03	1.31E+04	1.02	3.30E+04	-5.35E+02	-0.01	6.77E+03	1.01
	15	9.11E+04	3.08E+03	0.07	1.48E+05	1.21	9.25E+04	6.48E+03	0.15	1.35E+05	1.19
	25	2.08E+05	2.46E+04	0.57	3.33E+05	1.47	2.13E+05	2.96E+04	0.69	3.62E+05	1.51
	35	3.63E+05	5.57E+04	1.29	2.48E+05	1.35	3.74E+05	6.09E+04	1.41	2.88E+05	1.40

Table 29. Replicating portfolios under average natural gas price volatility.

	Net Cost (%)	Hydrological Insurance Volume (millions)	Inflow Strike (km^3)	Put Volume	Natural Gas Put Strike ($/MMBtu)	RMF
Spring	0.45	0.62	1.55	2	6.42	1.44
	1.25	0.96	1.72	2	4.49	1.74
	1.91	0.86	2.09	6	5.38	1.88
	2.59	1.12	2.46	6	7.26	2.29
	3.64	1.04	2.85	2	5.96	2.49
Summer	0.33	0.82	0.59	4	4.94	1.26
	1.13	1.92	0.74	6	4.94	1.34
	1.83	1.22	0.77	12	2.62	1.23
	2.63	0.70	1.67	8	4.40	1.46
Fall	0.19	1.02	1.17	16	7.23	0.93
	0.82	0.82	0.71	2	5.46	2.24
	1.67	1.06	0.88	0	n/a	3.35
	2.42	1.48	0.94	2	7.23	3.74
	3.93	1.02	1.35	2	2.28	4.65
Winter	0.28	0.24	1.28	2	4.44	1.18
	1.17	0.80	1.87	2	7.43	2.04
	2.22	1.04	1.94	2	3.14	2.16
	3.28	1.30	2.10	4	4.97	2.33
	4.32	1.10	2.82	4	1.78	2.35

APPENDIX 4: CHAPTER 4

1. Alternative Cost Model

An alternative formulation of the cost model based on exogenous environmental and market variables was also developed for use in calculating premiums associated with the third party collar agreement.

$$\hat{C}_T = (a * \hat{G}_T{}^3 + b * \hat{G}_T{}^2 + c * \hat{G}_T) * \gamma * \hat{S}_T \tag{1}$$

where, $\hat{C}_T$ = estimated cost of restrictions in season T

$\{a, b, c\}$ = multiplication coefficents

$\hat{G}_T$ = estimated generation at Roanoke Rapids Dam in season T

$\hat{S}_T$ = estimated price spread in season T ($\frac{\$}{MWh}$)

γ = multiplication coefficient for price spread

In the alternative model formulation, seasonal hydropower generation at Roanoke Rapids Dam is replaced by a function of seasonal inflows into upstream Kerr Reservoir (linear regression of seasonal generation at Roanoke Rapids Dam and Kerr Reservoir inflows yields an R^2 = 0.93).

$$\hat{G}_T = 0.113 * F_T + 962.2 \tag{2}$$

where, F_T = inflows to Kerr Reservoir in season T

Seasonal price spread is replaced with a linear combination of natural gas price and heating and cooling degree days (i.e., proxies for electricity demand) (regression of estimated price spread and actual price spread yields an $R^2 = 0.89$).

$$\hat{S}_T = -22.25 + .015 * HDD_T + .041 * CDD_T + 7.72 * NGP_T \tag{3}$$

$$HDD_T = \sum_{j=1}^{J} \max\left(65 - {}^\circ F_j\right) \tag{4}$$

$$CDD_T = \sum_{j=1}^{J} \max\left({}^\circ F_j - 65\right) \tag{5}$$

where, HDD_T = cumulative heating degree days in season T

CDD_T = cumulative cooling degree days in season T

NGP_T = natural gas price in season T ($\frac{\$}{MMBtu}$)

${}^\circ F_j$ = average temperature on day j

j = day in season T

J = total number of days in season T

Table 29 lists model parameters a, b, c, d, and γ and performance metrics (R^2 and mean squared error (MSE)) for the cost model shown in Equation 2 (row 1), as well as for the alternative model formulation (row 2). It shows that the use of exogenous inputs (Kerr inflows, gas prices, and degree days) in the alternative model formulation reduces the R^2 value to 0.84, and increases the MSE to $215,000/season.

Table 30. Model performance and parameters for the cost models calibrated with historical data from 2005-2013.

Model Inputs		Performance		Parameters			
		R^2	MSE ($100k)	a	b	c	γ
Generation	Price Spread	0.91	1.58	4.81E-10	-2.93E-04	41.3	0.0171
Kerr Inflows	Gas Prices, Degree Days	0.84	2.15	1.07E-09	-4.00E-04	38	0.025

2.   Premium Calculations

Premiums are calculated on a rolling, seasonal basis using empirical probability distributions of $Collar_T$ derived from synthetic input data and the alternative cost model. For each season T, 300 synthetic values of F_T, HDD_T, and CDD_T are simulated using a method outlined in Nowak et al. [26] that makes use of historical (1947-2012) streamflow and temperature records in the Roanoke River basin. Monte Carlo sampling from conditional probability distributions of natural gas prices one year in the future ($NGP_T | NGP_0$) is used to generate 300 years of synthetic natural gas prices for each season. Conditional probability distributions of natural gas prices are based on results of an Ornstein-Uhlenbeck (OU) stochastic difference model fit to historical natural gas prices over the period 1997-2012.

Synthetic weather inputs (F_T, HDD_T, and CDD_T) and natural gas prices (NGP_T) are paired to create 300 x 300 = 90,000 separate values of $\widehat{C}_T$. Estimated costs are then combined with a normally distributed error function ε_T that describes the distribution of errors between $\widehat{C}_T$ and C_T over the period 2005-2013. The 90,000 synthetic values of $\widehat{C}_T$ are used to calculate a corresponding empirical probability distribution for $Collar_T$, which is then transformed (see Equation 5), and the risk-adjusted expected value is taken as the seasonal premium.

Seasonal premiums (P_T) are found to fluctuate on a seasonal basis because the empirical

probability distribution of $Collar_T$ is influenced by price spread, which, in turn, depends on electricity

demand and the price of natural gas. In particular, premiums are larger for high demand seasons (winter

and summer) and following years of high natural gas prices. From the perspective of a hypothetical

downstream stakeholder, however, the goal of the collar agreements is to ensure relatively constant net

payments, and the ability of collar agreements to do this can be impacted by large fluctuations in

premiums. One option for reducing variability in premiums is to extend the coverage period of collar

agreements to one year (i.e., a downstream stakeholder would simultaneously purchase coverage for

spring, summer, fall and winter of the same year). A downstream stakeholder could then pay the average

seasonal premium over the one year period. Contracts can similarly be adjusted to apply over multi-year

periods (e.g., 5 or 10 years).

Table 30 shows how contract duration impacts the mean and standard deviation of net payments

made by the downstream stakeholder.

Table 31. Impact of contract duration on mean and standard deviation of net seasonal payments made by downstream stakeholder.

	Mean ($M)	Standard Deviation ($M)	Min ($M)	Max ($M)
C_T	1.15	0.69	0.17	2.80
Seasonal	1.25	0.36	0.56	2.08
1 year	1.34	0.19	0.99	1.58
9 years	1.55	0	1.55	1.55

Extending the contract duration (e.g., from seasonal to 1 year, and from 1 year to 9 years) results

in a greater reduction in the standard deviation of net payments experienced by the downstream

stakeholder because fluctuation in seasonal premiums is reduced. In order to eliminate all variability in seasonal net payments over the period 2005-2013, the downstream stakeholder must sign a single agreement for the entire 9-year period (2005-2013). However, engaging a downstream stakeholder in longer term contracts increases the risk exposure of the third party insurer. As a consequence, seasonal premiums (and therefore mean net payments) are higher.